INVESTIGATION ON ENHANCING FIRE PERFORMANCE OF CARBON FIBRE REINFORCED POLYMER (CFRP) STRENGTHENED CONCRETE COLUMNS

Maramba Widanage Chamodi Himasha

198036L

Degree of Master of Science

Department of Civil Engineering

University of Moratuwa
Sri Lanka

May 2021

INVESTIGATION ON ENHANCING FIRE PERFORMANCE OF CARBON FIBRE REINFORCED POLYMER (CFRP) STRENGTHENED CONCRETE COLUMNS

Maramba Widanage Chamodi Himasha

198036L

Thesis submitted in partial fulfillment of the requirements for the degree Master of Science

Department of Civil Engineering

University of Moratuwa
Sri Lanka

May 2021

DECLARATION

I declare that this is my own work and this thesis does not incorporate without acknowledgement any material previously submitted for a Degree or Diploma in any other university or institute of higher learning and to the best of my knowledge and belief it does not contain any material previously published or written by another person except where the acknowledgement is made in the text.

Also, I hereby grant to University of Moratuwa the non-exclusive right to reproduce and distribute the thesis, in whole or in part in print, electronic or other medium. I retain the right to use this content in whole or part in future works (such as articles or books).

Signature: *UOM Verified Signature* Date: 27/05/2021

The above candidate has carried out research for the Masters under my supervision

Name of the supervisor: Prof. (Mrs.) J.C.P.H. Gamage

Signature of the supervisor: Date:

ACKNOWLEDGEMENT

This research project provided me with the much needed exposure to both experimental work and numerical modelling. Further it helped in practically implementing the theoretical knowledge I gained from my undergraduate studies to develop an effective product to overcome issues in a commercially available product.

Lot of people helped me in achieving a greater success in this project and without their help it would have been very difficult to reach a successful completion. I feel honored to work under the guidance of my research supervisor. Prof. (Mrs.) J.C.P.H.Gamage, Senior lecturer in the Department of Civil Engineering, University of Moratuwa. She has always been the inspiration and her proper guidance is the spirit of the success of this research project. I would like to extend the gratitude to Dr. G.I.P. de Silva, Senior lecturer in the Department of Material Science and Engineering, University of Moratuwa and Prof. R.U.Halwathura, Senior lecturer in the Department of Civil Engineering, University of Moratuwa for their immense guidance. Further, the guidance given by Dr. H.M.Y.C. Mallikarachchi on numerical modelling needs to be acknowledged. I highly appreciate the help given by Eng. Buddhika Weerasinghe and my research group fellows throughout this whole time.

I would like to further extend my appreciation to non-academic staff members in Department of Civil Engineering, University of Moratuwa for the immense support given to conduct my experimental work.

Himasha M.W.C.

Department of Civil Engineering

University of Moratuwa

27.05.2021

ABSTRACT

This study focuses on the development of an adhesive to bond Carbon Fibre Reinforced Polymer (CFRP) fabric with a concrete substrate which performs well under elevated temperature. The epoxy adhesive which is the generally used adhesive for CFRP has a very low glass transition temperature that results in the loss of adhesive properties at higher temperatures. As a solution, Engineered Cementitious Composite (ECC) mortar mix was developed to function as a cementitious adhesive. ECC was developed using locally available materials. Effective bond length for the developed ECC adhesive is 150 mm and the achieved bond strength is 224.9 N/mm^2. The bond strength was further enhanced up to 570.28 N/mm^2 by sticking sand on top of CFRP fabric using epoxy adhesive before bonding it using cementitious adhesive as an interface bond enhancing technique. When the bond temperature was incremented up to 100 ^0C, bond strength reduction was less than 5.5%. Another attempt was made to enhance performance of the epoxy adhesive which has been used in CFRP/Concrete composite by blending with Polyethylene terephthalate (PET) fibres as a commercially viable option. Finally it indicated that developed epoxy can be used to strengthen cylinders using CFRP and a 7% of higher axial confinement was achieved when compared with the bond without modification. This modification has enhanced the performance of composite at ambient temperature as well as at elevated temperature when compared with the CFRP/Epoxy/Concrete bond.

LIST OF PUBLICATIONS

International Journal Papers

1. Bond characteristics of out of plane curved concrete beam strengthen for shear using Carbon Fibre Reinforced Polymer sheets (Processing)
2. Development of cementitious adhesive for bonding Carbon Fibre Reinforced Polymer fabric on concrete (Processing)
3. Modification of epoxy adhesive using Polyethylene terephthalate (PET) fibres to develop the thermal performance (Processing)
4. Investigation on Rice husk ash based insulation for Carbon Fibre Reinforced Polymer strengthened concrete members (Processing)

International Conference Papers

1. Finite element Modelling of reinforced concrete horizontally curved beams strengthened for shear using Carbon Fibre reinforced polymer, 7th International Symposium on Advances in Civil and Environmental Engineering Practices for Sustainable Development (ACEPS-2019) – Published
2. A Review on Cementitious Adhesives used to bond CFRP with Concrete, 10th International Conference on Structural Engineering and Construction Management – Published
3. Modification of engineered cementitious composite mortar to use as an adhesive for CFRP/Concrete bond, 11th International Conference on Sustainable Built Environment (ICSBE-2020) – Published
4. Enhancing the thermal performance of epoxy adhesive used in the CFRP/concrete bond (MERCon-2021) - Submitted

TABLE OF CONTENTS

LIST OF FIGURES

LIST OF TABLES

LIST OF ABBREVIATIONS

Abbreviation	Description
CFRP	Carbon Fibre Reinforced Polymer
ECC	Engineered Cementitious Composite
FRP	Fibre Reinforced Polymer
GO	Graphene Oxide
MPC	Magnesium Phosphate Cement
PVA	Poly Vinyl Alcohol
PET	Polyethylene terephthalate
PE	Polyethylene
PP	Polypropylene
ASTM	American Society for Testing and Materials
JSCE	Japan Society of Civil Engineers

1 INTRODUCTION

1.1 Research Background

CFRP strengthening has been one of the widely used retrofitting methods in the present world. Type of adhesive used as the bonding agent plays a major role in the long term performance of the strengthening setup[1]. Performance of the strengthening system under elevated temperature needs to be given a huge concern. CFRP strengthened concrete can reduce its strength by 65% at 300^{0}C[2]. Generally, epoxy (organic) adhesives are used as the bonding agent for fibre composites. But they have several disadvantages apart from its suitability with respect to better bonding behaviour. Strength of epoxy adhesive deteriorates rapidly with an elevated temperature higher than the glass transition temperature (60 ^{0}C –70 ^{0}C) [3]. At glass transition temperature (T_g) properties of the polymer adhesives suddenly drops and takes the form of a viscous material [4]. Apart from that, it possesses other disadvantages like the high cost of material[5], toxic fumes[6]. To overcome these issues, researchers suggest several options. Development of cementitious adhesives is one such option. Apart from that, modifications can be introduced to the existing epoxy adhesive to resist in higher temperatures.

1.2 Research Problem

Usually, organic adhesives have higher strength than cementitious adhesives. Therefore it is necessary to develop a cementitious adhesive with a better bonding ability. These cementitious adhesives are of two types; polymer-based cementitious adhesives and non-polymer based cementitious adhesives. When developing a new adhesive, several properties need to be checked to assess its compatibility to the purpose. Mechanical properties like tensile strength, compressive strength and pull-off strength need to be checked.

The modification to existing epoxy adhesives can be done either by a physical blending of a material or by chemical modification. Researchers have attempted several methods to enhance the bond strength of the epoxy adhesive [7]–[10]. A good amount of research has been focused on the chemical modification of epoxy adhesives [8],

[11]. However, the analysis of the thermal performance of epoxy under these modifications has not been discussed deeply. Researchers have also focused on the introduction of fibres to epoxy as the modification which can be categorized as a modification done by physical blending [12]–[15]. However, there is a huge research gap in determining the enhancement of adhering quality of epoxy resin by reinforcing it using fibres.

1.3 Research Scope

The overall research comprises of two parts. Part one is to develop a cementitious adhesive which could resist higher temperatures while maintaining a sound bonding capability. The other part is to introduce an effective modification agent to the epoxy adhesive so that it enhances the bond strength along with the ability to resist higher temperatures.

1.4 Significance and Innovation of the Research

Most of the cementitious and the modified epoxy adhesives which are in the research stage show a higher material cost. Thus, they are not economically feasible for large scale projects. Moreover, some raw materials used are locally unavailable. Hence, it is important to consider both cost and the availability of the materials used in the process of developing a feasible product.

1.5 Objectives

1. To develop a cementitious adhesive to create the bond between CFRP and concrete using locally available materials (Adhesive A)
2. To modify the epoxy adhesive to increase the glass transition temperature of the polymeric bond (Adhesive B)
3. To evaluate the strength and elevated temperature performance of adhesives A and B

1.6 Thesis Outline

Chapter 1: This chapter contains details under sub-topics research background, objectives and methodology

Chapter 2: This contains the literature review done in order to attain the objectives of the research. An extensive study was done in related areas to develop effective products and research significance and further research needs are also included.

Chapter 3: This chapter highlights the properties of the materials used in the research and a detail description of the testing methodologies.

Chapter 4: The details of the modification of epoxy adhesive using a fibre and performance analysis are also included both in ambient and elevated temperature conditions.

Chapter 5: The chapter focuses on the development of the cementitious adhesive, its production and evaluation of performance. Evaluation of performance is done in both ambient and elevated temperature conditions.

Chapter 6: A comparison is carried out on the performance of two developed adhesives and pure epoxy adhesive. Application of the developed adhesives on concrete elements is assessed to evaluate the performance.

Chapter 7: A finite element model was developed to predict the performance of the single shear lap test and several parametric studies are included which asses the performance of ECC adhesive in different aspects.

Chapter 8: Final chapter includes the overall conclusions and recommendations of the research study.

2 LITERATURE REVIEW

2.1 Introduction

Reinforced concrete jackets and iron bands were used as retrofitting procedures in concrete columns in past. But currently, in the process of retrofitting, new approaches have yielded outstanding results and ultimately they are often used in the industry. Carbon Fibre Reinforced Polymer (CFRP) is such a new approach that is already been used in retrofitting purposes. For column strengthening, CFRP fabrics are used to enhance axial confinement as well as to increase the bonding capacity.

Rocca, Galati and Nanni [16] performed a comparison on four Fibre Reinforced Polymer (FRP) design guidelines confined members. The formulae used in evaluating the ultimate compressive strength of columns wrapped with FRP underestimate the actual results [17]. Columns exhibit a transverse expansion as they are compressed axially. Therefore, when the transverse strain limit is exceeded, cracks appear parallel to the compressive force [17].

Several factors affect the performance of the bond between the fibre and concrete substrate. Some of them are the type of fibre, concrete surface preparation method, type of adhesive, adhesive thickness, bonded surface area and method of application [1].

2.2 The behaviour of CFRP/Epoxy/Concrete bond

2.2.1 At ambient temperature

Epoxy is one of the versatile polymer based adhesives. It shows a higher adhesion to almost all types of surfaces. It’s bonding ability in CFRP- Concrete bond has been proved by number of researchers [3], [18], [19]. Therefore, it has been used in the industry for a long time as the adhesive for CFRP-Concrete bonding system. The epoxy adhesives are applied on surfaces in both dry and wet lay-up methods. Dai and Ueda [20] investigated the effect of adhesive stiffness on bonding ability and they concluded that the lower stiffness enhances the bond capacity. The epoxy adhesives do not let any vapour through which might ultimately cause durability issues[21].

2.2.2 At elevated temperature

Generally, epoxy (organic) adhesives are used as the bonding agent for fibre composites. They have several disadvantages apart from its suitability with respect to better bonding behaviour. Strength of epoxy adhesive deteriorates rapidly with a temperature greater than the glass transition temperature (T_g) which is between 60 ^{0}C – 70 ^{0}C [3]. The properties of a polymer undergo a sudden drop at T_g and it becomes a more viscous material [4].

2.3 Problem identification

Low thermal performance is one of the major drawbacks in epoxy adhesives. Epoxy is a proven adhesive used in CFRP retrofitting works. In order to perform as an ideal adhesive for structural works, it should show a better resistance towards the fire. The lower T_g value of epoxy adhesive turns the adhesive to a viscous material soon. Eventually, the bond deteriorates causing a sudden failure. Apart from that the epoxy adhesives show a relatively high material cost [5] and the emission of toxic fumes during combustion [6]. Due to above-mentioned reasons, cementitious adhesives have suggested being used in external bonding. Minimum application temperature of epoxy adhesive is often around 10°C. Moreover, the hardening process of thermosetting adhesives is moisture and temperature-dependent [6]. Epoxy needs around 10^{0}C to start the exothermic hardening [6].

2.4 Research studies focused on developing new bonding system

The weaknesses in the performance of epoxy have motivated researchers to explore alternative bonding agents with improved thermal. However, the majority of them have not assessed in application or reached commercialization stages. Among those explored options, cementitious adhesives take a significant place due to its resistance to elevated temperatures and the consistency shown in between concrete and adhesive [5].

CFRP fabric has a greater surface area which helps cementitious adhesives to achieve better penetration. Therefore, it results in an increase in bond strength [6], [22]. Usually, the polymer-based adhesives have a higher bonding strength than the cement-based adhesives. The adhesive bonding capability can be assessed by different test configurations such as the single-lap shear and double lap shear tests [23]. Badanoiu and Holmgren [24] stated that the number of fibres in the tow directly influence the load carrying capacity of the cementitious carbon fibre composite. To reach the strengthening level of epoxy, a cementitious adhesive system requires double the amount of carbon fibre needed by epoxy [21]. Loading capacity can be increased if the cementitious adhesive penetrates into the carbon fibre tow [24]. This can be termed as the wettability of a cementitious adhesive. Wetting is the process where the adhesive is diffused to the substrate creating the bond [21]. Usually, a cementitious mix cannot be wetted individual strands in a bundle of carbon fibres like epoxy which is a fluid-like material. Therefore wettability is a major requirement of a good adhesive which accounts for the sound bond between fibre and the resin[21].

Surface preparation before applying a cementitious adhesive enhances the bonding ability. In external bonding of CFRP, shear stresses get concentrated [25]. As a result, CFRP gets debonded from concrete [25]. When developing a new adhesive, several properties need to be checked to assess its compatibility to the purpose. Setting time and flowability evaluates the suitability of the adhesive for practical applications. Apart from that mechanical properties like tensile, compressive and pull-off strengths are needed to be checked. Thermal performance of the developed adhesive is a major concern since the existing polymeric adhesives do not perform well under elevated temperature. Therefore the replacement should be a solution to overcome this issue. In most of the instances of developing a cementitious adhesive for CFRP, a polymeric material was included as a major component. However, those adhesives are affected by hydrothermal conditions [1]. It is also said that FRP-mortar systems are less effective in strengthening[26].

2.4.1 Cementitious adhesives developed by Hashemi and Al-Mahaidi [22]

Hashemi and Al-Mahaidi [22] tested 4 types of Cement-based adhesives as given in Table 2.1. Polymer modified mortar (OL) obstruct the release of moisture out of the concrete member [22]. This is due to the reduced permeability by the polymer [22]. The performance of silica fume incorporated mortar (OS) was better than the ordinary portland cement mortar (OC) and polymer modified mortar (OL) [22]. Experimental application of cement based-adhesive developed by Hashemi and Al-Mahaidi [22] for externally-bonded CFRP textile enhanced the ultimate capacity by 25%. Hashemi and Al-Mahaidi [23] stated that the addition of silica fumes to the cementitious adhesive is able to improve the bond strength.

Table 2.1 - Contents in the cement based adhesives[22]

Type	C[1] (kg)	MC[2] (kg)	CA[3] (kg)	FA[4] (kg)	W[5] (kg)	F[6] (kg)	SF[7] (kg)	SBR[8] (kg)	SP[9] (kg)
Concrete	306	-	1275	685	177	-	-	-	-
OC[10]	888	-	-	-	426	754.8	-	-	8.9
OS[11]	813	-	-	-	406	691	81.3	-	40.6
OL[12]	776	-	-	-	310	659	-	194	3.9
MS[13]	613	153	-	-	437	651.5	76.7	-	42.2

1. Ordinary Portland Cement
2. Micro-cement
3. Coarse aggregate
4. Fine aggregate
5. Water
6. Filler (Silica 200G)
7. Silica fume
8. SBR LATEX (Barra Emulsion 157)
9. Superplasticizer (Viscocrete5-500)
10. Cement-based mortar without any other additives
11. Silica fume incorporated mortar
12. Latex modified mortar
13. Micro-cement added to OS mortar

Hashemi and Al-Mahaidi further developed the cementitious adhesive [22] by mixing with MBrace primer and superplasticizer [27]. This approach has improved the viscosity of the adhesive and has enabled the ease of penetration of adhesive through fibres [27]. Higher viscosity it possesses is an essential requirement in order to use it as an adhesive for column confinement.

Table 2.2 shows the content ratios of the 4 types of cementitious adhesives developed by Hashemi and Al-Mahaidi [27]. Among them, Mortar M4 depicted a considerably better results when used as a bonding agent for Near Surface Mounted (NSM) CFRP textile. The interfacial bond failure between textile and concrete was observed with longitudinal cracks on cementitious adhesive[27].

Table 2.2 - Contents in the cementitious adhesive[27]

Mix type	Cement (g)	Micro cement (g)	Water (g)	Filler (Silica 2000) (g)	Silica fume (g)	Super plasticizer (g)	Primer (g)
Mortar M1	674.3	168.6	35.4	716.5	84.3	42.1	227.5
Mortar M2	674.3	168.6	35.4	716.5	84.3	33.7	151.2
Mortar M3	674.3	168.6	35.4	716.5	84.3	25.3	101.2
Mortar M4	674.3	168.6	35.4	716.5	84.3	16.9	88.6

2.4.2 Cementitious adhesive developed by Mohammed, Al-Saadi and Al-Mahaidi [28]

Mohammed, Al-Saadi and Al-Mahaidi [28] developed a High-strength self-compacting non-polymer cementitious adhesive (IHSSC-CA) using cementitious materials and graphene oxide. The smoothness in the surface of the adhesive prevents possible brittle failure in the concrete [28]. According to pore structure analysis results, it was observed that this developed adhesive effectively maintains the composite behaviour between concrete and CFRP [28] which result in a higher load-carrying capacity. Three-dimensional (3D) laser profilometery showed that the use of IHSSC-CA as the adhesive has increased the roughness on CFRP surface [28]. Meanwhile, a low relative deformation on the CFRP surface was also noticed [28].

2.4.3 Cementitious adhesive developed using Graphene oxide

Graphene oxide is a nanomaterial. Researchers have highlighted the advantages of Graphene oxide (GO) over other cement-based materials [29], [30]. Adhesive mixture developed by Mohammed et al. [31] incorporating GO in cementitious adhesive showed a pot life of 120 min with a 7.5% flow. The tensile strength is 13.8 N/mm^2

while the compressive strength is 101 N/mm^2. Pull-off strength was observed as 1.2 N/mm^2.

Cement-based adhesive with GO (GM) has slightly higher initial and final setting times than control mix without GO (CM) [31]. A higher amount of plasticizer increased the setting time. The surrounding environment also affects the setting time of cementitious adhesive. Hence, superplasticizer content needs to be reduced in a wet environment. Compared to CM, GM showed an increment in tensile strength up to 45% [31]. Enhancement of compressive strength in GM compared to CM is around 13.5% [31]. Mohammed et al. [31] stated that the strength enhancement was achieved as a result of pore structure modification which occurs due to the addition of GO. Failure patterns of CM and GM indicated that GM can arrest and restrict crack propagation while GO has the ability to arrest crack propagation [29]. Presence of nanomaterial increases the tensile strength by delaying crack initiation [32].

2.4.4 Magnesium Phosphate Cement (MPC) as a cementitious adhesive

Advantages of MPC over ordinary portland cement are high bond strength, rapid hardening and good permeability [33]. MPC is a stable material at higher temperatures compared to Portland cement [34]. These mortars release ammonia during both formation and even after. Therefore potassium dihydrogen phosphate was used in this study instead of ammonium dihydrogen phosphate in preparing the cement mix. However, at elevated temperature, the MPC stability differs with the material used in formation [34]. Effective binding coefficient of epoxy resin is lesser than that of MPC [35].

Chang et al. [36] conducted experiments on using MPC as the bonding agent for CFRP fabric in retrofitting corroded reinforced concrete columns. Magnesium oxide with a density of 3460 kg/m^3, borax retarder with a purity of 99.5% and industrial-grade KH_2PO_4 with a purity of 98% was used in the preparation of MPC [36]. The compressive strength of cementitious adhesive reached 42 N/mm^2 at the end of 7 days of curing and 28 days strength is 53 N/mm^2. Experimental results showed that the bonding of CFRP using MPC is an effective method to enhance the ultimate displacement and ultimate bearing capacity of corroded reinforced concrete columns[36]. Moreover, Chang et al. [36] concluded that the compressive strength of reinforced concrete columns which are fully wrapped with CFRP fabric is greater than that of discontinuously wrapped columns.

Li et al. [34] conducted experiments on several mix proportions of MPC to identify the most suitable mix proportion (Table 2.3). The colour of all the specimens had become lighter at 500 ^{0}C. When the temperature was increased up to 1000 ^{0}C, cracks have started appearing. Li et al. [34] stated that the cracks increased with the increase of fly ash content. Volume deformation of MPCs with quartz sand became more pronounced with the increase of quartz sand content [34]. The residual compressive strength of MPC specimens with fly ash under elevated temperature decreased with the increase of fly ash content [34] (Table 2.4). MPC with 40% of fly ash content showed the highest strength [34] (Table 2.4).

Table 2.3 - Mixing proportions of MPCs [34]

Mixes	P/M	Retarder %	Fly ash %	Sand ratio
C	1/4	5	0	0
F_1	1/4	5	10	0
F_2	1/4	5	20	0
F_3	1/4	5	40	0
S_1	1/4	5	0	1/0.5
S_2	1/4	5	0	1/1.0
S_3	1/4	5	0	1/1.5

Table 2.4 - Initial and residual compressive strengths [34]

Mix	Control strength 20 ^{0}C (N/mm^2)	Residual strength					
		130 ^{0}C		500 ^{0}C		1000 ^{0}C	
		(N/mm^2)	(%)	(N/mm^2)	(%)	(N/mm^2)	(%)
C	72.4	44.6	61.6	27.4	37.8	24.6	34.0
F_1	73.3	42.8	58.4	24.6	33.5	20.8	28.4
F_2	74.8	40.9	54.5	23.3	31.1	19.8	26.5
F_3	76.7	37.2	48.5	22.6	29.5	18.8	24.5
S_1	68.7	32.7	47.5	18.4	26.8	13.5	19.6
S_2	66.2	31.1	47.0	17.2	26.0	11.3	17.1
S_3	65.2	30.5	46.7	16.4	25.1	10.6	16.2

Li and Chen [33] analyzed the factors which influence on the properties of MPC. They identified casting temperature and w/c ratio as the key factors which affect on the setting time of MPC. The increase of w/c ratio was proportional to the setting time while inversely proportional to the compressive strength gain [33]. For a constant w/c ratio, setting time increased by increasing casting temperature [33]. MPC shows a higher early strength. It reaches 70% of its 28 days compressive strength within 3 hours. Calcium fly ash can improve the properties of MPC and while reducing the cost [33].

2.4.5 Engineered Cementitious Composite as an adhesive

In this bonding system, CFRP composite is embedded inside the Engineered Cementitious Composite (ECC) matrix. The composite is engineered to behave in a ductile manner under tensile and flexural loading[37]. ECC is developed by mixing cement, silica sand, water, fly ash and fibres. The polymeric fibres are usually used as the fibre type in preparation of ECC. The ECC shows a strain capacity which ranges in between 3% - 7%, whereas the OPC shows only 0.1% of strain capacity[38]. Thus, ECC shows ductile behaviour. This is basically because of the fibres which tend to create micro-cracks within the mortar mix. Even though other cementitious adhesives perform well under elevated temperature, it shows low ductility. This creates a negative effect on the load transferring from the concrete substrate to CFRP [39], [40]. ECC achieves the desired ductility by microcracking in strain hardening stage [41] with a micro-crack width less than 100 mm [42].

A lot of research has been carried out so far using Poly Vinyl Alcohol (PVA) as the fibre in ECC [26], [40], [43]–[49]. Melting of Poly Vinyl Alcohol (PVA) fibres in ECC resists spalling failure up to 800 ^{0}C [45]. ECC cementitious adhesive developed by Wu and Li [26] achieved a compressive strength of 45.7 N/mm^2 and tensile strength of 3.5 N/mm^2 under room temperature. Average compressive strength ECC developed by Wu and Li [40] was 50.9 N/mm^2 while it is noted as 52.6 N/mm^2 for ECC mortar without PVA fibre. Pull out stress is proportional to the CFRP embedded length [40]. For 170 mm embedded length, the bond stress reached 174.2 N/mm^2. The average tensile strain capacity of ECC is 2.8% that is 252 times higher than that of the cement mortar [40].

The cubes were cast for ECC as per ASTM C190/C190M [50] to conduct the compressive strength test. Dog bone shaped specimens were used to determine the tensile strength as per the recommendation of the Japan Society of Civil Engineers (JSCE) [51].

2.4.5.1 The behaviour of fly ash in ECC

Fly ash is a waste material disposed from the coal power generation. Fly ash contributes to reduce both free drying shrinkage and crack width in ECC [46]. According to micromechanics analysis, this tight crack width is caused by the increase of fibre-binder interface frictional bond. As per the findings of Yang et al. [46], the higher fly ash content in ECC reduces its compressive strength and increases its tensile ductility.

2.4.5.2 Influence of different types of fibres in ECC

Length to the diameter of a fibre is defined as its aspect ratio. The pullout resistance of fibres out of the matrix increases with the increase of aspect ratio [38]. Katz, Li, and Kazmer [52] developed different cement matrices deviating silica fume content and ratio between water and binder (w/b) to analyze the effect on interfacial bond properties of the fibres. Mortar mix without silica fumes and with a higher w/b showed a bond strength of 0.5 N/mm^2 between fibres and cement matrix when carbon fibres of 10 μm were used. However, the bond strength was improved by 50%-100% by lowering the w/b or by adding silica fumes as it densifies the matrix. The fibre-cement matrix interaction behaviour is determined by the fibre pull out test [37].

Fibres in ECC involves in enhancing the tensile behaviour of the mortar mix. The most prominently used fibres are polymer fibres like PVA, Polyethylene terephthalate (PET), Polyethylene (PE) and Polypropylene (PP). PVA fibres are the generally used fibre type in ECC due to the better bonding they showed with the cement mix [38]. Sathishkumar et al. [38] conducted tests on ECC developed using different fibre types to determine the mechanical properties. By analyzing the results they concluded that

PVA fibres perform well for ECC compared to PET, PE and PP fibres (Figure 2.1). Further, they tested ECC by changing the fibre percentage in the mix. For all the fibre types, 2% fibre content showed the highest tensile strength, compressive strength and flexural strength values [38]. However, PVA fibres are not locally produced in Sri Lanka.

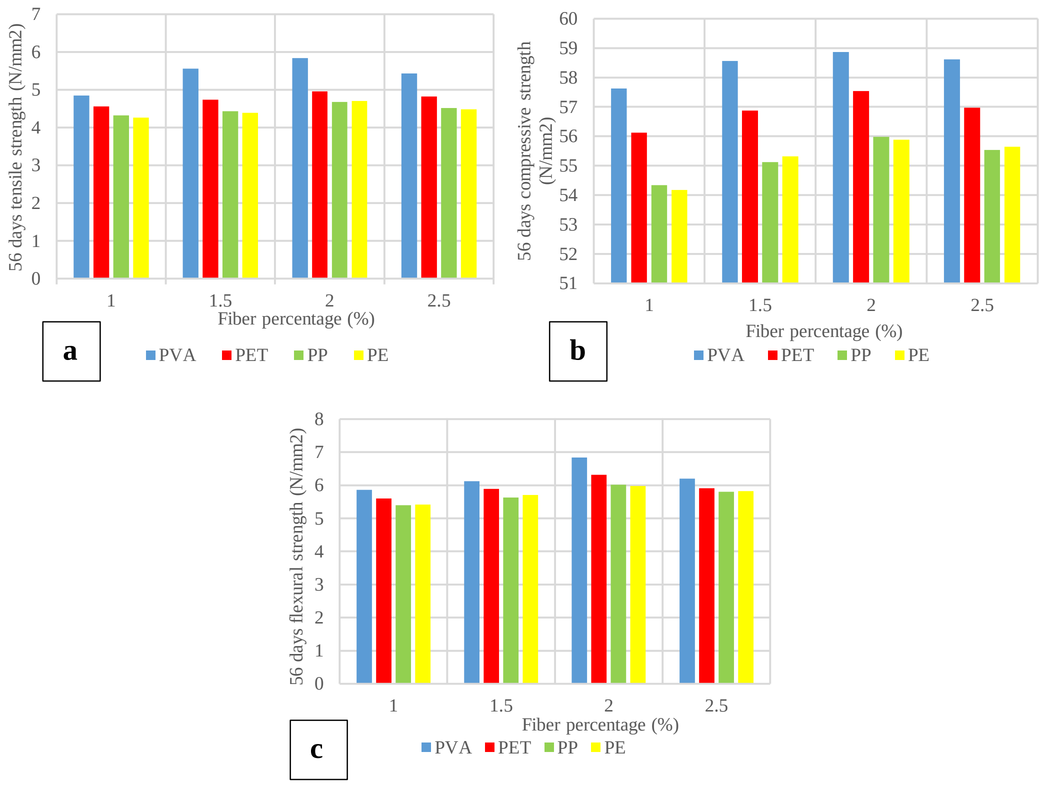

Figure 2.1. (a) Tensile strength variation of ECC prepared with different fibres [38] (b) Compressive strength variation of ECC prepared with different fibres [38] (c) Flexural strength variation of ECC prepared with different fibres [38]

When PVA fibre is used, approximately 75% of the cost for preparing ECC is spent on the fibres [53]. When equal volumes are concerned, the cost of PE fibres is 8 times the cost of PVA fibres [54]. Therefore the use of PVA fibres and PE fibres in developing ECC is not economically feasible. PET solid waste is a serious environmental issue. Therefore to minimize the disposal of PET to the environment, the use of recycled PET fibres in the process of preparation of ECC is a sustainable approach. However, the wettability of PET fibres in the cement matrix is low since PET fibres exhibit a limited chemical reactivity and lower surface energy [55].

2.4.5.3 Thermal performance of ECC

Wu and Li [26] investigated the thermo-mechanical behaviour of ECC as a cementitious adhesive for bonding CFRP. Up to 500 ^{0}C, ECC showed anti-spalling behaviour [26]. Table 2.5 shows the mix proportions of developed ECC adhesive. Both cubes and dogbone shaped specimens were cast to determine the variation occur in the compressive strength and tensile strength respectively once it is exposed to the elevated temperature.

Table 2.5 - Mix proportion of ECC developed (All the quantities are in kg/m^3) [26], [40]

Water (W)	Cement (C)	Fly ash (FA)	Silica sand	PVA fibres	Water reducer	W/(C+FA)	FA/C
311	393	865	457	26	5	0.25	2.20

The compressive and tensile strengths were measured at each 100 ^{0}C intervals up to 500 ^{0}C. When the samples reached the targeted temperature, they were left to remain in the same temperature for 1 hour and then it was taken out and left to cool down to room temperature before performing the test [26]. When exposed to elevated temperature, the compressive strength started to drop at 300 ^{0}C and tensile strength started to drop at 200 ^{0}C as shown in Figure 2.2 (a) and Figure 2.2 (b), respectively. Up to 200 ^{0}C, multi cracking and strain hardening behaviour were observed.

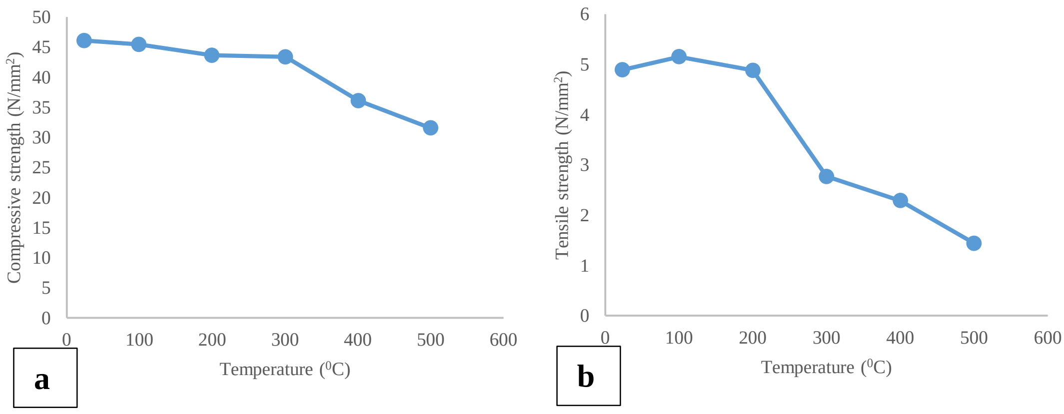

Figure 2.2. (a) Compressive strength variation under elevated temperature[26] (b) Tensile strength variation under elevated temperature[26]

The surface bond between ECC adhesive and concrete is sensitive to elevated temperature [26]. Hence the concern has to be given on enhancing the bond between ECC and concrete substrates. Exposure to elevated temperatures melts down the PVA fibres within the ECC specimens and interconnected channels started to create within ECC mortar as shown in Figure 2.3. These channels let water vapour to escape and minimize the internal pressure which helps in reducing the internal crack formation [26].

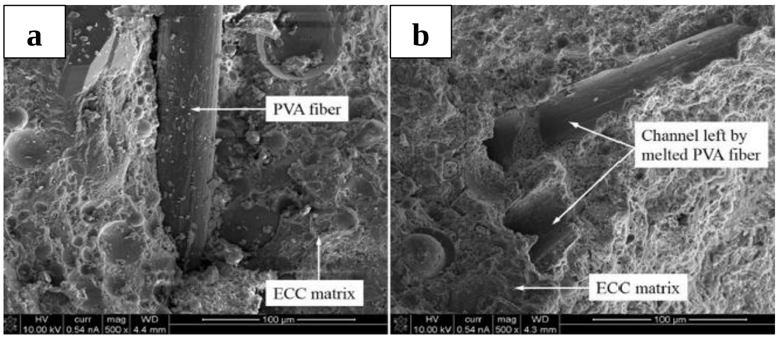

Figure 2.3. SEM images of ECC at (a) room temperature (b) 500 ^{0}C [26]

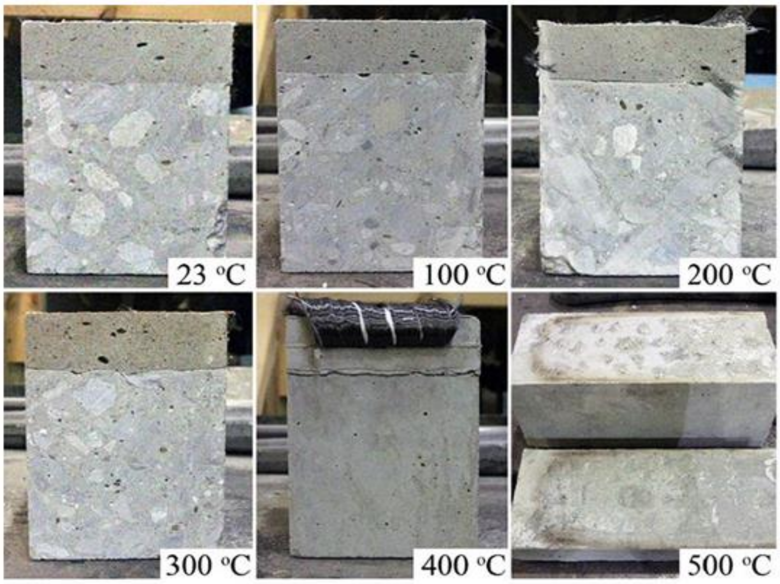

Figure 2.4. ECC-Concrete substrate bond at different temperatures[26]

Wu and Li [26] performed the direct pull-out test on the adhesive system to determine its bonding capability. Figure 2.4 shows the appearance of CFRP bonded samples when exposed to elevated temperature. At 200 ^{0}C, small cracks have emerged and after 300 ^{0}C, cracks emerged in the interface between ECC and concrete. The CFRP sheet got debonded when interface reached 200 ^{0}C and at temperatures higher than that, interface separation took place in between ECC and concrete substrate (Figure 2.5 (a)). Wu and Li [40] performed a series of direct pull-out tests to determine the effective bond length for CFRP-ECC strengthening system and it was observed that the ultimate pullout strength is directly proportional to the CFRP embedded length (Figure 2.5 (b)).

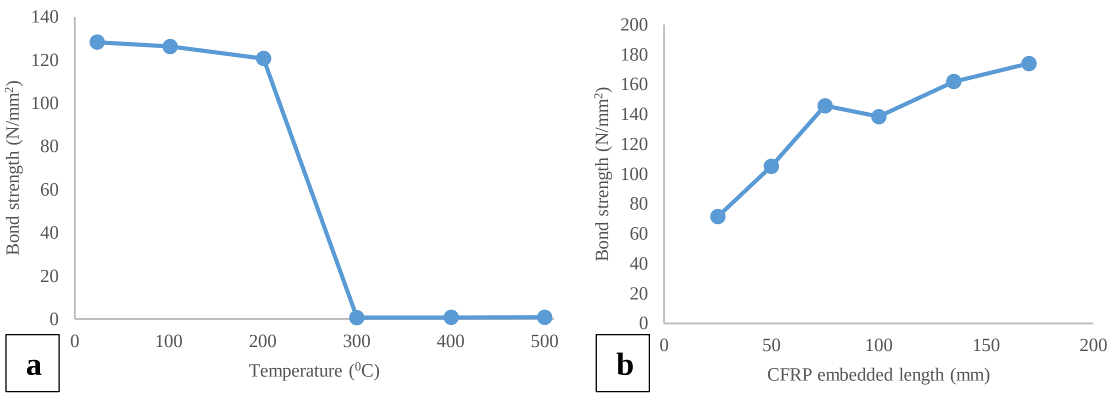

Figure 2.5. (a) Bond strength variation under elevated temperature[26] (b) Bond strength variation under different CFRP embedded lengths[40]

2.5 The research found on modifying the existing bond

The epoxy adhesives are thermoset resins which prevail in a liquid state at room temperature when it is uncured. During the curing process, resin molecules create strong bonds within each other and turn in to a solid-state. After the curing process epoxy adhesive becomes a brittle material. The epoxy adhesive performs well as an adhesive for fibre composites in ambient temperature conditions. But under elevated temperature conditions, its performance is very low, since it generally has a low T_g. To overcome these kinds of weak performances in epoxies, they are modified with various additives and fillers [7]. These modifications are done in different ways such as using curing agents, modifying using thermoplastic polymers, blending chopped fibres [7]. Plasticization and rubber toughening are two other prominent ways of modifying epoxy. Both are chemical procedures. In general practice, fire retardant epoxies are produced by introducing fire retardant additives to them [7].

As a sustainable approach, researchers have investigated the use of natural fibres over synthetic fibres to modify epoxy resin. Depending on the aspect ratio of natural fibres, they can be utilized in different ways; as a filler, as randomly dispersed short fibres and as continuously laid fibres [7]. Natural fibres have a lower thermal conductivity. Researchers have investigated the effect of natural fibres on the mechanical and thermal properties of natural fibre polypropylene composite [56]. But the blend of natural fibres has lowered T_g of the composite [56]. The T_g of a composite is governed by several factors. Tajvidi et al. [56] stated that in this case, the factors which lower the glass transition might have dominated over the factors which enhance it. Pujari et al. [12] investigated the thermal conductivity of natural fibre blended epoxy composite. As per the results, the thermal conductivity of composite decreased with the increase of fibre content [12]. This is because of the non-conductive property of natural fibres [12].

Manjunath et al. [13] modified epoxy using fibre reinforcement to investigate in performance as a structural material. They used PET fibres in the experiment and tested on mechanical properties of the composite. With the addition of PET fibres, epoxy showed a ductile nature during failure [13]. Further, this modification incremented the glass transition temperature [13].

2.6 Adhesives used in aerospace engineering structures

Retrofitting structures using FRP composites is more economical than replacing it. Therefore, it is a common practice in the aerospace industry [57]. The concern is given regarding the long term durability of joints repaired with composites [57]. If an adhesive withstands a stress of 6.9 N/mm^2 in a lap shear coupon test it is said to be a structural adhesive [58]. In the aerospace industry, the structural adhesives are used either in adhering two composites or composites to metal. They are also being used as a shim material.

Adhesives for aerospace engineering structures can be either a paste or a film mainly. The adhesive films are ideal for composites with low resin content and high fibre content [58]. The structural adhesives based on Polyimide and Bismaleimide (BMI) can also be processed at elevated temperatures[58].

Generally, the adhesives used in aerospace applications get exposed to a greater range of temperatures (-55 ^{0}C – 200 ^{0}C) [57]. Epoxies, phenolics, silicones, polyimides and ceramics are few adhesives which resist high temperatures [59]. Tensile strength variation of different adhesives along with the exposed temperature is given in Figure 2.6 [57], [60]–[66]. In Figure 2.6, tensile strength values of all the adhesives are normalized with respect to the temperature 22^{0}C. Therefore, it can be clearly understood that the tensile strength of adhesives gets reduced with the increase of exposed temperature [57].

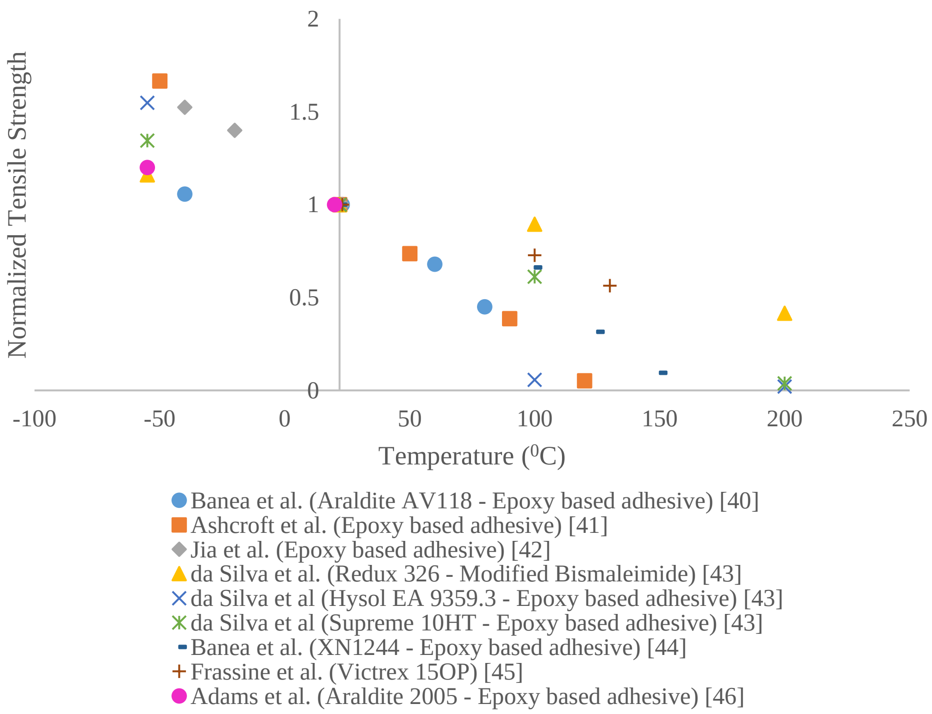

Figure 2.6. Temperature-dependent tensile strength properties of structural adhesives [57]

The strength of the adhesive depends on T_g [65], [66] and T_g usually depends on the curing temperature of the adhesive [65], [66]. T_g can be incremented by curing the adhesive at a higher temperature for a short time. However, this causes the formation of voids in the adhesive layer which directly affects the bond strength[67]. Therefore, Cebrain et al. [68] suggested the dual step curing process. It is a dual step process at which the samples are cured in a specific lower temperature for a certain time and then cured in a higher temperature in the second stage. Thus, it comparatively lowers the void formation in the adhesive layer. Cytec Solvay Group [69], Henkel Adhesive Technologies[70], Hexcel [71], Permabond Engineering Adhesives Ltd. [72] and Renegade Materials Corporation [73] are few prominent companies which produce aerospace adhesives. These are with the capability to resist high temperature and resist several other harsh environmental conditions.

2.7 Further Research needed

Poor thermal performance of epoxy adhesive has encouraged the researchers to explore more on developing a new adhesive for the CFRP-concrete bond. The thermal resistivity in cementitious mortar led the researchers to focus more on developing a cementitious adhesive to replace epoxy. The most common issue examined in developed cementitious adhesives is the lack of bond strength. This issue has to be addressed differently since the cementitious adhesives do not wet the CFRP fabric properly similar to epoxy adhesives. Therefore the bond between cementitious adhesive and CFRP is usually low. The cementitious adhesive-CFRP bond can be strengthened by incrementing the surface free energy. The simplest way is to abrade the bonding surface. However, if the abrading is done on composite, the concern should be given to avoid possible damaging on fibres. Apart from that, the attention needs to be focused on developing new techniques to create friction on fibre composite with other means.

Generally, the cementitious adhesive-concrete bond is enhanced by shearing away the top layer of concrete which create the broken atomic bonds. This improves the chemical bond between cementitious adhesive and concrete. However, this attempt is usually not enough to attend the bond strength issue. The cementitious adhesives are usually brittle in nature. Therefore, issues arose when transferring load from concrete to cementitious adhesive. Thus, a priority needs to be given upon avoiding cementitious adhesive-concrete bond interface failure.

Limited researches have been focused on enhancing the thermal performance of epoxy by blending it with fibres. However, the enhancement of both the bond strength and the thermal performance of epoxy adhesive by blending fibres have not been investigated by researchers. Manjunath et al. [13] have concluded that the addition of PET fibres to epoxy increased the ductile nature of composite. This ductile nature could further improve the load transfer in the CFRP-concrete bond. Therefore, investigations can be made on how this modification influence on the bonding ability. Use of recycled polymeric fibres in this modification purpose can be considered as a sustainable approach.

3 MATERIAL CHARACTERISTICS AND TESTING METHODOLOGIES

3.1 Introduction

Part of Chapter 3 focuses on materials used in the experiment and their properties. Other parts of the chapter describe the details of the major experiments conducted in the research. Within this chapter, the general procedure of the experiment is discussed.

3.2 Collection of raw materials

Objectives of this research comprise of two parallel driven test series. The first objective is to develop a cementitious adhesive as a substitute for epoxy adhesive. The selected cementitious adhesive to develop using the locally available materials is ECC. Materials used to develop ECC adhesive are Portland cement, silica sand, fly ash, water and Polyethylene Terephthalate (PET) fibres (Figure 3.1). Silica sand was obtained from Piramal Glass Ceylon PLC located in Naththandiya, Sri Lanka (Figure 3.2). Fly ash was obtained from the Norochcholi power plant located in Sri Lanka (Figure 3.2). BPPL Holdings PLC, Horana, Sri Lanka provided the required PET fibres (Figure 3.2).

Figure 3.1 – Materials used to develop ECC adhesive, (a) Portland cement (b) Fly ash (c) Silica sand (d) Water (e) PET fibers

In this test series where the epoxy adhesive is modified using fibres, the PET fibres were being used. The unidirectional normal modulus CFRP fabrics were used in the testing work (Figure 3.3 (a)) and two-part epoxy adhesive was used for sticking CFRP fabric as shown in Figure (Figure 3.3 (b) and (c)).

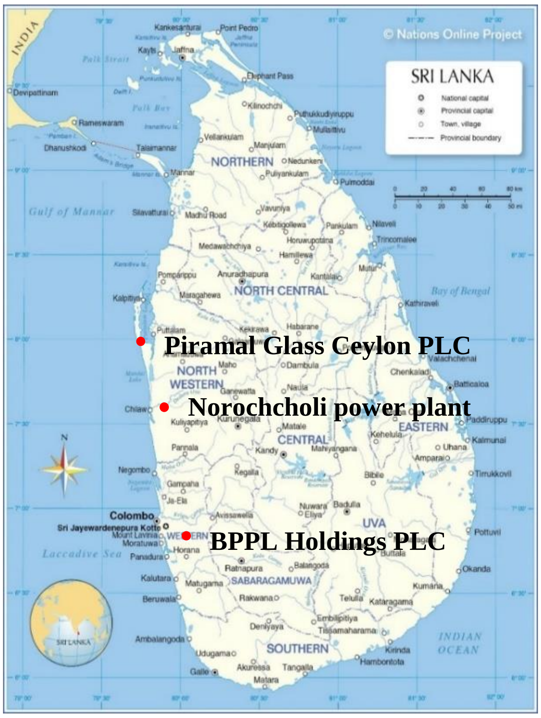

Figure 3.2 – Material collected locations[74]

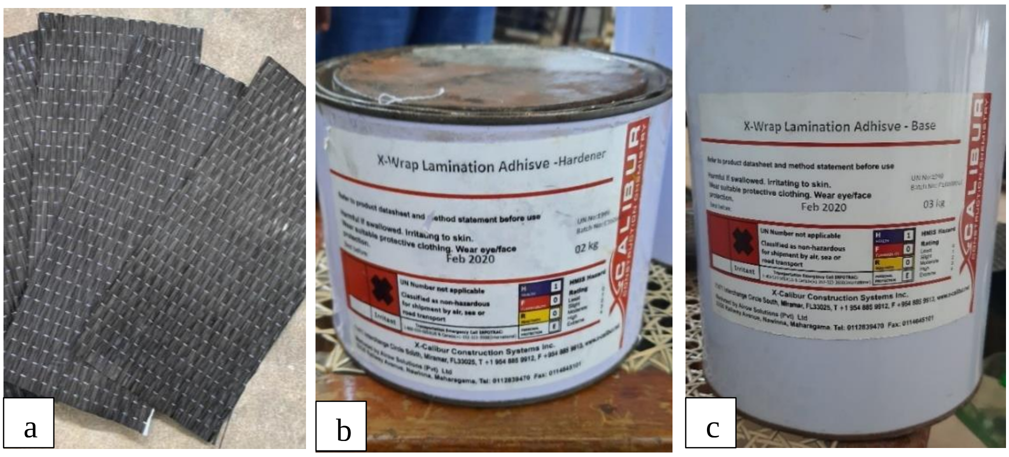

Figure 3.3 - (a) CFRP fabric (b) Epoxy adhesive-Hardener (c) Epoxy adhesive-Base

3.3 Material properties

Chemical analysis for fly ash was done at Geological Survey and Mines Bureau of Sri Lanka. The chemical composition results are given in Table 3.1. But the chemical composition of fly ash drastically differs depending on the source from where it is obtained. This can be seen when comparing with the chemical composition of fly ash used by Wu and Li [40] to develop ECC as an adhesive. Properties of PET fibres are mentioned in Table 3.2. The thickness of a PET fibre was measured using a micrometre screw gauge. The manufacturer provided properties for CFRP fabric is given under Table 3.3[75]. The manufacturer provided properties for the epoxy adhesive is given under Table 3.4 [76].

Table 3.1 – Chemical composition of fly ash

Component	Norochcholai power plant, Sri Lanka	DTE Monroe Power Plant, State of Michigan, USA[40]
SiO_2 (%)	46.89	42.20
Al_2O_3 (%)	30.69	22.51
MgO (%)	1.56	3.20
CaO (%)	7.56	15.66
Na_2O (%)	0.23	0.98
K_2O (%)	0.64	1.53
P_2O_5 (%)	2.67	-
Fe_2O_3 (%)	1.88	9.20
SO_3	-	1.85
Loss on ignition	5.59	1.34

The fly ash obtained from Norochcholai power plant can be categorized as class F type according to ASTM C618-19 [77]. The content of CaO in fly ash is a key factor which influences the behaviour of mortar. The CaO content in Norochcholai plant is below 10%. Therefore this fly ash mainly shows the pozzolanic characteristics [78]. The pozzolanic materials need the presence of $Ca(OH)_2$ for the formation of solid matter [78]. Therefore water requirement might be high in cement blended with this kind of fly ash for the hydration process. Increase of SiO_2 and Al_2O_3 accelerate the setting time of mortar [79]. Fly ash with low CaO shows a lower early strength [78]. High fly ash content in a mortar paste increases its tensile ductility while reducing the compressive strength [46].

Table 3.2 – Properties of PET fibre

Nominal strength (N/mm^2)	Modulus (GPa)	Density (kg/m^3)	Melting point (^0C)	Average fibre thickness (mm)	Average fibre length (mm)
1700 [80]	50 [80]	1410 [80]	265 [80]	0.4	10

PET fibres were used as the fibre component in developing the ECC adhesive. These fibres provide the required ductility for the brittle mortar by performing as a reinforcement. Thus, the randomly dispersed fibres increase the tensile strength of ECC adhesive. In the modification of epoxy adhesive, PET fibres were used as a reinforcement within the epoxy resin. It is expected to retard the sudden loss of strength in the epoxy adhesive.

Table 3.3 – Manufacturer-provided properties of CFRP fabric [75]

Parameter	Value
Sheet weight	300 g/m^3
Carbon content	95%
Net effective thickness	0.166 mm
Modulus of elasticity	240 GPa
Tensile strength	4000 N/mm2
Elongation at break	2%

Table 3.4 - Manufacturer-provided properties of epoxy adhesive [76]

Parameter	Value
Pot life	40 mins at 25 ^0C
Tensile strength at 7 days	45 N/mm^2 at 20 ^0C
Flexural strength at 7 days	60 N/mm^2 at 20 ^0C
Compressive strength at 7 days	1.67 GPa at 20 ^0C
Glass transition temperature	65 ^0C
Viscosity	5000 cps at 20 ^0C

3.4 Thermal conductivity test

Thermal conductivity is the property which indicates the ability of a material to conduct heat [81]. The temperature gradient in the sample results in conduction [81]. Lee's disc method which was used here is commonly used to determine the thermal conductivity of bad heat conductors [81]. Figure 3.4 shows Lee's disc apparatus. The circular samples with a diameter of 60 mm and a thickness of 5 mm were cast to test for the thermal conductivity of developed cementitious adhesive (Figure 3.5). For each category, 3 circular samples were cast for the thermal conductivity test as per mentioned in the test procedure [82].

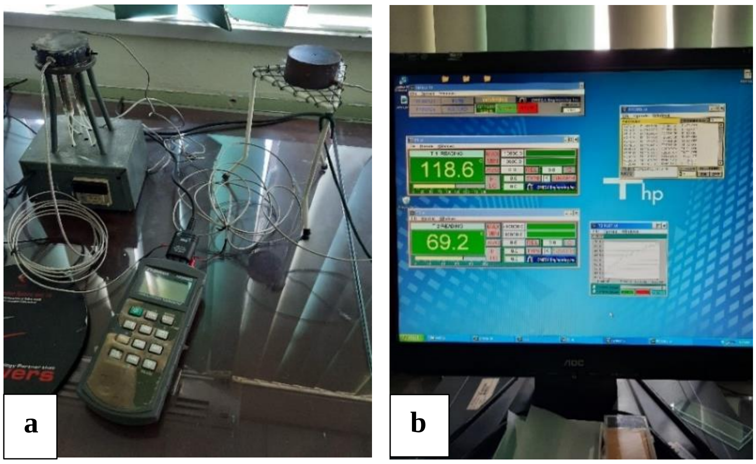

Figure 3.4 – (a) Lee's disc apparatus (b) Software used to record data from Lee's disc apparatus

Prepared samples were demoulded after 1 day of curing and then the samples were kept for curing in a water bath for 27 days. Then they were dried for a day in the air (26 ± 3 ^{0}C; 74 ± 5%) prior to being used in the thermal conductivity test.

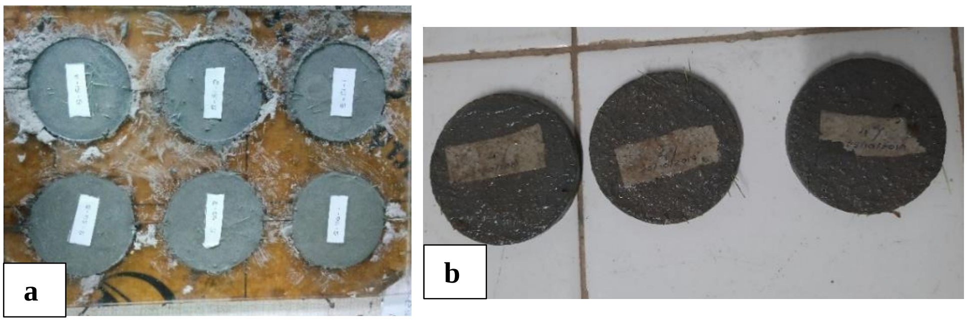

Figure 3.5 – (a) Casting samples in the mould (b) Casted samples

In order to obtain a smooth surface for the samples, a silicone heat sink compound was applied on both sides of the sample. During the test, the sample was kept in between 2 copper discs and heat conducted through the sample since a temperature gradient is created between 2 copper discs (Figure 3.6). The test was conducted in accordance with ASTM D7340 - 07(2018) [82]. Heating curve and the cooling curve for the sample were recorded. To calculate the thermal conductivity, Fourier's Law on conductive heat transfer (Equation 3.1) and Specific heat capacity equations (Equation 3.2) was used.

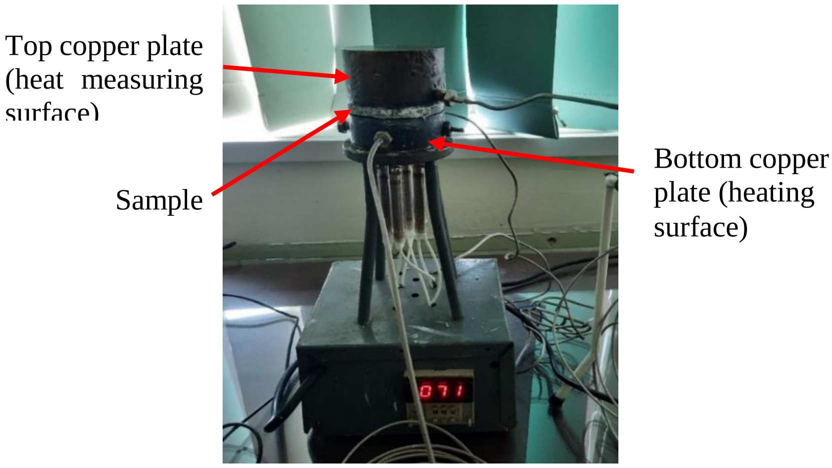

Figure 3.6 – Mounting the sample in the apparatus

$$H = kA\frac{(T_2 - T_1)}{x} \quad \text{Eq. (3.1)}$$

Where H is for the steady-state rate of heat transfer,

k is for the thermal conductivity of the sample,

A is the cross-sectional area of the sample,

x is the sample thickness,

(T_2-T_1) defines the temperature raise.

$$H = mc\frac{dT}{dt} \quad \text{Eq.(3.2)}$$

Here, m is the mass of the lower copper disc,

c is the specific heat of copper,

(dT/dt) is the heat radiated per second.

3.5 Direct pull out test

The direct pull out test was conducted to determine the bond strength of an adhered sample. Figure 3.7 presents the schematic diagram of the experimental setup which was fabricated to conduct pull out test using the Universal Testing Machine. Grade 30 concrete blocks with the dimensions of 100 mm x 100 mm x 250 mm were used to bond CFRP fabric using the adhesive. First, these concrete blocks were cast and demoulded after a day and kept for curing in a water bath for 27 days. Then the bonding surface of the concrete block was grinded. Dust on the grinded surface was wiped out using a wet cloth and blocks were dried under room temperature. Next, the CFRP fabric was bonded to the grinded surface using the adhesive. CFRP fabric was cut into 75 mm wide strips before adhering it and the strip was laid in a way such that it maintains a 100 mm long part of the strip outside the bonding region to fix the grip to pull out the CFRP strip during testing. The grip was fabricated by fixing 2 aluminium sheets, each with the dimension of 75 mm x 100 mm on either side of the CFRP fabric strip part left for the grip, using epoxy adhesive. The prepared samples were demoulded after 1 day and curing was done for 7 days under air (26 ± 3 ^{0}C; 74 ± 5%).

All the bolts shown in Figure 3.7 are 10 mm diameter bolts. The long vertical bolt restrained the 70 x 50 x 6 mm^3 angle movement in the vertical direction. This 70 x 50 x 6 mm^3 angle restrained the vertical movement of the concrete block. Horizontal bolts fastened to the 70 x 50 x 6 mm^3 angle avoided the block from overturning when the CFRP fabric was pulled. The 50 x 50 x 6 mm^3 angle at the bottom of the setup avoided the horizontal movement and overturn of the block. The 50 x 50 x 6 mm^3 angle was kept restrained to the block using the two horizontal bolts fastened between 300 x 175 x 10 mm^3 mild steel plate and the angle. Therefore, setup restrained all the movements of the concrete block letting only the CFRP fabric to be pulled. The setup was fixed to the bottom clamp using the bottom grip.

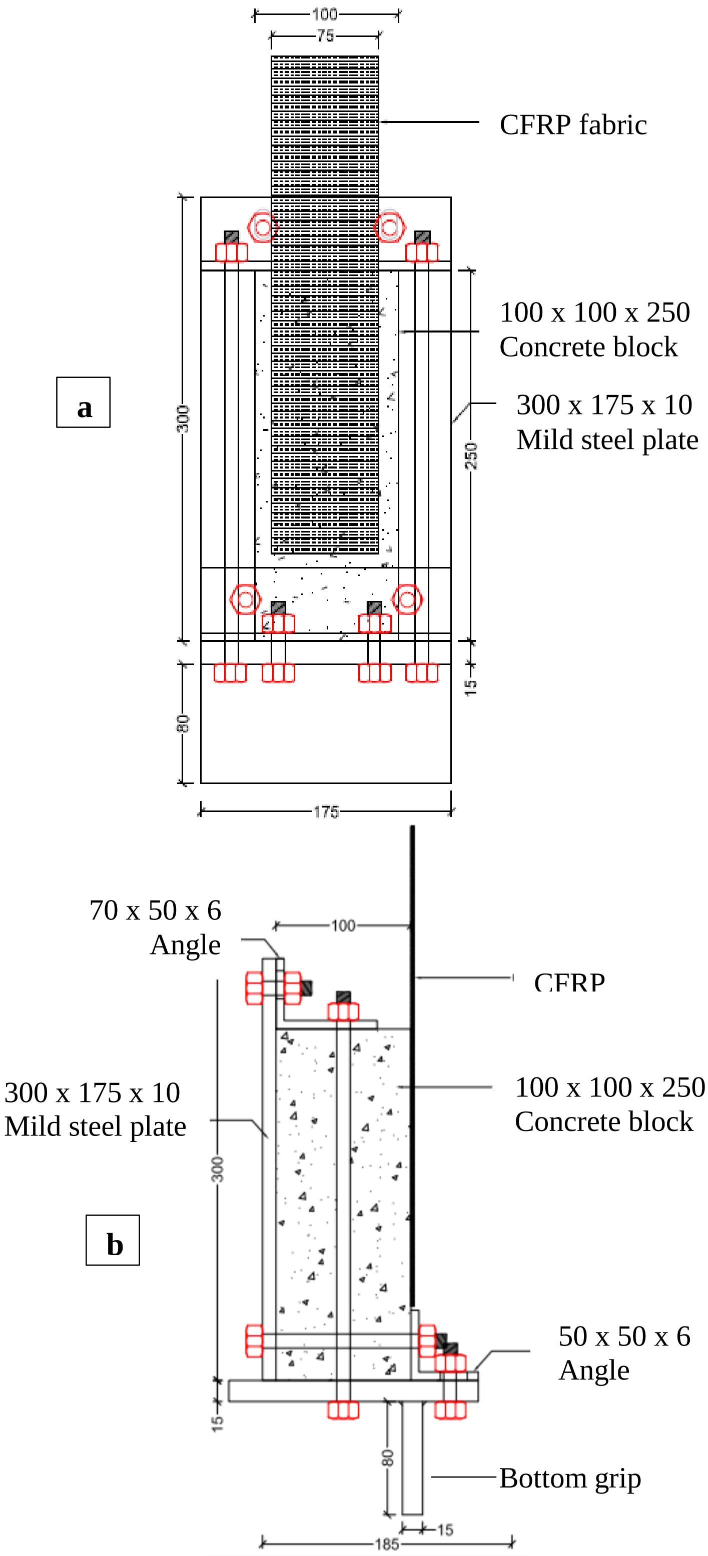

Note: All dimensions are in millimeters

Figure 3.7 – Schematic diagram of setup used to mount pull out test samples (a) Front view (b) Side view

Sample preparation for the cementitious adhesive is shown in Figure 3.8. Figure 3.9 shows the test setup mounted on the Universal Testing Machine for testing.

Figure 3.8 – Preparing samples for direct pull out test

Figure 3.9 – Testing samples in Universal Testing Machine

3.6 Chapter summary

Under this chapter, the properties of the materials used in the experiment are highlighted. Manufacturer-provided material properties of CFRP fabric and epoxy adhesive are included. The chemical composition of fly ash was tested to analyze the behaviour of fly ash in a mortar. Both manufacturer-provided material properties and properties obtained by conducting tests on materials are included. A section in the chapter describes the procedure of conducting the thermal conductivity test. Lee's disc method was identified as an effective method for measuring the thermal conductivity of materials. The procedure of sample preparation and testing are included. Further description is given on the calculation of thermal conductivity using the obtained readings. Another section in the chapter gives a comprehensive detailing on the procedure followed to conduct the direct pull-out test which is repeatedly used in the experiments. The direct pull out test is one of the popular methods which can be used to measure the bond between a substrate and adhesive. The sample configurations, test setup and procedure for direct pull out test are also included in this chapter.

4 DEVELOPMENT OF EPOXY ADHESIVE FOR ELEVATED TEMPERATURE PERFORMANCE (PETCO-EPOXY)

4.1 Introduction

Chapter 4 presents the overall details of epoxy adhesive modification using PET fibre and analysis on its performance. Use of fibres can enhance the tensile strength of epoxy. Moreover, it can function as reinforcement inside epoxy adhesive avoiding a brittle failure in the adhesive layer. Amount of fibres used in modifying epoxy is a crucial factor in the modification process. Therefore, it is the preliminary check done in the development stage of this study. Thereafter experiments were carried out analyzing its performance under different aspects. After developing the adhesive, the next step is to analyze its performance under elevated temperature. Therefore, the direct pull out test was carried out once again for the developed adhesive systems, while exposing the setup into elevated temperature.

4.2 Preparation of the fibre modified epoxy adhesive

A two-part epoxy adhesive was used for this [76]. In order to prepare the epoxy adhesive, one part of hardener was mixed with two parts of the base. Then it was mixed thoroughly for about 2 to 3 minutes to obtain a homogenous mix. PET fibres used to modify the adhesive was cut into 10 mm long fibres. The fibre diameter is 0.4 mm. Since the fibres have a considerable diameter it was hard to cut it in to smaller strands. However, to maintain a uniform dispersion, long strands of PET fibres were cut in to 10 mm long pieces. These fibres were mixed with the prepared adhesive mix for about another 2 to 3 minutes until the fibres get homogeneously dispersed in the adhesive. Since the pot life of epoxy adhesive under 20 ^{0}C is 40 minutes, the application process needs to be done quickly and the amount of adhesive prepared at a time should be an amount which could be applied within the specified pot life.

4.3 Selection of optimum fibre content

4.3.1 Optimum fibre content under ambient temperature

To determine the optimum fibre content for the modified epoxy adhesive, pull out test was performed as explained in Chapter 3.5. After the fabrication of the samples, they were kept 28 days for curing prior to the testing (Figure 4.1 (a)). Samples were pulled at a rate of 1 mm/min as shown in Figure 4.1 (b) till the failure. Depending on the bond strength acquired by each sample, optimum fibre content which was needed to develop the adhesive could be decided. The samples were fabricated to test for pull out test with different fibre volume contents as 0%, 10%, 20%, 30%, 40% and 50% of epoxy volume. The wet lay-up method was used while applying modified epoxy adhesive to adhere CFRP fabric and concrete block. A 75 mm wide CFRP fabric strip was adhered to the concrete block with a bond length of 150 mm. The first attempt to find the optimum fibre content was failed due to the errors that occurred in the process of sample fabrication. Those test results are given in Table 4.1. Two samples were tested under each category. Most of the samples failed as a result of CFRP rupturing in between bond and the grip of the CFRP strip except, samples S-10 and S-20 which failed in debonding (Figure 4.2). Therefore, the results were discarded.

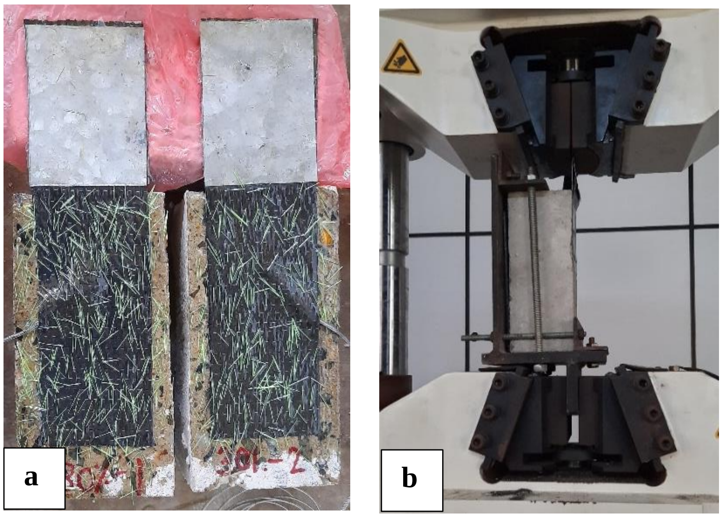

Figure 4.1 – (a) Fabricated samples (b) Testing a sample

In the first attempt, 3 mm thick steel sheets were adhered to the CFRP fabric to use as the grip for the application of tensile load on CFRP fabric. Due to the relatively high weight of these steel sheets, it was hard to maintain the correct vertical level in CFRP fabric while loading it to the setup to conduct the direct pull-out test. This was one of the reasons which caused the unexpected failure of the samples during testing.

Table 4.1 – Test results of checking optimum fibre content

Sample code	PET content as a % of the epoxy volume	Failure load (kN)	Average failure load(kN)	Average bond strength(N/mm^2)
S-0-1	0	9.50	7.9	634.54
S-0-2	0	6.35		
S-10-1	10	9.00	9.5	763.05
S-10-2	10	10.00		
S-20-1	20	8.10	7.5	602.41
S-20-2	20	6.95		
S-30-1	30	10.15	9.15	734.94
S-30-2	30	8.15		
S-40-1	40	2.10	3.35	269.08
S-40-2	40	4.60		
S-50-1	50	9.30	6.55	526.10
S-50-2	50	3.80		

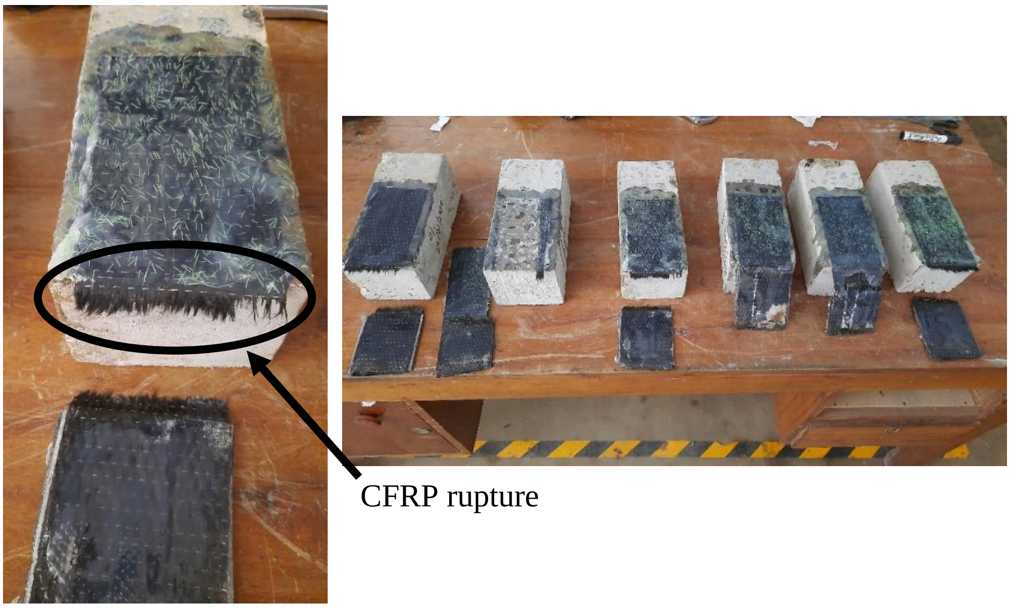

Figure 4.2 – (a) CFRP rupture at the gap between steel plate grip and concrete block (b) Failure modes of samples

Apart from that, a considerable gap was maintained between the steel plate and concrete block while adhering the steel plate to the CFRP fabric. When the CFRP fabric was pulled out, the applied load get concentrated in the CFRP fabric within this gap, rather than transferring it to the CFRP fabric part adhered to concrete block. As a result, CFRP got ruptured as shown in Figure 4.2 (a).

Therefore, another set of samples were fabricated overcoming the issues in the previous test series. Overall 12 samples were fabricated with 2 samples for each fibre content. Table 4.2 shows the results of the second attempt where the bond length of all the samples was set to 100 mm and Figure 4.4 shows the graphical interpretation of the results. Due to the sudden outbreak of Covid-19 pandemic, the samples were tested for their pull out strength after 3 months. Given below is the sample calculation of bond strength for sample S-0.

CFRP strip width = 75 mm Thickness of CFRP strip = 0.166 mm

Failure load of S-0 sample = 7.6 kN

Bond strength of S-0 sample $= 7.6\ kN/(75 \times 0.166 \times 10^{-6})\ m^2$

$$= 610441.77\ kNm^2 = 610.44\ Nmm^2$$

Table 4.2 – Test results of the second attempt to find the optimum fibre content

Sample code	PET content as a % of the epoxy volume	Average failure load (kN)	Average bond strength (N/mm^2)	% Strength enhancement
S-0	0	7.6	610.44	-
S-10	10	14.55	1168.67	91%
S-20	20	12.3	987.95	62%
S-30	30	11.9	955.82	57%
S-40	40	11.3	907.63	49%
S-50	50	9.2	738.96	21%

According to Figure 4.3, it is clearly seen that the modification of epoxy by mixing PET fibres is an overall success since all the samples with different fibre proportions reached a higher bond strength than the pure epoxy bond strength which is obtained through sample S-0. The bond strength at failure of pure epoxy/CFRP/concrete bond was 610.44 N/mm^2. The bond strength of epoxy-bonded CFRP depends on the concrete surface preparation method, type of adhesive, adhesive thickness, bonded surface area and method of application [1]. This was evident in the experimental results found in the literature [83]–[85]. According to the test results of Issa, Rahman and Alrousan [83], bond strength of CFRP bonded with epoxy for a bond width of 75 mm and bond length of 113 mm was about 1810 N/mm^2. For a bond width of 100 mm and a bond length of 125 mm, the bond strength obtained by Gamage, Wong and Al-Mahaidi [84] was around 1193 N/mm^2. A further lower bond strength value of 397 N/mm^2 was obtained through the experiments conducted by Soares et al. [85]. It was for a bond length of 250 mm and a bond width of 15 mm.

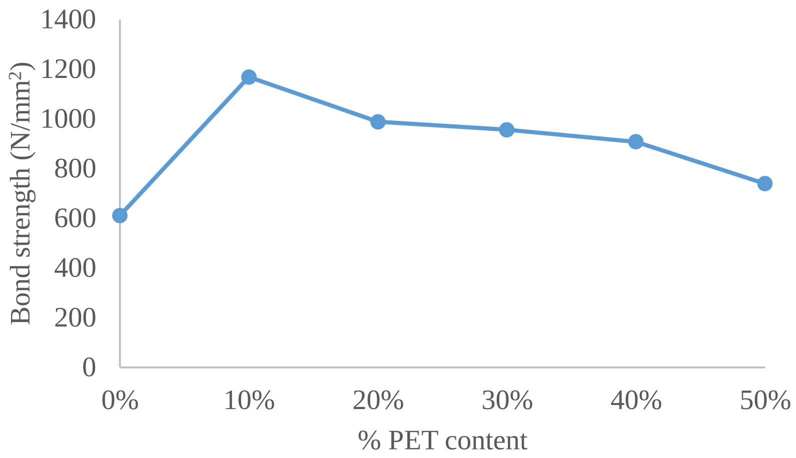

Figure 4.3 – Graphical interpretation of test results to find the optimum fibre content

Among all the other modified epoxy samples, the highest bond strength is reached by the sample with the fibre content 10% (S-10) of epoxy volume. It shows a strength enhancement of 91% compared with the bond strength of S-0 sample. This strength enhancement gradually decreases with the increase of fibre volume and in S-50 sample, strength enhancement decreases up to 21%. Therefore, from these results, it can be concluded that the highest bond strength at room temperature was gained when the fibre volume reached 10% of the epoxy volume. The blended fibre functioned as a reinforcement within the epoxy resin. It enhanced the tensile strength of the modified epoxy adhesive. The addition of PET fibre to the epoxy resin further enhances the ductility of Epoxy-PET fibre composite [13]. Therefore the load transfer within the modified epoxy layer might have become more effective with its ductile nature rather than failing in a more brittle nature. This could be the cause for 91% of strength enhancement recorded at 10% PET fibre content.

In samples S-0, S-10, S-20, S-30 and S-40 failure occurred as a concrete splitting failure (Figure 4.4). However, in the S-50 sample, failure occurred in CFRP-epoxy interface along with a slight concrete wedge failure (Figure 4.4).

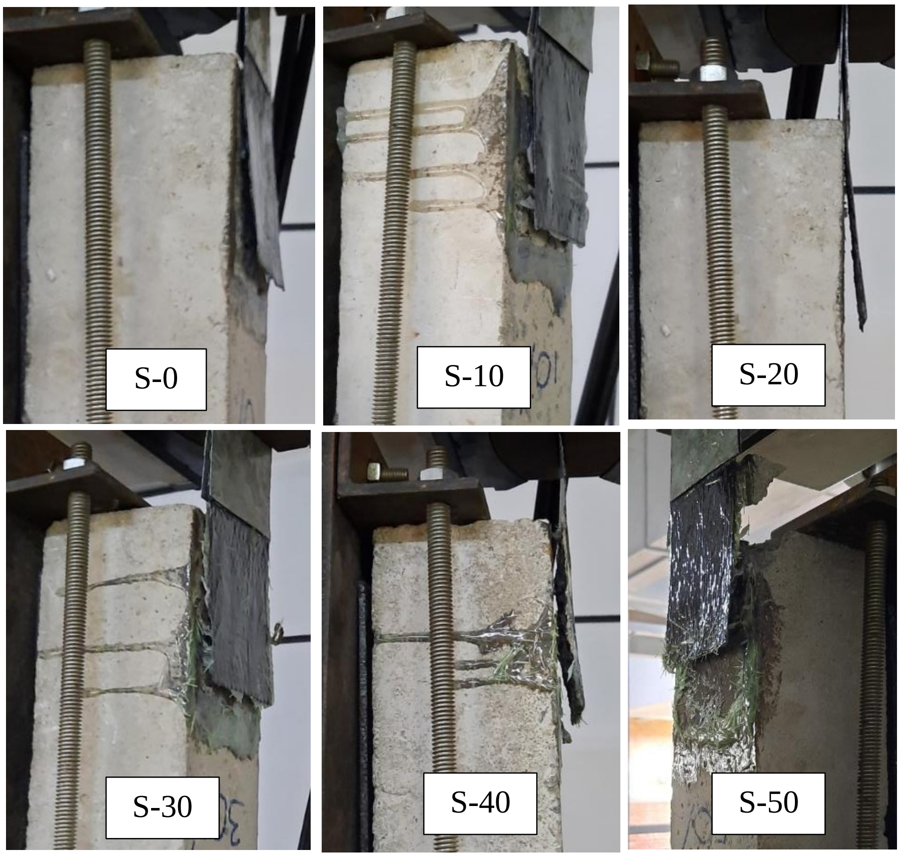

Figure 4.4 – Debonding failure occurrence

Figure 4.5 shows the nature of failures occurred in each sample. All the samples except S-50, CFRP strip got detached from concrete block with a layer of concrete. This was evident throughout the adhered surface. In S-50 sample failure occurred mainly within the modified epoxy adhesive. As mentioned before, a concrete block failure was closer to the edge of the concrete block. The amount of fibre distribution in modified epoxy near the edges of concrete is low. With the failure occurred in CFRP-modified epoxy interface, a stress concentration might have occurred closer to the edge of the concrete block where the bonding is better due to the lower fibre distribution. This might have caused the concrete wedge failure. This failure mechanisms further proves the fact that the increase of fibre content beyond 40% of epoxy volume disturbs the uniform bonding of CFRP to the concrete block. The fibre content change from 10% to 50%, depicted a gradual decrease in bond strength. Even though those bond strengths showed a strength enhancement compared to the epoxy sample, a gradual decrease in bond strength with the increase of fibre content showed that higher fibre contents decrease the bonding ability. Therefore, a conclusion can be made that even though the epoxy modification enhanced the bond strength due to effective load transferring within the modified epoxy adhesive, a higher amount of fibre content disturbs the bond interface between modified epoxy and concrete.

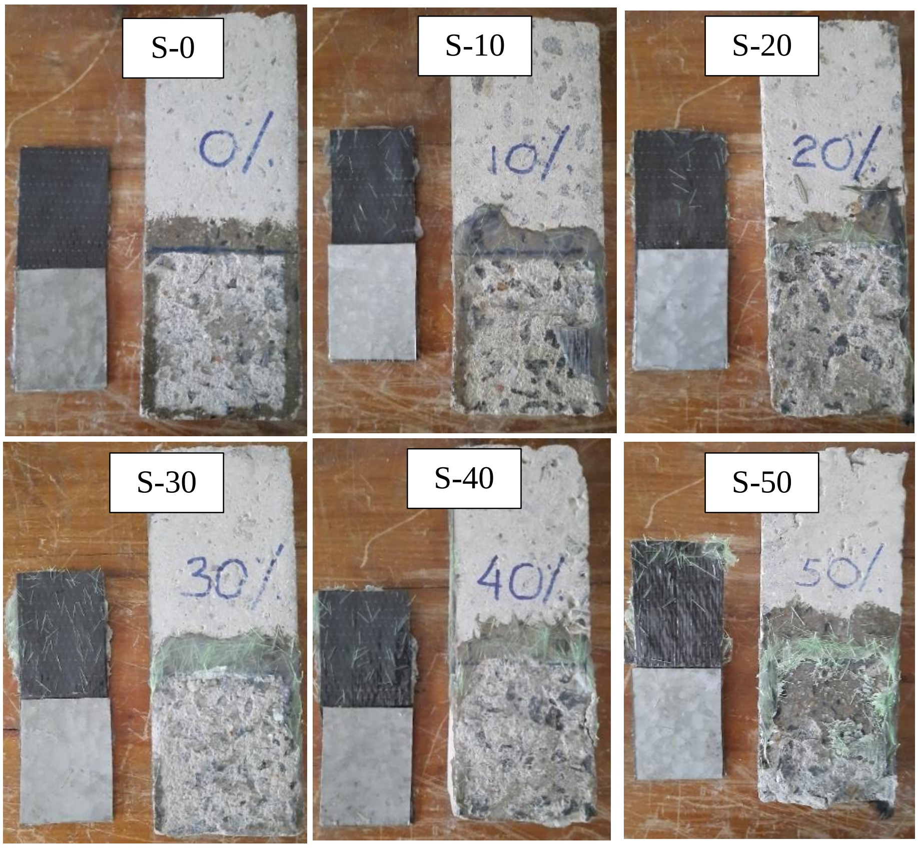

Figure 4.5 – Nature of failure mode

4.3.2 Optimum fibre content under elevated temperature

Even though the optimum fibre content concluded from the above test is 10% of epoxy volume, there is a tendency for these results to vary under elevated temperature. Therefore, another set of samples were cast to check the influence of elevated temperature on the bond strength for the adhesive modified with different fibre contents. Two samples from each S-10, S-30 and S-50 were fabricated again. These samples were heated using flashlights until the bond temperature rises to 150^{0}C (Figure 4.6 (a)). For temperature increment, two flashlights of 1000 W and 500 W were used (Figure 4.6 (b)). During the fabrication of a sample, a thermocouple was kept in the bond between CFRP and concrete as shown in Figure 4.6 (a). This thermocouple was fixed to the data logger to monitor the temperature rise during application of the load (Figure 4.6 (c)).

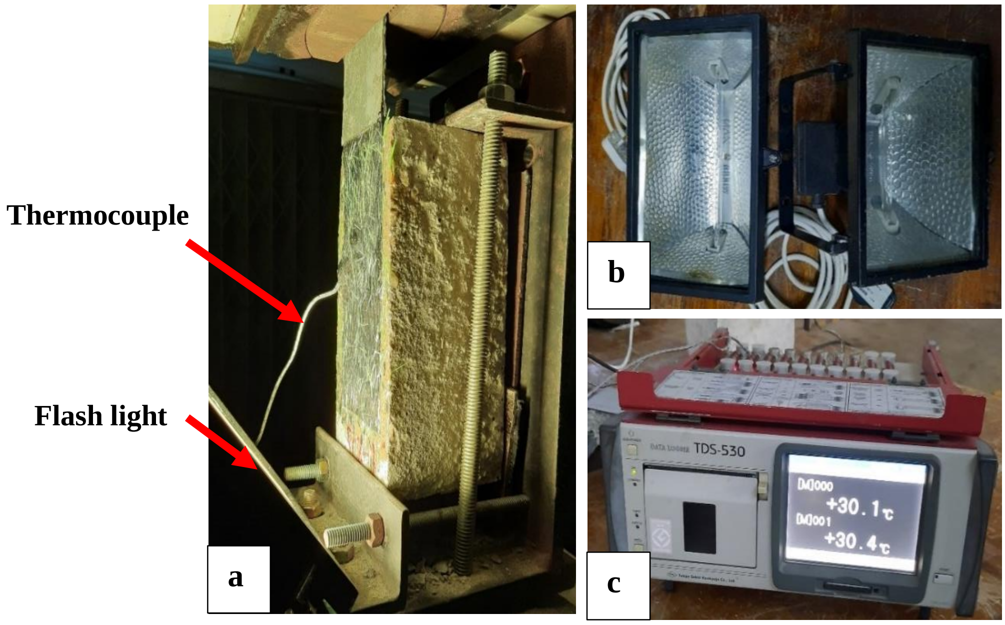

Figure 4.6 – (a) Testing the sample (b) Flashlights (c) Data logger

Table 4.3 gives the results of the experiment at 150 ^{0}C and Table 4.4 compares the bond strength difference at room temperature and elevated temperature. Figure 4.7 further depicts the strength deviation in a graphical format.

Table 4.3 – Bond strength of CFRP/concrete bond at 150 ^{0}C

Sample code	PET content as a % of the epoxy volume	Failure load (kN)	Average bond strength (N/mm^2)
S-10-1	10	5.50	433.73
S-10-2	10	5.30	
S-30-1	30	5.90	489.96
S-30-2	30	6.25	
S-50-1	50	5.40	441.77
S-50-2	50	5.64	

The highest bond strength was achieved by the sample S-30. Here the lowest bond strength was shown by the S-10 sample. This might be because the epoxy content in the S-10 sample is at a greater amount compared to S-30 and S-50 sample. Therefore, the behaviour of epoxy dominates in this specific sample. However, in S-30 and S-50 samples, fibre content is high. Therefore, it seems that the influence created by the fibres dominate in these samples since the bond strength is higher than that of the S-10 sample.

Figure 4.7 shows the fabricated samples and Figure 4.8 shows the failure modes in each sample category. As per Figure 4.8, all the samples showed interface failure between modified epoxy and concrete. But S-30 sample showed a slight concrete wedge failure with debonding. This indicates the relatively sound bond between CFRP and concrete.

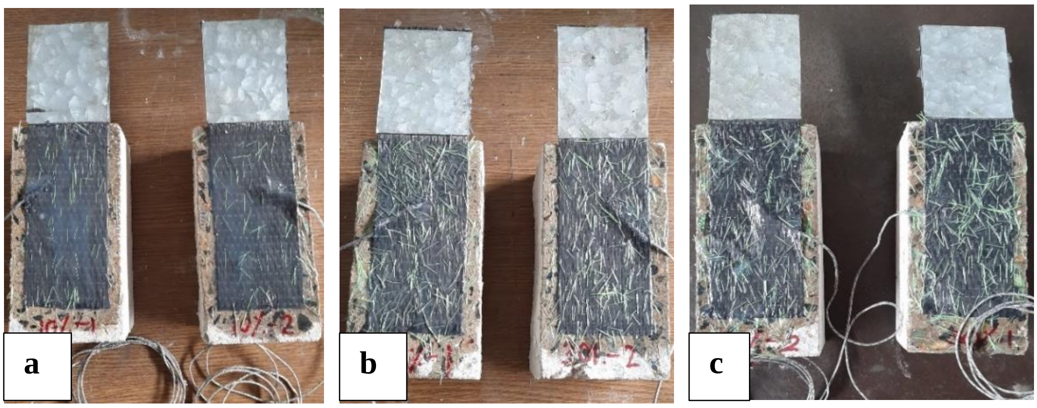

Figure 4.7 – Fabricated samples

Figure 4.8 further shows that both S-10 and S-50 samples did not show a concrete layer attached to the detached CFRP strip. This is because, both the samples started losing their stiffness with the exposure to heat. In S-30 samples, CFRP detached with a concrete layer attached to the strip. Thus, it can be deduced that the bond between the concrete substrate and CFRP is strong despite the exposure to elevated temperature and the effect from the elevated temperature on CFRP/Concrete bond is comparatively low in S-30 sample. The appropriate amount of fibre in epoxy might have delayed the loss of stiffness in adhesive or in other words, it might have incremented the glass transition temperature of the polymeric adhesive. The percentage reduction of strength is low with the incremented fibre content when the system was exposed to the elevated temperature.

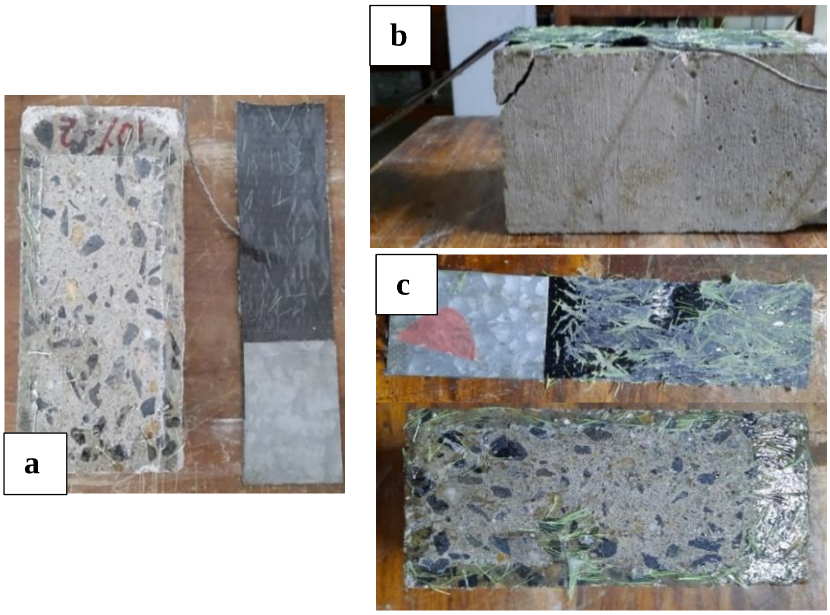

Figure 4.8 – Failure mode in samples (a) S-10 (b) S-30 (c) S-50

4.3.3 Selection of optimum fibre content under overall performance

According to the results shown in Figure 4.9, it is clear that the highest bond strength at 150 ^{0}C is achieved by the sample S-30. For the samples at room temperature, the highest bond strength was achieved by S-10. The main drawback in the normal epoxy adhesive is its poor performance at elevated temperature. The main intension of modifying epoxy adhesive is to achieve a better bonding performance at elevated temperature.

Table 4.4 – Bond strength at room temperature and elevated temperature

Sample	Average bond strength at room temperature (N/mm^2)	Average bond strength at 150 ^{0}C (N/mm^2)	Percentage strength reduction
S-0	610.44	160.51	74%
S-10	1168.67	433.73	62%
S-30	955.82	489.96	49%
S-50	738.96	441.77	40%

Even though the S-10 performed better under room temperature, S-30 performed well in elevated temperature. Moreover, the percentage strength reduction at 150 ^{0}C is low in S-30 compared to S-10 (Table 4.4). The introduction of low fibre content created a positive impact on epoxy adhesive at ambient conditions while increased fibre content indicated relatively better performance at elevated temperature. Therefore considering the overall performance, the S-30 sample was selected as the best fibre proportion to perform well in both room temperature and elevated temperature.

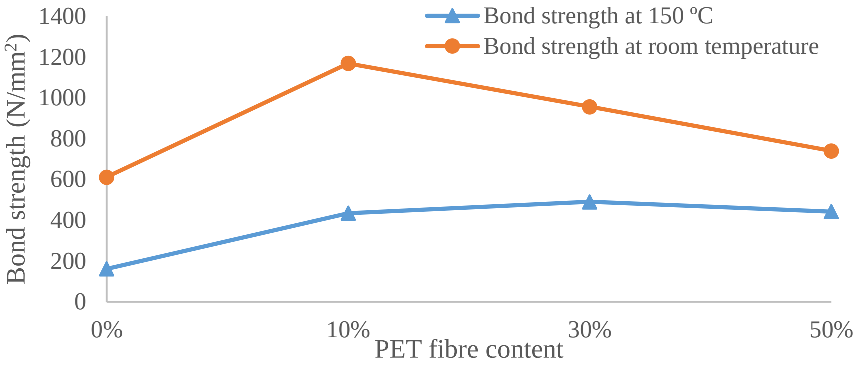

Figure 4.9 – Bond strength - % of PET addition

4.4 Effective bond length

After selecting the optimum fibre content to develop the modified epoxy adhesive depending on both ambient and elevated temperature conditions, the selected proportion was tested to determine the effective bond length of CFRP in the concrete application using the developed adhesive. Samples were kept 7 days for curing after the fabrication. Figure 4.10 shows the fabricated samples.

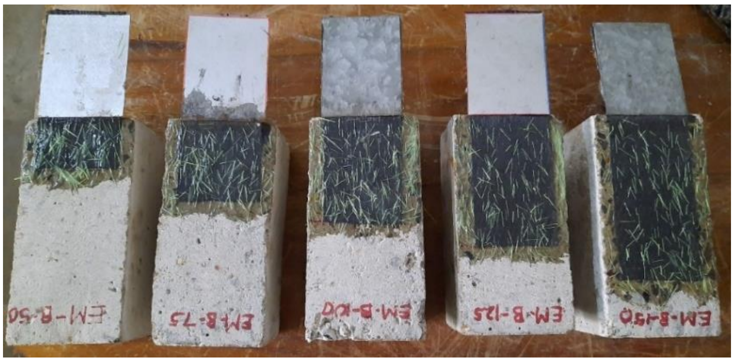

Figure 4.10 – Samples used to check the effective bond length

Test results are briefed under Table 4.5. A set of samples were fabricated with pure epoxy as the bonding agent for the comparison purpose. Figure 4.11 shows the graphical interpretation of the test results. When the bond length exceeds 75 mm, samples with modified epoxy showed a drastic development in bond strength and beyond 100 mm, the bond strength reached a stable state with no significant strength enhancement. Therefore the maximum 7 days bond strength of modified epoxy for CFRP fabric ranges in between 827 N/mm^2 – 832 N/mm^2. The effective bond length for the modified epoxy adhesive can be concluded as 100 mm. Figure 4.12 shows how the samples fail in each instance.

Table 4.5 – Test results of single lap shear test

Sample code	CFRP bond length (mm)	Failure load (kN)	Bond strength (N/mm^2)	Failure mode
EM-B-50	50	9.55	767.07	Concrete wedge failure
EM-B-75	75	9.60	771.08	Top concrete layer failure
EM-B-100	100	10.30	827.31	Top concrete layer failure
EM-B-125	125	10.35	831.33	Top concrete layer failure
EM-B-150	150	10.35	831.33	Top concrete layer failure
E-B-50	50	4.6	369.48	Top concrete layer failure
E-B-75	75	5.95	477.91	Top concrete layer failure
E-B-100	100	6.9	558.23	Top concrete layer failure
E-B-125	125	8.5	682.73	Top concrete layer failure
E-B-150	150	8.55	686.75	Top concrete layer failure
E-B-175	175	8.6	690.76	Top concrete layer failure

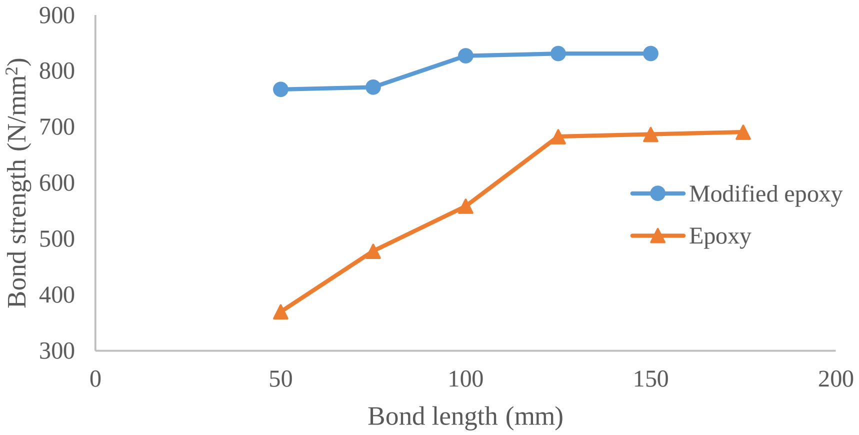

Figure 4.11 – CFRP bond strength - Bond length

The samples fabricated with pure epoxy adhesive showed a gradual increment in bond strength from bond length 50 mm to 125 mm and bond strength was relatively stable from 125 mm to 175 mm. Therefore, the effective bond length of pure epoxy can be deduced as 125 mm. Results showed that the PETCO-Epoxy adhesive showed a higher bond strength than pure epoxy adhesive for all the bond lengths.

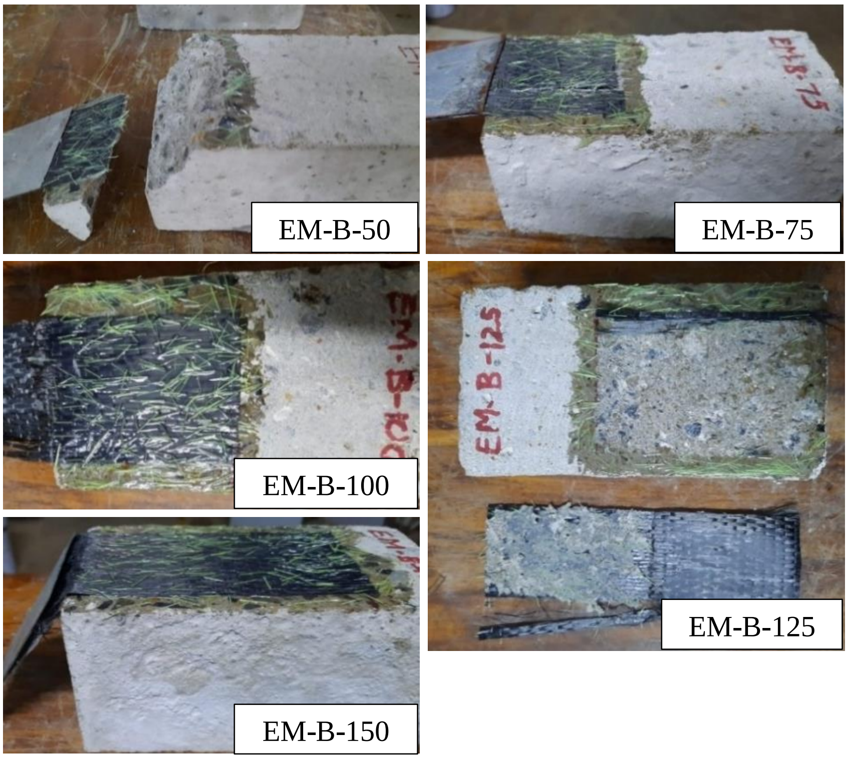

Figure 4.12 - Failure modes of samples with modified epoxy in direct pull out test

Except for EM-B-50 sample, top concrete layer failure was present in all the other samples. Concrete wedge failure took place in sample EM-B-50. In all the other cases, a concrete layer got detached with CFRP strip. This shows that the adhesive has good bonding with the concrete substrate. The concrete wedge failure in sample EM-B-50 might have caused due to the concentration of the applied load on a small area where a weak concrete region has prevailed. Figure 4.13 shows the failure modes of samples which used pure epoxy adhesive as the bonding agent.

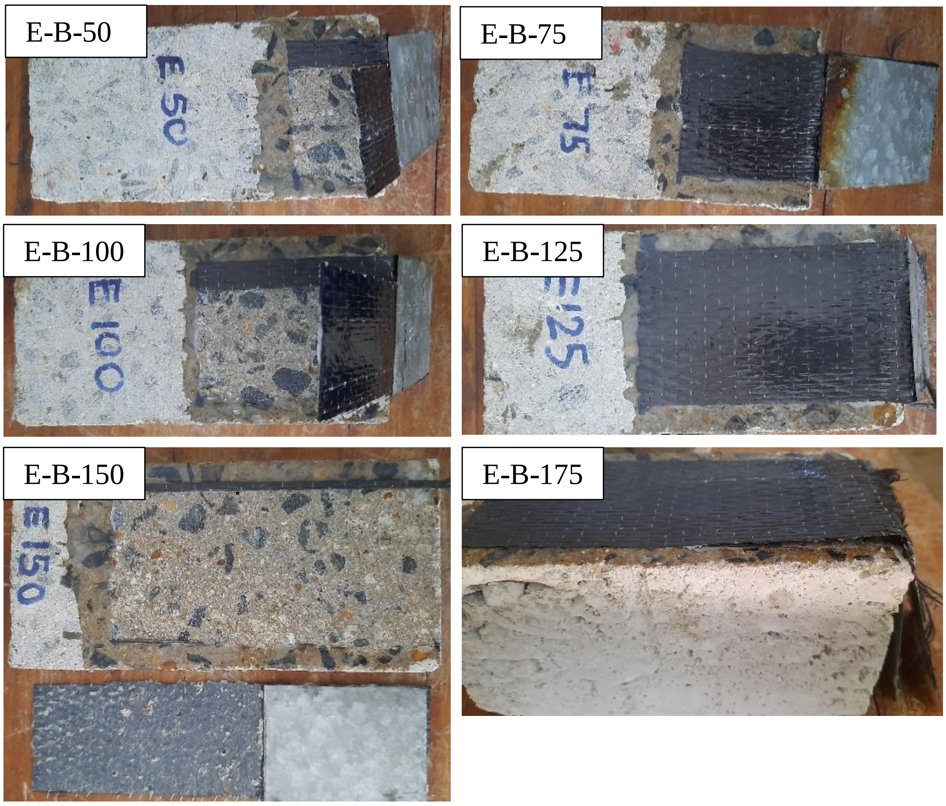

Figure 4.13 - Failure modes of samples with pure epoxy in direct pull out test

4.5 Material properties of modified epoxy adhesive

After deciding the appropriate fibre content for the modified epoxy adhesive, the developed adhesive was tested for its tensile, compressive and flexural strengths. Uniaxial tensile test for modified epoxy adhesive was done following the guidelines given in ASTM D638 - 14 - Standard Test Method for Tensile Properties of Plastics [86]. Figure 4.14 (a), (b) and (c) show a sample used to perform the test, how the sample was tested in Hounsfield Tensometer and how the sample failed, respectively. Table 4.6 summarizes the test results.

According to the manufacturer provided material properties, 7 days tensile strength of the epoxy adhesive is 45 N/mm^2 [76]. After the modification, the average tensile strength of adhesive has reached 63.24 N/mm^2, showing tensile strength enhancement of 40.5%. Therefore, it is clear that the blended short PET fibres have functioned as a reinforcement for the epoxy resin and enhanced its tensile strength. The tensile strengths were tested at the end of 7 days and 14 days of curing periods to observe the strength gain with time.

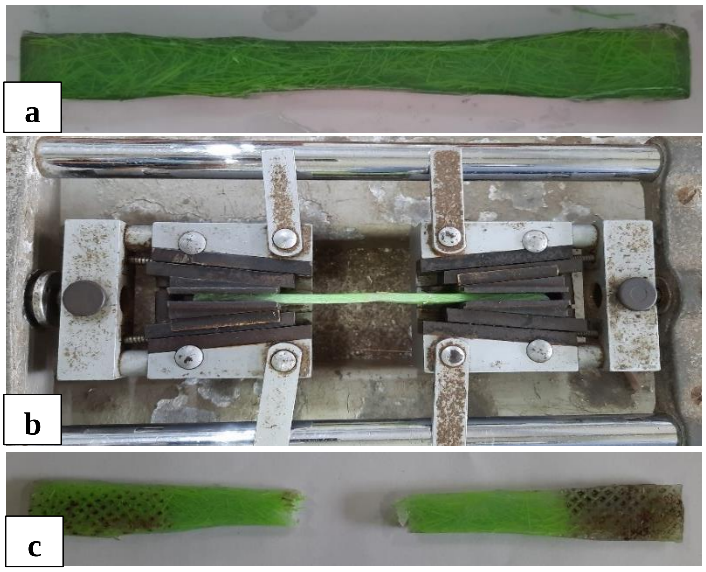

Figure 4.14 – (a) Tensile strength testing sample (b) Conducting the test (c) Failure mode of a sample

Table 4.6 – Tensile strength test results

Number of days cured	Sample	Width (mm)	Thickness (mm)	Load (N)	Tensile strength (N/mm^2)
7 days	1	13.1	6.8	5710.15	64.10
	2	12.9	7.2	5709.6	61.47
	3	12.9	6.9	5709.9	64.15
	Average tensile strength at 7 days				63.24
14 days	1	14	7.0	6542.8	66.76
	2	14	7.22	6510.9	64.41
	3	13.4	6.88	6512.0	70.64
	Average tensile strength at 14 days				67.27

Compressive strength of modified epoxy was tested in accordance with ASTM - D 695-02a - Standard Test Method for Compressive Properties of Rigid Plastics [87]. The tested samples are with dimensions of 12.7 mm x 12.7 mm x 25.4 mm (Figure 4.15). The samples were tested at the end of 7 days and 14 days of curing (Table 4.7).

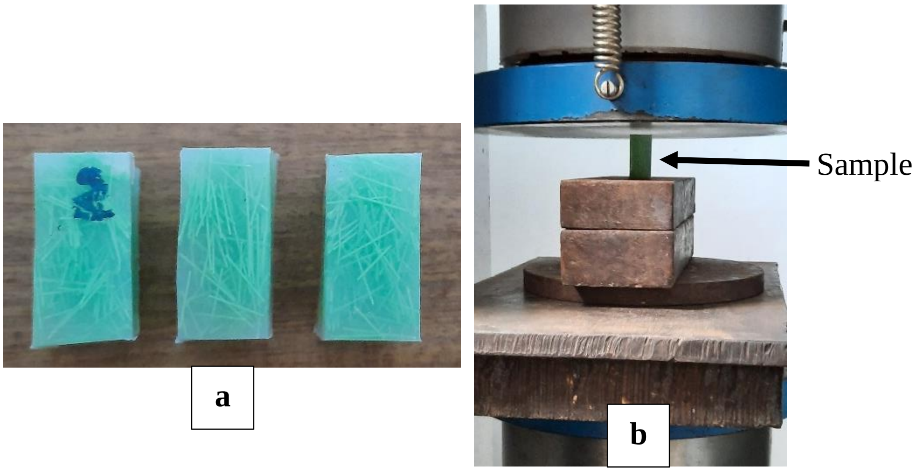

Figure 4.15 – (a) Fabricated samples (b) Testing a sample

Table 4.7 - Compressive strength test results

Number of days cured	Sample	Width (mm)	Thickness (mm)	Load (N)	Tensile strength (N/mm^2)
7 days	1	13.9	13.6	3924	20.76
	2	13.3	13.74	4120	22.55
	3	13.4	13.3	3826	21.47
	Average compressive strength at 7 days				21.59
14 days	1	13.6	13.42	5690	31.17
	2	13.32	13.7	5788	31.72
	3	13.3	13.5	5788	32.24
	Average compressive strength at 14 days				31.71

The flexural strength of the modified epoxy adhesive was tested according ASTM - D 790 – 03 - Standard Test Methods for Flexural Properties of Unreinforced and Reinforced Plastics and Electrical Insulating Materials [88]. Figure 4.16 (a) and (b) present a tested sample and three point bending test conducted on the sample, respectively. Table 4.8 shows the respective test results.

Figure 4.16 – (a) Flexural strength testing sample (b) Testing a sample

Accuracy of the flexural strength was low due to the low sensitivity of the testing apparatus used. The smallest measurement of the testing apparatus is 0.05 kN which resulted in difficulty to record minor load deviations.

Table 4.8 – Flexural strength test results

Number of days cured	Sample	Width (mm)	Thickness (mm)	Load (kN)	Flexural strength (N/mm^2)
7 days	1	12.52	3.58	0.1	47.86
	2	12.72	3.3	0.05	54.14
	3	12.68	3.62	0.05	45.14
	Average flexural strength at 7 days				49.05
14 days	1	12.62	3.42	0.05	50.81
	2	12.86	3.48	0.1	96.31
	3	12.84	3.36	0.05	51.74
	Average flexural strength at 14 days				66.29

Pot life of an epoxy is the time taken to double the initial viscosity of the fluid [89]. Therefore, to determine the pot life of the developed PETCO-Epoxy, viscosity should be measured. The falling ball method was used to determine the viscosity of the developed PETCO-Epoxy adhesive. It can be used to measure dynamic viscosity based on Stokes' law [90]. Initial viscosity was measured right after the preparation of the PETCO-Epoxy adhesive and viscosity was continuously measured at 10 minute intervals starting from 20 minutes after the preparation. Pot life of epoxy is 40 minutes at 20 ^{0}C as per manufacturer provided data. Therefore, viscosity was measured from 20 minutes to 60 minutes from the initial time of preparation of the PETCO-Epoxy adhesive.

The respective viscosity of the adhesive was calculated by recording the time taken by a spherical ball to travel a particular distance through the adhesive. The test results are mentioned in Table 4.9 and the viscosities are normalized with respect to the initial viscosity of the adhesive. Figure 4.17 (a) shows the test results in a graph to interpret how viscosity changes with the time and Figure 4.17 (b) shows how the test was conducted. According to the test results, time spent to double the initial viscosity was 25 minutes and 34 seconds. Therefore, the pot life of PETCO-Epoxy adhesive is 25 minutes and 34 seconds.

Table 4.9 – Results of viscosity test

Time (min)	Distance (mm)	Time (s)	Normalized viscosity
0	45	165	1
20	30	180	1.64
30	24	198	2.25
40	21	225	2.92
50	15	240	4.36
60	15	280	5.09

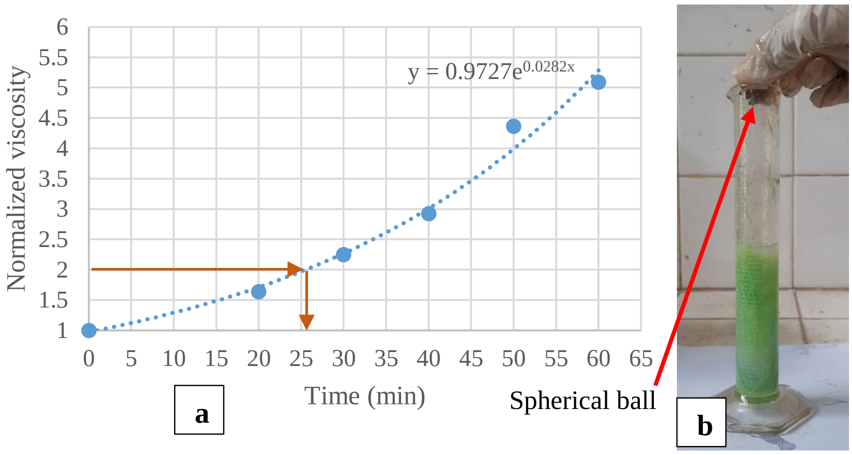

Figure 4.17 – (a) Normalized viscosity – Time graph (b) Conducting the test

4.6 Thermal performance

Thermal performance of the modified epoxy adhesive can be analyzed by performing the direct pull-out test after exposing the bond to different elevated temperatures. Therefore a set of samples were fabricated by bonding CFRP to concrete blocks using a modified epoxy adhesive (Figure 4.18 (a)).

Another set of samples were fabricated by bonding CFRP using epoxy (Figure 4.18 (b)). These were used to compare the performance deviation between the pure epoxy adhesive and modified epoxy adhesive under elevated temperature. Bond length for all the samples was set to 150 mm. The fabricated samples were exposed to different temperature levels; 40 ^{0}C, 60 ^{0}C, 80 ^{0}C, 100 ^{0}C and 120 ^{0}C. Figure 4.18 (c) shows how the experiment was conducted.

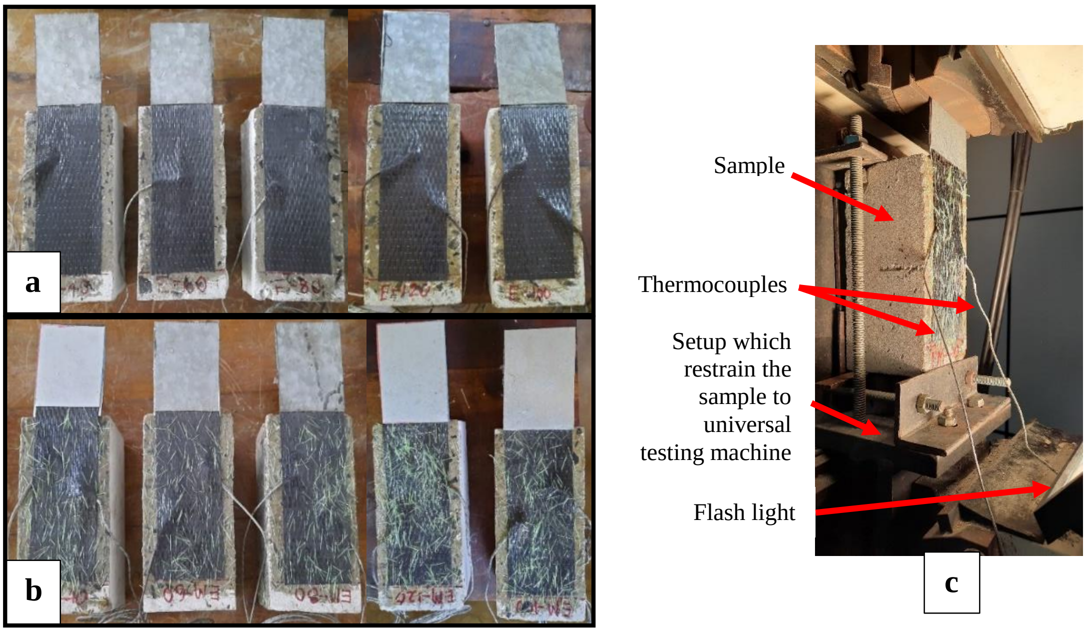

Figure 4.18 – Samples fabricated by bonding CFRP using (a) epoxy adhesive (b) modified epoxy adhesive (c) Testing the sample

The bond temperature was incremented using a flashlight system by elevating the environmental temperature. Two thermocouples were fixed within the bond in each sample to monitor the bond temperature. These thermocouples were fixed to a data logger to take the temperature readings. Table 4.10 summarizes the test results.

Table 4.10 – Comparison of thermal performance between pure epoxy and modified epoxy adhesives

Adhesive type	Sample code	Bond temperature (^{0}C)	Failure load (kN)	Bond strength (N/mm^2)	*Strength enhancement in modified epoxy
Modified epoxy	EM30	30	10.35	831.33	24%
	EM40	40	10.10	811.24	22%
	EM60	60	9.95	799.20	23%
	EM80	80	9.55	767.07	181%
	EM100	100	9.30	746.99	265%
	EM120	120	9.00	722.89	339%
Epoxy	E30	30	8.35	670.68	-
	E40	40	8.25	662.65	-
	E60	60	8.10	650.60	-
	E80	80	3.40	273.09	-
	E100	100	2.55	204.82	-
	E120	120	2.05	164.66	-

*With respect to the non-modified epoxy at same temperature

Figure 4.19 shows the test results in a graphical format. Room temperature during the testing was 30 ^{0}C. Bond strength for the modified epoxy sample at room temperature was obtained from the previous test done on determining the effective bond length. Bond strength enhancement in the modified epoxy adhesive with respect to pure epoxy adhesive for each temperature exposure was calculated as a percentage (Table 4.10). According to Figure 4.19, it is clear that in both adhesives bond strength reduces with the exposure to elevated temperature. In epoxy adhesive, with the gradual increase of exposed temperature, bond strength decreased in a relatively linear manner until 60 ^{0}C and afterwards the bond strength underwent a drastic drop. From 80 ^{0}C to 120 ^{0}C, bond strength kept on decreasing gradually. However, for each temperature exposure, bond strength of modified epoxy was much higher than that of the pure epoxy adhesive. Generally, this enhancement ranges in between 22%-24% for temperature exposures below 60 ^{0}C. Afterwards, the strength enhancement reached to a higher level since the pure epoxy adhesive has reached its T_g of the bond. Thus, epoxy adhesive loses its bonding ability and bond strength of pure epoxy shows a relatively low value.

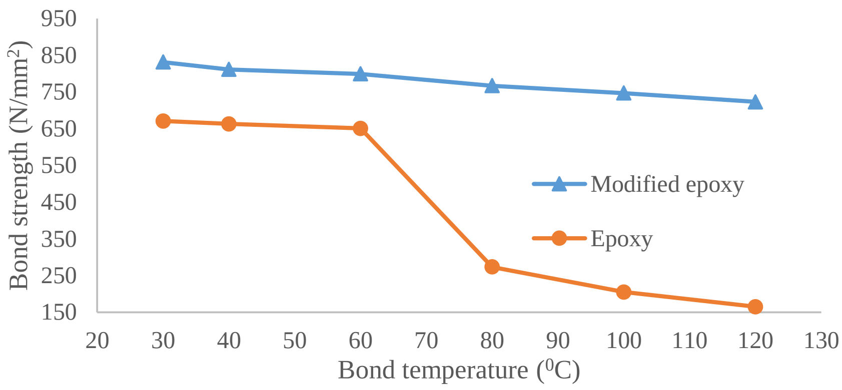

Figure 4.19 – Bond strength vs. Bond temperature

Meanwhile, the bond strength of modified epoxy deteriorated linearly till 120 ^{0}C. Until 120 ^{0}C, the modified epoxy adhesive did not show any drastic drop in the bond strength. Therefore, it is clear that the modified epoxy adhesive performs well in both room temperature and elevated temperature up to 120 ^{0}C. Thus a conclusion can be made that the modified epoxy adhesive bond has not reached its glass transition temperature till 120 ^{0}C.

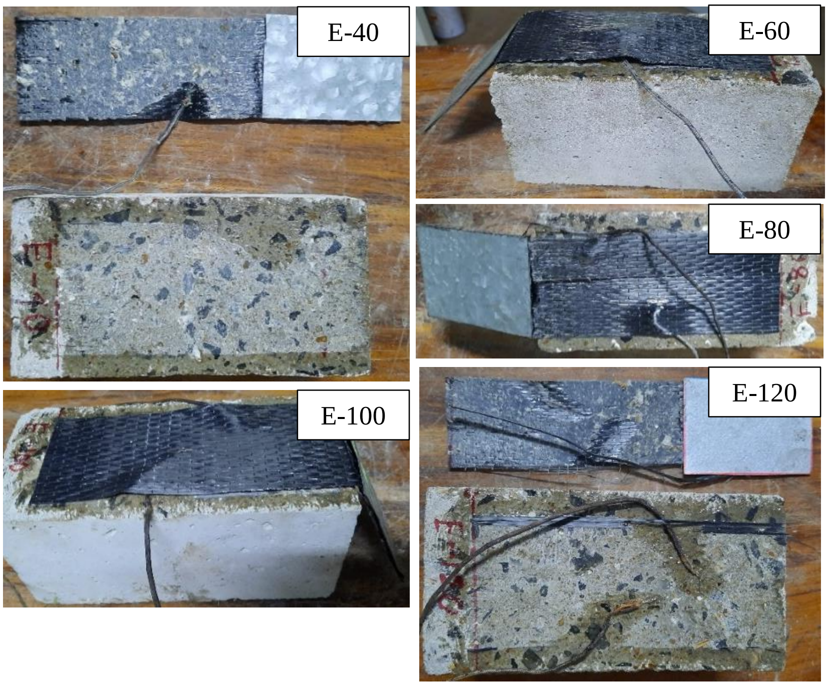

Figure 4.20 – Failure modes of samples with the pure epoxy adhesive

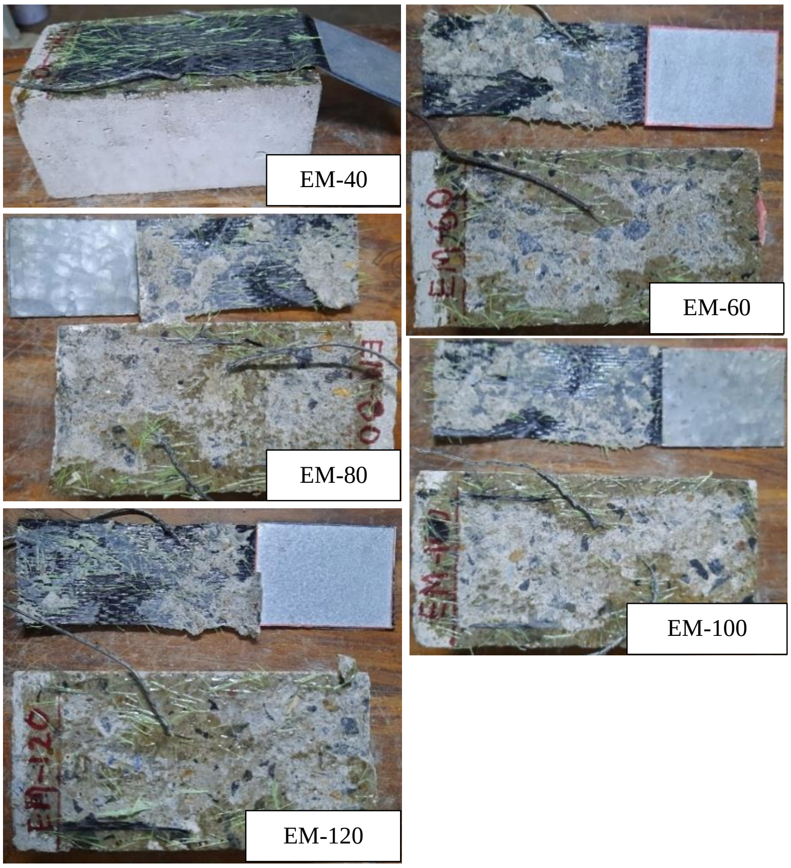

Figure 4.21 - Failure modes of samples with the modified epoxy adhesive

Figures 4.20 and 4.21 show how pure epoxy adhesive and modified epoxy adhesive applied samples failed when the system was exposed to elevated temperature while loading. The CFRP strip detached from samples which adhered using pure epoxy adhesive while the CFRP bonded with modified epoxy failed with concrete cover layer failure. Figure 4.21 clearly shows that a uniform concrete layer got detached from concrete substrate along with CFRP strip except for the places where thermocouples were fixed.

4.7 Chapter summary

Initially, an optimum fibre content to modify the epoxy adhesive was decided by conducting the direct pull-out test with the samples using epoxy modified with a range of PET contents. According to the results of sample with fibre volume is of 10% of the epoxy volume showed the highest bond strength. Since the temperature influences on the adhesive are concerned, fibre volume as 30% of the epoxy volume was selected as the best choice because it showed the lowest percentage strength reduction under elevated temperature. Another series of pull out tests were conducted to determine the effective bond length for modified epoxy adhesive and the results indicated 100 mm CFRP length as the effective bond length for the selected materials and application technique. The effective bond length for pure epoxy adhesive was 125 mm. The thermal performance of modified epoxy was further compared with the thermal performance of the pure epoxy adhesive. The test results concluded that the bond strength of the modified epoxy adhesive is higher than that of pure epoxy adhesive even under the elevated temperature. The bond strength reduction indicated by modified epoxy samples at 120 ^{0}C bond temperature was 13.04% while it was 75.45% for pure epoxy bonded samples. This depicts that the modification of epoxy adhesive has yielded better results in both room temperature and under the exposure to the elevated temperatures.

5 DEVELOPMENT OF CEMENTITIOUS ADHESIVE FOR ELEVATED TEMPERATURE PERFORMANCE (ECC ECO)

5.1 Introduction

This chapter includes the details of developing Engineered Cementitious Composite (ECC) mortar mix as an adhesive. Initially, a proper mix proportion for developing the adhesive was decided through literature and preliminary experiments. After finalizing the mix proportion to develop the cementitious adhesive several tests were conducted to determine its bond performance under ambient and elevated temperature conditions.

5.2 Preparation of ECC

Sample preparation was done in accordance with ASTM C305 [82]. In the preparation of ECC, Portland cement, silica sand, fly ash and PET fibres were mixed in a mechanical mixer initially and then water was added to the paste gradually (Figure 5.1).

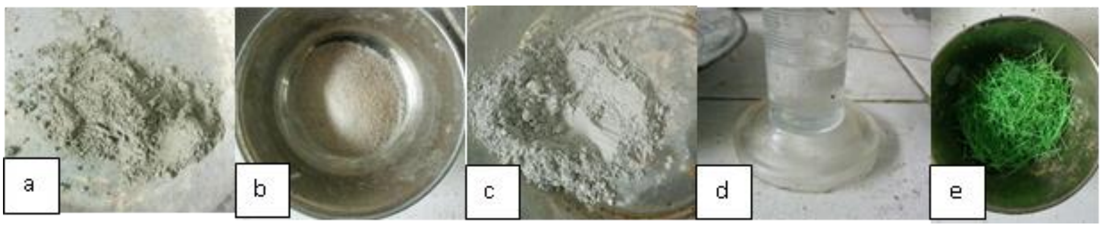

Figure 5.1 - (a)Cement (b) Silica sand (c) Fly ash (d) Water (e) PET fibres

The whole paste was kept for mixing in the mechanical mixer for 10 minutes with an angular velocity of 50 rpm, to get a homogenous mixture. ECC adhesive mix was developed in two different mix proportions which were modified from the literature [40], [45], [49], [91] as given in Table 5.1.

Table 5.1 – Mix Proportions

Sample mix	Mix proportions (Cement: Water: Silica sand: Fly ash)
MP-1	1 : 0.85 : 1 : 1.6
MP-2	1 : 0.85 : 0.8 : 1.2

Here, MP-2 is the same as the ECC mortar mix defined as ECC-M45 [91] with a modification introduced to the water-cement ratio (w/c). The w/c of ECC-M45 is 0.56 [91]. It is a typical mix design with self-consolidating properties [91]. Mix proportion of ECC-M45 was tailored to attain multiple cracking and to maintain a controlled crack width [91]. This mix design uses PVA fibres and fibre content is 2% of the volume of cement [91]. This specified fibre volume is slightly higher than the critical fibre content needed to achieve the desired strain hardening properties. But when producing the mortar mix MP-2 according to the specified w/c of ECC-M45, the result is a dry mix without proper adhering qualities. In order to achieve the expected adhering qualities in the mortar mix, ECC mortar was developed by changing w/c to 0.6, 0.7, 0.8 and 0.9. A sticky nature was evident in ECC mortar with 0.8 and 0.9 w/c. The ECC mortar with w/c of 0.9 showed a high flowability. Therefore, 0.85 was selected as the ideal w/c ratio to achieve the desired sticky nature in mortar.

5.3 Selection of best mix design proportion for ECC adhesive

In the selection of the best mix design proportion to develop ECC, the thermal performance of the adhesive was given a huge concern. Therefore, the fibre content in each mix design proportion was deviated to understand the effect of the amount of fibre on the thermal conductivity of the developed adhesive. For each mix proportion, samples were cast deviating the fibre volume as 2%, 3%, 4% and 5% of cement volume. PET fibres used for the adhesive mix were cut into 10 mm length. Even though the literature suggests the use of fibre content on the cementitious adhesive mix as 2% of the cement content to obtain desired strain hardening qualities and ductile behaviour, the thermal conductivity test was performed on samples by varying the fibre content, starting from 2% of cement content up to 5% of cement content to determine whether the increment of fibre content on the adhesive mix affects positively in reducing thermal conductivity with proper adhesion at elevated temperature.

Table 5.2 shows the measured thermal conductivities of the samples in both mix proportions.

Table 5.2 – Thermal conductivity values of samples

Mix proportions (Cement: Water: Silica sand: Fly ash)	Sample code	Fibre content as a percentage of cement content (% of cement)	Measured thermal conductivity (W/mK)
1 : 0.85 : 1 : 1.6	MP-1-2-1	2	0.198
	MP-1-2-2	2	0.175
	MP-1-2-3	2	0.170
	MP-1-3-1	3	0.192
	MP-1-3-2	3	0.203
	MP-1-3-3	3	0.254
	MP-1-4-1	4	0.210
	MP-1-4-2	4	0.295
	MP-1-4-3	4	0.183
	MP-1-5-1	5	0.223
	MP-1-5-2	5	0.249
	MP-1-5-3	5	0.235
1 : 0.85 : 0.8 : 1.2	MP-2-2-1	2	0.180
	MP-2-2-2	2	0.165
	MP-2-2-3	2	0.145
	MP-2-3-1	3	0.231
	MP-2-3-2	3	0.195
	MP-2-3-3	3	0.179
	MP-2-4-1	4	0.218
	MP-2-4-2	4	0.241
	MP-2-4-3	4	0.286
	MP-2-5-1	5	0.234
	MP-2-5-2	5	0.279
	MP-2-5-3	5	0.231

By equating Equations (3.1) and (3.2),

$$mc\frac{dT}{dt} = kA\frac{(T_2 - T_1)}{x} \qquad \text{Eq.(5.1)}$$

Sample calculation for MP-2-3-2,

Cooling curve gradient = Heat radiated per second = dT/dt = 0.0162 ^{0}C/s

m = 880 g

c = 0.385 J/g^{0}C

$mc\frac{dT}{dt} = 5.48856$

A = 0.002829 m^2

T_2-T_1 = 49.7 ^{0}C

x = 0.005 m

$\frac{x}{A(T_2 - T_1)} = 0.035567$

$k = 0.195\ W/mK$

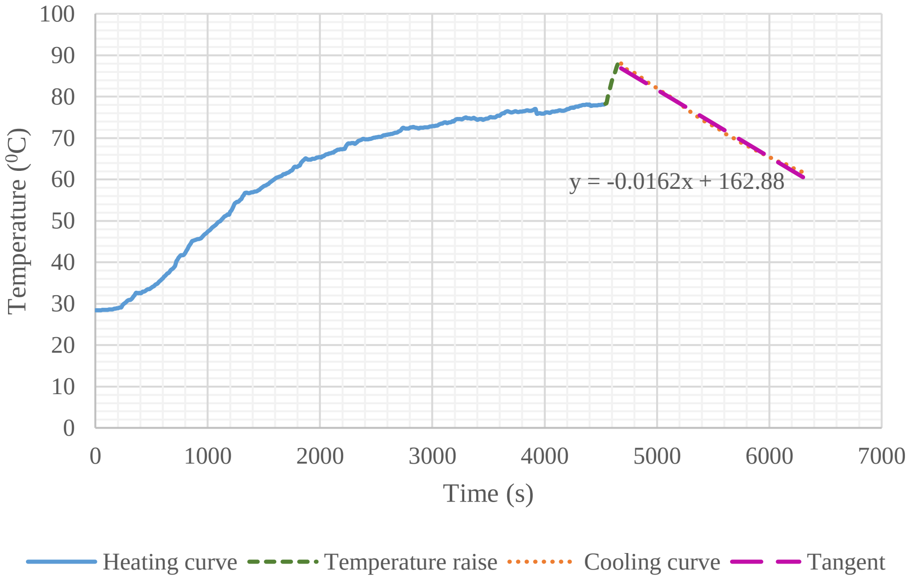

Figure 5.2 – Temperature deviation curve for sample MP-2-3-2

Figure 5.2 shows the temperature deviation curve obtained for the sample MP-2-3-2 which is the second sample of the MP-2 proportion with PET fibre content as 3% of cement content. Heat radiated per second (dT/dt) value is the gradient of the tangent drawn to the cooling curve at a steady temperature, T2. In order to obtain the exact tangent for this particular temperature, the top copper plate needs to be heated for some time after removing the sample from the setup. Usually, this temperature rise is maintained for about 10 ^{0}C (Temperature raise curve). Then the heating is halted and the setup is kept for cooling to obtain the cooling curve. For this considered sample, the gradient of the tangent drew on the cooling curve at a steady temperature is 0.0162 ^{0}C/s. Temperature rise (T2-T1) is 49.7 ^{0}C. According to the experimental values obtained, the thermal conductivity of the sample was calculated as 0.195 W/mK.

Figure 5.3 presents the temperature deviation graph for the sample MP-2-4-1 which is the first sample of the MP-2 proportion with PET fibre content as 4% of cement content. Heating and cooling curves are shown in two different colors.

Figure 5.4 shows the comparison of thermal conductivity values obtained for all the samples in a graphical manner. It clearly shows that the increment of the percentage of fibre content in the adhesive mix increases its thermal conductivity. Fibres within the cementitious adhesive behave as a reinforcing material to the paste. Higher the fibre content, higher the strength gain by the adhesive mix. Through these thermal conductivity results, it is clear that the increment of fibre content within the cementitious adhesive increases its thermal conductivity.

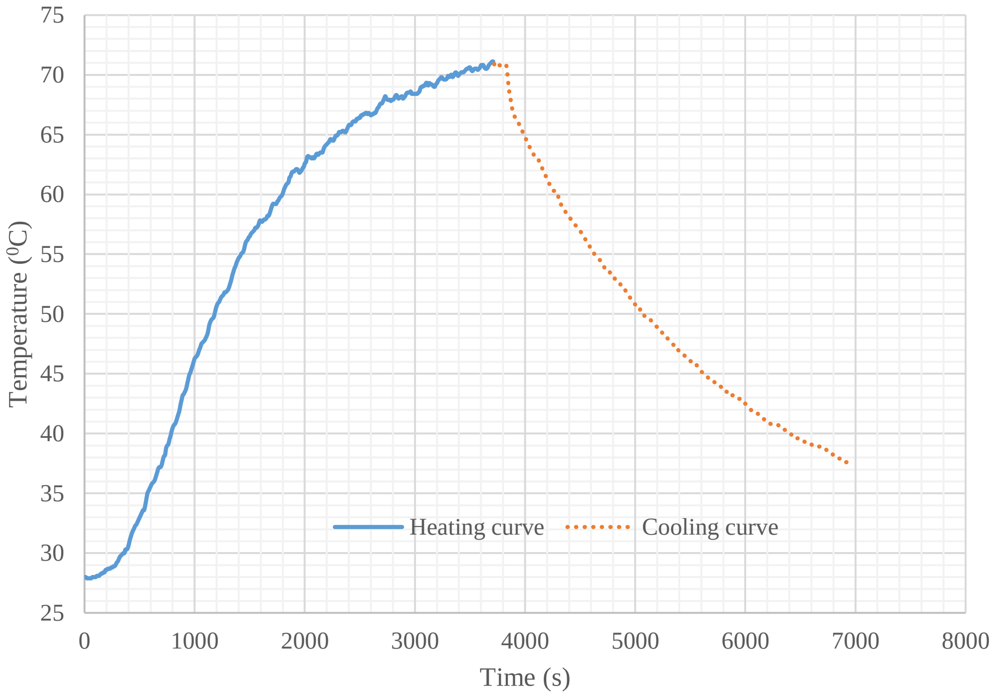

Figure 5.3 – Temperature deviation graph for sample MP-2-4-1

Researchers also suggest that the use of fibre content as 2% of cement volume due to the optimum tensile ductility and strain hardening stage which ECC achieve in this fibre content [92]. Sathishkumar et al. [38] concluded that 2% of PET fibre content in ECC showed the highest compressive strength, tensile strength and flexural strength values compared to other PET fibre volume percentages. Therefore, fibre content as 2% of cement content is taken as the ideal fibre content to carry out further testing for the properties depending on both thermal conductivity results and literature provided details.

Both the two proportions, MP-1 and MP-2 shows very similar conductivity results. However, both MP-2-2 and MP-2-3 samples have shown lower thermal conductivities than their respective MP-1 samples. Therefore the MP-2 proportion was selected for further testing among MP-1 and MP-2 proportions. Moreover, MP-2 mix proportion is a modified version of ECC-M45 mortar mix proportion. The original ECC-M45 mortar mix has yielded good results experimentally. Higher fly ash content slightly affects the reduction in compressive strength of the ECC[44]. Fly ash content in MP-2 is low compared to MP-1.

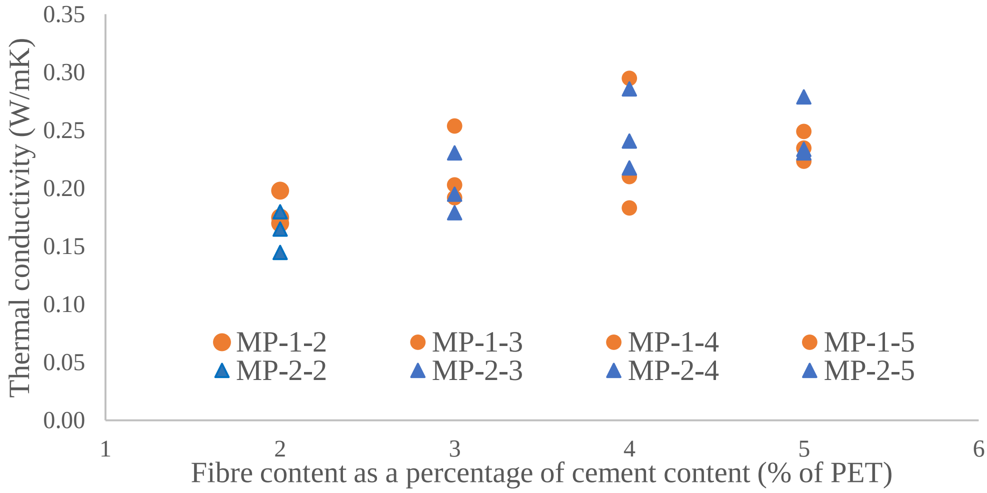

Figure 5.4 – Thermal conductivities of samples

5.4 Effective bond length and bond strength

Direct pull out the test was performed to determine the effective bond length for the developed ECC adhesive mix (MP-2-2). The samples were prepared by bonding CFRP fabric to the concrete block using selected ECC adhesive mix with bonding lengths; 50 mm, 75 mm, 100 mm, 125 mm, 150 mm and 175 mm.

Table 5.3 - Results of direct pull out test

Sample code	Bond length (mm)	Failure load (kN)	Bond slip at failure (mm)	Bond strength (N/mm^2)
MP2-2-50	50	0.35	1.6	28.11
MP2-2-75	75	0.75	2.566	60.24
MP2-2-100	100	1.5	2.851	120.48
MP2-2-125	125	2.7	2.998	216.87
MP2-2-150	150	2.8	3.265	224.90
MP2-2-175	175	2.75	4.372	220.88

Initial preparations of the concrete block were done as described in Chapter 3.5. Then, a 5 mm thick layer of ECC adhesive mix was applied and on top of it, a 75 mm wide CFRP fabric was laid. Finally, another 5 mm thick layer of ECC adhesive was applied.

For all the samples, bond failure occurred at ECC-CFRP interface. This can be seen in Figure 5.5.

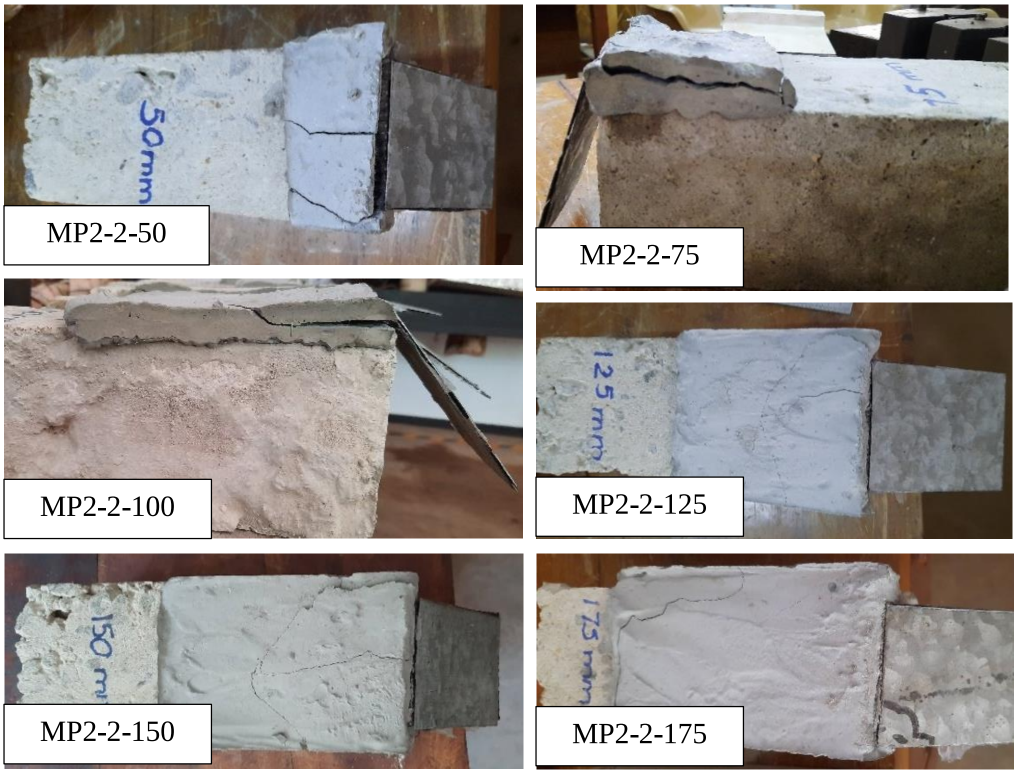

Figure 5.5 – Failure modes in samples

Wu and Li [40] fabricated the direct pull-out test samples with an adhesive thickness of 25 mm for their developed ECC adhesive. For a higher thickness of a cementitious adhesive layer, the addition of extra dead load to the structure is considerable high. The ECC adhesive developed by the authors has a unit weight of 1895.04 kg/m^3. The unit weight of epoxy is around 600 kg/m^3 if 1 mm thick layer of epoxy is applied. Therefore, it is more productive to maintain a lower ECC thickness to reduce the loading on the structure. To make the product economical feasible, the cementitious adhesive should be developed such that it gains the expected strength with a lower cementitious adhesive thickness. Therefore, a 5 mm thick bond was maintained between concrete and CFRP fabric. Another 5 mm layer of ECC was applied on top of ECC to enhance both bonding ability and thermal performance. Table 5.3 shows the results of the direct pull-out test performed.

Figure 5.6 presents the bond strength vs. bond length relationship to determine the effective bond length of the developed cementitious adhesive. From the bond length 50 mm to 150 mm, bond strength was kept on increasing rapidly. For bond lengths, 150 mm and 175 mm, the respective bond strengths deviated in the range of 220 N/mm^2 – 225 N/mm^2. Therefore within that bond length range, bond strength has not deviated considerably. It shows that after the bond length reached 150 mm, bond strength has reached a limiting state. Hence, it can be concluded that the effective bond length of ECC adhesive is 150 mm.

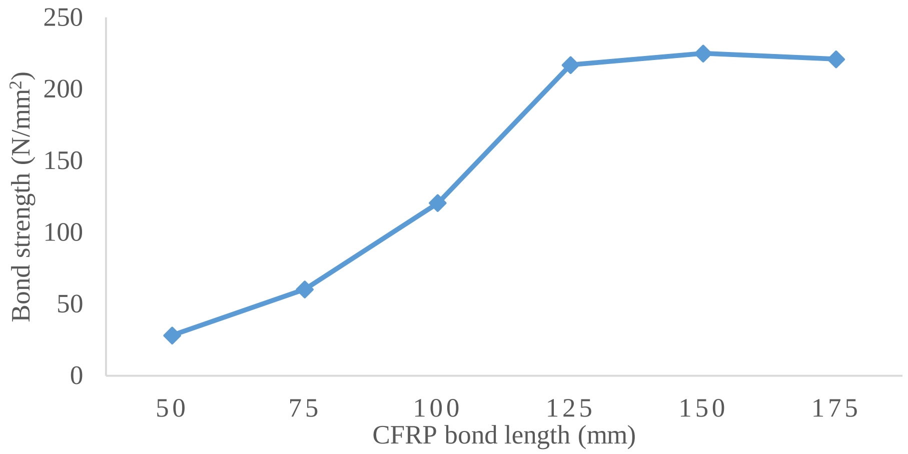

Figure 5.6 – Bond strength vs. bond length

5.5 Enhancing bond strength

Since the bond failure occurred in between the cementitious adhesive and CFRP fabric, appropriate strategies need to be followed to further enhance the bond strength. This could be done by increasing the surface energies. One way of enhancing the surface energies is by creating surface friction between two surfaces. Therefore, attempts were taken to roughen the contact surface. As the first attempt, sand was adhered on both sides of CFRP fabric using epoxy adhesive before adhering it to concrete block using the cementitious adhesive (E-M-S-1/2) (Figure 5.7 (a)). Sand used to stick on CFRP fabric was taken after sieving from 1.7 mm sieve.

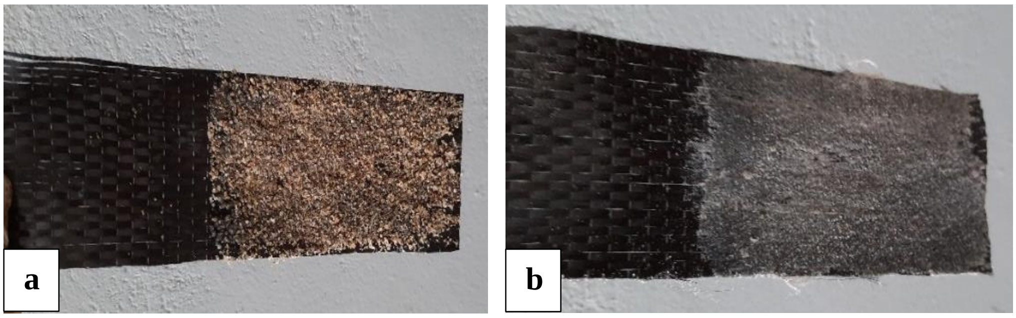

Figure 5.7 (a) Sticking sand on CFRP fabric (b) Sticking silica sand on CFRP fabric

In the next option, sand was replaced with silica sand (E-M-SS-1/2) (Figure 5.7 (b)). The third option was to change the nature of the cementitious adhesive. This was done by producing cementitious adhesive slurry instead of mortar mix (E-S-N-1/2). To develop ECC slurry, silica sand content was removed from the paste. No attempt was taken to enhance the surface friction along with this option.

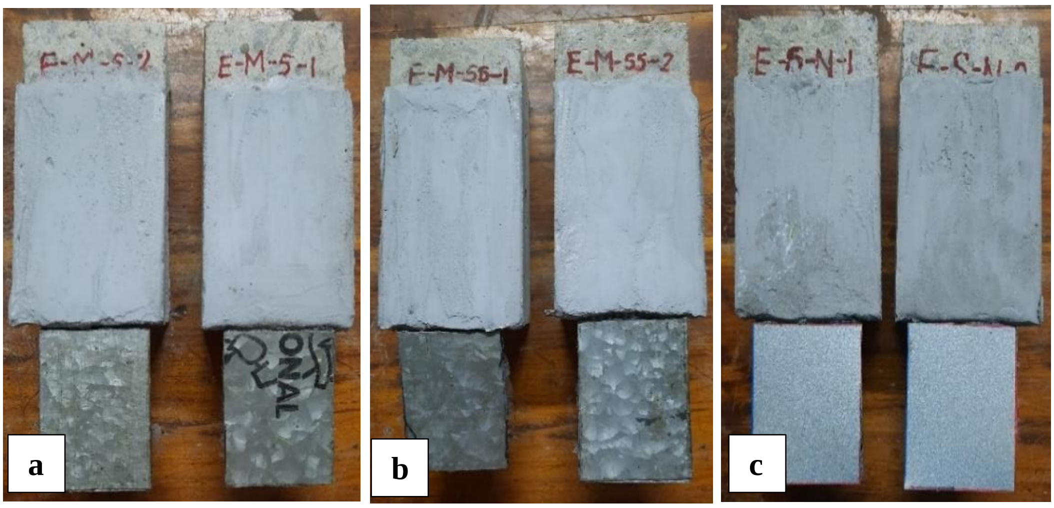

Figure 5.8 – Fabricated samples to perform direct pull out test (a) E-M-S-1/2 (b) E-M-SS-1/2 (c) E-S-N-1/2

Symbol: E-M-S-1

ECC mix

Mortar – M / Slurry - S

Sample number

CFRP Surface roughening technique

SS - Adhesion of silica sand
S – Adhesion of sand
NS – No modification

Two samples for each option was fabricated. 150 mm is the bond length used in all the samples. Figure 5.8 shows all the fabricated samples to perform the direct pull-out test. Test results are given in Table 5.4.

Table 5.4 – Test results of bond strength enhancing techniques

Sample code	Failure load (kN)	Average bond strength (N/mm^2)	Percentage strength enhancement with respect to the control sample	Failure mode
Epoxy	8.35 (Average)	670.68	-	Bond failure between the epoxy adhesive and CFRP fabric
MP-2-150 (Control sample)	2.8 (Average)	224.90	-	Bond failure between the cementitious adhesive and CFRP fabric
E-M-SS-1	5.50	449.80	100%	Bond failure between the cementitious adhesive and CFRP fabric
E-M-SS-2	5.75			
E-M-S-1	7.15	570.28	158%	Bond failure between the cementitious adhesive and concrete surface
E-M-S-2	7.1			
E-S-N-1	1.65	124.50	-45%	Bond failure between the cementitious adhesive and CFRP fabric
E-S-N-2	1.45			

As mentioned in Table 5.4, all the other options instead of E-M-S showed the bond interface failure between CFRP fabric and cementitious adhesive.

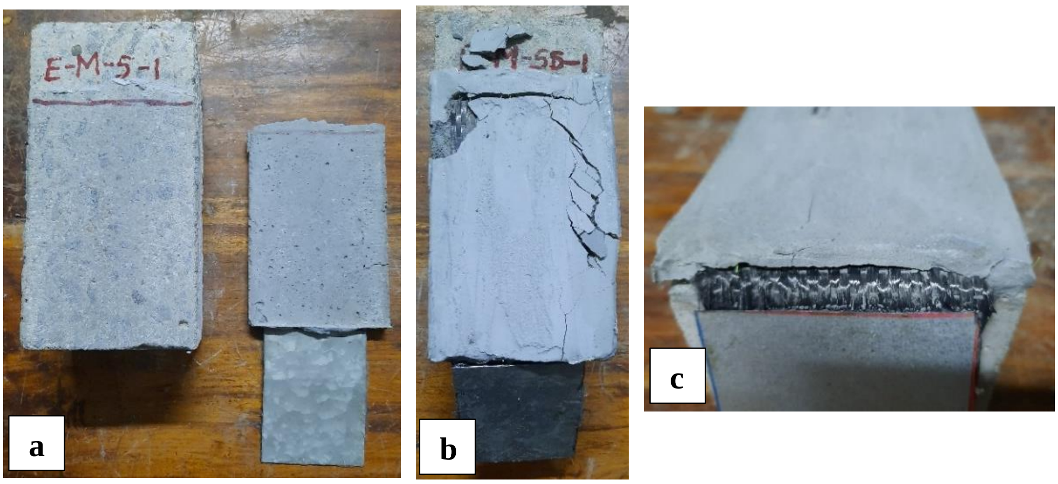

Figure 5.9 – Bond failure occurred in each bond strength enhancing technique

Results depict that both samples which used surface roughening technique yielded higher strength enhancement. Use of ECC slurry for bonding CFRP has reduced the bond strength. Therefore, it is clear that expected strength enhancement was not achieved by that option. The option where the sand adhered to CFRP achieved the expected bond failure and the highest strength enhancement. The bond strength achieved by this option shows a 14.97% deviation from epoxy bond strength which is relatively low when compared with other options. Its failure mode concludes that the bond between CFRP and the cementitious adhesive has reached to a better state. Figure 5.9 further clarify the bond failure occurred in each option.

5.6 Material properties of ECC adhesive

Prepared ECC adhesive mix was poured into six moulds with the dimensions of 70 mm x 70 mm x 70 mm to prepare samples for compressive strength test (Figure 5.10). After leaving samples in the mould for 1 day, they were demoulded. Then these samples were cured in the air (26 ± 3 ^{0}C; 74 ± 5%). The test was done in accordance with ASTM C109 [50]. Three cubes were used to measure the 7 days compressive strength and remaining 3 was used to measure 28 days strength. Results are mentioned in Table 5.5.

Table 5.5 – Compressive strength test results

Sample	Failure load (kN)	Compressive strength (N/mm^2)		
		7 days	14 days	28 days
1	92.8	18.94	-	-
2	83.6	17.06	-	-
3	73.0	14.90	-	-
4	148.2	-	30.24	-
5	150.4	-	30.69	-
6	149.0	-	30.41	-
7	273.9	-	-	55.90
8	246.5	-	-	50.31
9	255.3	-	-	52.10
Average compressive strength		16.97	30.45	52.77

The uniaxial tensile test was done in accordance with ASTM C190-85 to determine the tensile strength of the ECC adhesive [93]. Hounsfield Tensometer was used to conduct the test (Figure 5.11 (a)). Dumbbell shaped samples were cast as given in Figure 5.11 (b) and they were loaded in Hounsfield Tensometer as shown in Figure 5.11 (c). Mixing of the adhesive sample was done in accordance with ASTM C305 [94]. Uniaxial tensile strength results are given in Table 5.6.

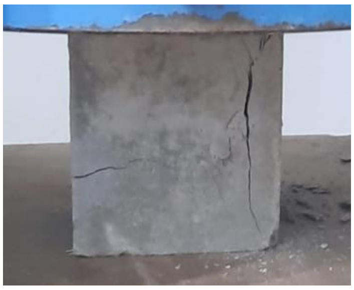

Figure 5.10 – Testing the compressive strength

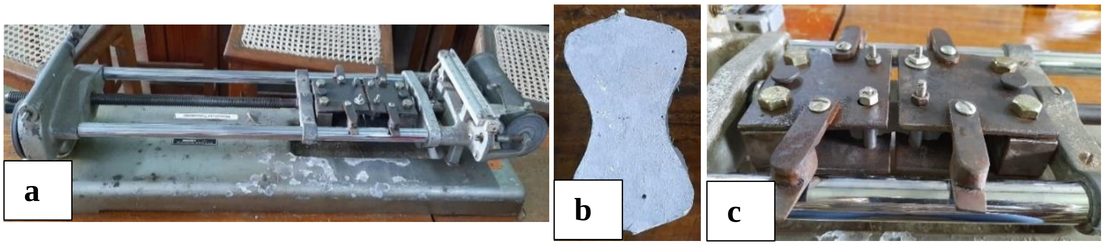

Figure 5.11 - (a) Hounsfield Tensometer (b) Dumbbell shaped sample (c) Mounting the sample

The 28 days compressive strength achieved by modified ECC mortar at room temperature is higher than that of the compressive strength of ECC developed using PVA in several other studies [38], [40], [48], [49]. But the experimental studies on tensile strength of ECC developed using PVA fibres deviates from 3 MPa to 5 MPa [40], [48], [49]. The current study gives a tensile strength within this range. As per book chapter by Li [91], the typical tensile strain of ECC ranges between 1-8%.

The flexural strength of the developed ECC adhesive was tested in accordance with EN 1015-11 - Methods of test for mortar for masonry [95]. Figure 5.12 (a) presents how the test was conducted and Figure 5.12 (b) shows the failure mode of a sample. Test results are summarized in Table 5.7. The 28 days flexural strength for ECC was not able to test as result of the interruptions caused due Covid-19 pandemic.

Table 5.6 – Tensile strength test results

Number of days cured	Sample	Width (mm)	Thickness (mm)	Load (kN)	Tensile strength (N/mm^2)
7 days	1	26.6	24.42	0.9	1.39
	2	26.6	24.48	0.97	1.48
	3	26.58	24.48	1.01	1.55
	Average tensile strength at 7 days				1.47
14 days	1	26.44	24.52	1.52	2.34
	2	26.5	24.5	1.47	2.26
	3	26.58	24.42	1.59	2.45
	Average tensile strength at 14 days				2.35
28 days	1	26.8	24.4	2.40	3.67
	2	26.6	24.5	2.58	3.96
	3	26.3	24.5	2.49	3.86
	Average tensile strength at 28 days				3.83

The average mass of the samples was 0.65 kg. According to the block dimensions, the density of the ECC adhesive was calculated as 1895.04 kg/m^3.

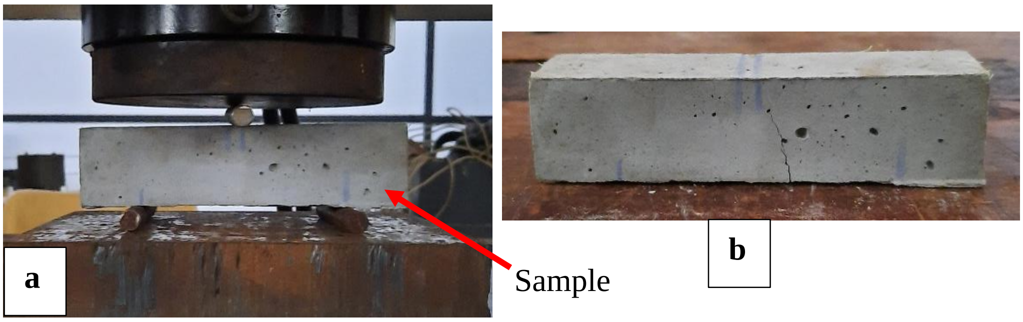

Figure 5.12 – (a) Conducting the three point bending test (b) Failure mode of a sample

Table 5.7 – Flexural strength test results

Number of days cured	Sample	Width (mm)	Depth (mm)	Load (kN)	Flexural strength (N/mm^2)
7 days	1	39.98	40	2.3	5.39
	2	39.72	39.8	2	4.77
	3	39.8	40.12	2.5	5.85
	Average flexural strength at 7 days				5.34
14 days	1	40.08	39.88	3	7.06
	2	40.32	40.3	3.3	7.56
	3	39.82	39.74	2.8	6.68
	Average flexural strength at 14 days				7.10

5.7 Thermal performance

In order to determine the thermal performance of cementitious adhesive, pull out test was done elevating the bond temperature up to 150 ^{0}C. While fabricating the samples for the test, the bonding length of CFRP was maintained as 150 mm. When preparing the samples, a K-type stainless steel shield thermocouple was laid on the bond line to monitor the bond temperature during testing. Figure 5.13 shows the test setup used for elevated temperature testing.

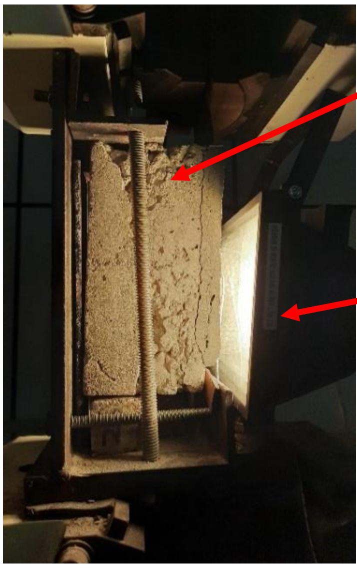

Figure 5.13 – Testing the sample

Table 5.8 shows the results of the test and results are presented in a graphical format in Figure 5.14. Figure 5.15 shows the failure mechanism observed during testing. This also shows that the temperature increment does not create a considerable influence on the bond between CFRP fabric and cementitious adhesive even though the bond strength enhancement between CFRP and cementitious adhesive was achieved by sticking sand on CFRP using the epoxy adhesive which is sensitive to the high temperature. It further proves that the bond strength enhancement technique implemented in the current study enables to resist the higher temperature of bondline than the epoxy bond.

Table 5.8 – Test results of the thermal performance of ECC adhesive

Adhesive type	Sample code	Bond temperature (^0C)	Failure load (kN)	Bond strength (N/mm^2)
ECC	ECC30	30	7.13	572.69
	ECC40	40	7.1	570.28
	ECC60	60	6.9	554.22
	ECC80	80	6.88	552.61
	ECC100	100	6.73	540.56
	ECC120	120	1.18	94.78
	ECC150	150	0.43	34.54
Epoxy	E30	30	8.35	670.68
	E40	40	8.25	662.65
	E60	60	8.10	650.60
	E80	80	3.40	273.09
	E100	100	2.55	204.82
	E120	120	2.05	164.66

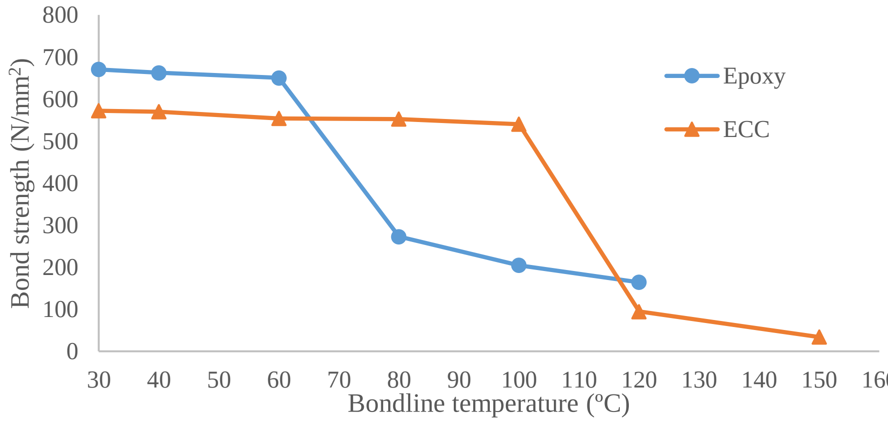

Figure 5.14 – Bond strength – Bondline temperature graph

With increased surrounding temperature, the bond strength between cementitious adhesive and concrete maintained a stable state up to 100 ^0C. From 100 ^0C to 120 ^0C, the bond strength underwent a drastical drop as shown in Figure 5.14 and it further lowered when bondline temperature reached 150 ^0C. This showed that the ECC-concrete bond becomes weak between 100 ^0C to 120 ^0C. The bond is sensitive to higher temperatures. Beyond 120 ^0C, the bond reached to a further weaker state.

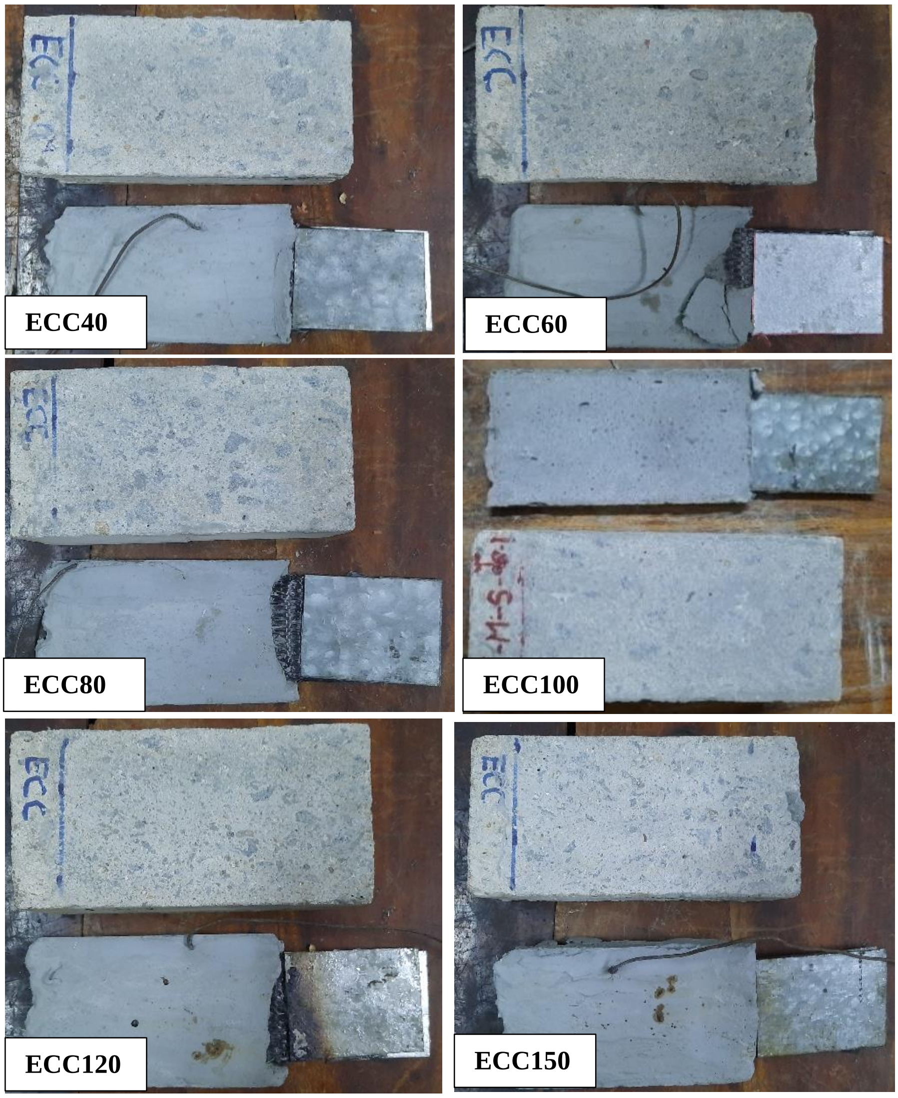

Figure 5.15 – Failure modes of samples

5.8 Chapter summary

A cementitious adhesive to bond CFRP fabric with concrete was developed using ECC mortar. ECC was developed using locally available materials. Preliminary experiments on the mortar mix were done in order to develop it as an adhesive. Initially, two ECC was developed with two different proportions adapted and modified from literature. Depending on the results obtained through thermal conductivity test and considering the literature on previous experiments done by researchers, a suitable proportion was selected to develop ECC adhesive. The selected weight proportion of cement: silica sand: fly ash: water is 1: 0.8: 1.2: 0.85. The PET fibre content is 2% of the volume of cement. The effective bond length for the particular mortar mix was decided as 150 mm depending on the direct pull-out test results. Since the bond strength was comparatively lower than that of pure epoxy, different techniques were employed to find a better way to enhance the bond strength. As per the final test results, sticking sand on CFRP fabric using epoxy adhesive before bonding it to concrete using cementitious adhesive was found out as the best option to improve the interface between CFRP and ECC based adhesive. The bond glass transition temperature of ECC adhesive lies in between 100 ^{0}C – 120 ^{0}C while it is between 60 ^{0}C – 80 ^{0}C for epoxy adhesive. This indicated that the ECC upgraded adhesive performs well at the ambient condition as well as in elevated temperature.

6 COMPARISON OF DEVELOPED PRODUCTS AND APPLICATION FEASIBILITY

6.1 Introduction

Checking the applicability of a product is another important stage in its development process. Therefore the developed adhesive systems were used to bond CFRP to a column prototype to assess the feasibility in the application. After a proper curing process, the fabricated samples were checked for enhancement of axial confinement to observe whether the adhesive systems have achieved the expected outcomes. Then the adhesive systems were checked for their mechanical properties. Due to the time constraints and prevailing situation in the country (Covid-19 pandemic), application on thermal shear and torsional strengthening were could not be assessed.

6.2 Comparison of developed products

Table 6.1 compares the performance of the pure epoxy, modified epoxy and ECC adhesives. The modified epoxy adhesive showed a 28.8% enhancement in tensile strength at 7 days when compared with pure epoxy adhesive. The addition of PET fibres has resulted in this increment. However, the ambient conditions at the time of testing tensile strength in two adhesive types are different. The tensile strength achieved by ECC adhesive is higher than the tensile strength of cement mortar containing fly ash [96], [97]. The tensile strength of ECC mortar developed using PVA fibres deviate between 3 N/mm^2 to 5 N/mm^2 [40], [48], [49].

Table 6.1 – Comparison of adhesives

	Pure epoxy	Modified epoxy (PETCO-EPOXY)	ECC adhesive (ECC-ECO)
Tensile strength (N/mm^2)	45 (7 days at 20 ^{0}C) [76]	63.21 (7 days at 30 ^{0}C)	3.82 (28 days at 30 ^{0}C)
Glass transition temperature of bond	60 ^{0}C - 80 ^{0}C	> 120 ^{0}C	> 100 ^{0}C
Effective bond length (mm)	-	100	150
Percentage bond strength reduction when the bond temperature was increased to 100 ^{0}C	69.46%	10.15%	5.21%

CFRP fabrics bonded using pure epoxy showed a bond glass transition temperature between 60 ^{0}C to 80 ^{0}C. However, it was higher than that for modified epoxy and ECC (Table 6.1). Therefore the thermal resistivities of both the developed adhesives are better than pure epoxy. The effective bond length of ECC adhesive is higher than the modified epoxy adhesive. When the bond temperature of samples fabricated with each of the adhesives was increased to 100 ^{0}C, the indicated bond strength reduction in both developed adhesives are lower than the reduction observed in pure epoxy fabricated samples. Further, then ECC adhesive showed the lowest bond strength reduction. Therefore, it can be concluded that the performance of both developed adhesives is better than the performance of pure epoxy at elevated temperatures.

6.3 Application of developed adhesives on column prototypes

Application in real scale members in the laboratory conditions is not feasible. Hence, the concrete cylinders of 200 mm height and 100 mm diameter were used to retrofit using CFRP with developed adhesives. These concrete cylinders were cast using Grade 25 concrete. Initially, 3 concrete cylinders were tested for their compressive strength after 28 days of curing, without any strengthening technique.

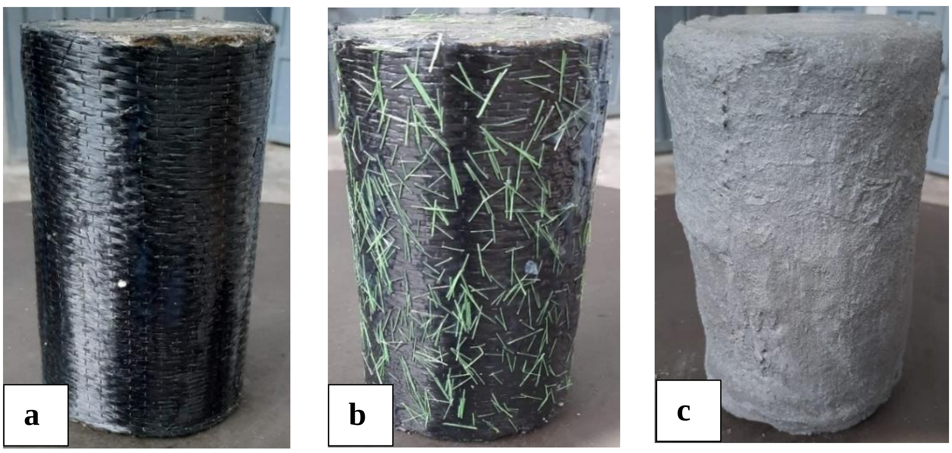

Figure 6.1 – CFRP bonded using (a) pure epoxy adhesive (b) modified epoxy adhesive (c) ECC adhesive

Before applying any adhesive, cylinders were grinded for better bonding. Then the grinded surfaces were wiped using a wet cloth to remove the dust particles. These cylinders were kept to dry for about 30 minutes. Three cylinders were strengthened using epoxy adhesive. A set of cylinders were strengthened using modified epoxy adhesive while another set was wrapped with CFRP fabric using ECC adhesive. All these samples were kept for 7 days of curing prior testing. The fabricated samples are shown in Figure 6.1. The acquired results are given in Table 6.2.

Table 6.2 – Test results of CFRP strengthened cylinders

Sample	Average failure load (kN)	Compressive strength (N/mm^2)	Strength enhancement
Concrete cylinder	187.5	23.87	-
Concrete cylinder bonded with CFRP using epoxy adhesive	463.9	59.07	147%
Concrete cylinder bonded with CFRP using modified epoxy adhesive	496.85	63.26	165%
Concrete cylinder bonded with CFRP using ECC adhesive	250.35	31.88	34%

According to the experimental results obtained, in all the cases, the compressive strength of strengthened samples has increased. However, the highest strength increment can be observed in the concrete cylinders strengthened with CFRP using modified epoxy adhesive. The strength enhancement achieved by wrapping CFRP on concrete cylinders using pure epoxy adhesive is about 147%. This enhancement has been further incremented up to 165% by modifying the epoxy adhesive using PET fibres. Therefore, the feasibility in the application of the modified epoxy adhesive in strengthening columns is apparent. The strength achieved by wrapping CFRP using epoxy adhesive can be incremented by 12% if the epoxy adhesive is replaced with modified epoxy adhesive. The strength enhancement achieved by wrapping CFRP using ECC adhesive is about 34%. This strength enhancement is a comparatively less value when compared with the strength enhancement gained using epoxy adhesive. This lagging in the performance can be lowered by implementing techniques to enhance the bond between ECC adhesive and concrete substrate.

Figure 6.2 shows how each category of samples failed under compressive loading. In both cases where epoxy adhesive and modified epoxy adhesive were used, failed in both CFRP rupture and debonding. In samples where ECC adhesive was used, failed mainly due to the debonding between the adhesive and concrete substrate.

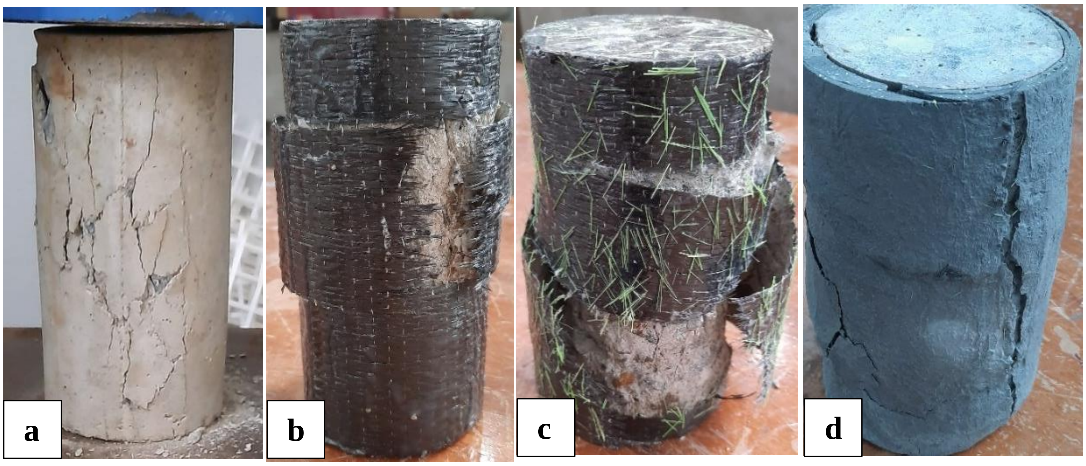

Figure 6.2 – Failure modes of concrete cylinders (a) without CFRP (b) CFRP wrapped with pure epoxy adhesive (c) CFRP wrapped with modified epoxy adhesive (d) CFRP wrapped with ECC adhesive

6.4 Chapter summary

A study was carried out on pure epoxy, modified epoxy and ECC adhesives to compare performance. Both developed adhesives showed better performance at elevated temperatures when compared with the response of pure epoxy at elevated temperature. In order to determine how efficiently the developed adhesives perform under real scenarios, they were used to bond CFRP fabric to small scale concrete cylinders. Then these samples were tested for their compressive strength to determine whether the adhesives function properly in bonding the CFRP fabric to the concrete substrate. Samples, where the modified epoxy adhesive was used, showed the highest strength enhancement. It showed a strength enhancement which is higher than that of the samples bonded using pure epoxy. Therefore, it can be considered as a better product than the epoxy adhesive. Even though the samples adhered using cementitious adhesive showed a strength enhancement compared to unstrengthened concrete cylinders, it did not exceed the strength enhancement of samples where pure epoxy was used.

7 NUMERICAL MODELLING

7.1 Introduction

Carrying out experimental studies to perform extensive research consumes higher cost and time. To avoid this drawback, a computer-simulated Finite Element (FE) Model can be developed. Development of such a model can be used to address a wide range of the research gap and even the prediction of the performance of structure can be made. This chapter describes the model developed to simulate the CFRP bonded concrete composite using the developed ECC based adhesive.

7.2 Finite Element Analysis (FEA)

Manual application of FEA theories in complex structures is a time consuming hard task. To overcome this issue, different FE modelling software which were developed by applying FE theories in the algorithm can be used. Abaqus FEA is a suite of FE analysis modules used in this study [98]. An Abaqus analysis follows three different stages to complete a task;

- Preprocessing
- Simulation
- Post-processing

In the preprocessing stage, a virtual model of the real scenario is defined. The model is usually created graphically. In the next stage, the defined model is analyzed using Abaqus/Standard or Abaqus/Explicit. Analysis time depends on the complexity of the problem. Once the simulation completes, results can be evaluated. Therefore in the post-processing stage evaluation is generally done visually.

7.3 Finite Element Model

A three-dimensional FE model was developed for the direct pull-out test using a FE modelling software [98]. A computer with an Intel(R) Core(TM) i5-4200U processor and an 8 GB RAM was used to run the model.

7.3.1 Model geometry

Table 7.1 gives the dimensions of the model developed to simulate the behaviour of CFRP/concrete system when testing using the single lap shear method. Both the dimensions of the top ECC layer and bottom ECC layer are the same. Figure 7.1 shows the image of the developed model.

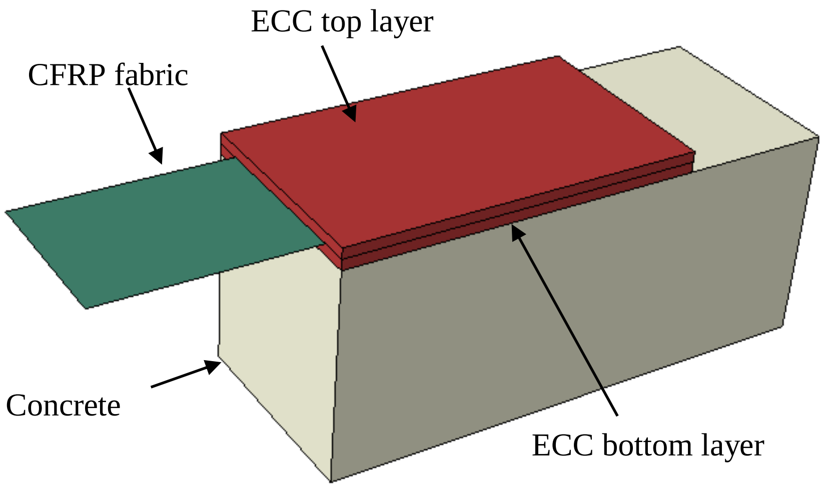

Figure 7.1 – Developed model

Table 7.1 – Dimensions of the model

Part	Length (mm)	Width (mm)	Height (mm)	Thickness (mm)
Concrete block	250	100	100	-
ECC adhesive layer	Vary	100	-	5
CFRP fabric	Vary	75	-	0.166

7.3.2 Defining Elements

The eight-node linear hexahedral solid element with reduced integration (C3D8R) was used to model both concrete block and ECC adhesive layers (Figure 7.2 (a)) [98]. The four-node quadrilateral membrane shell element with reduced integration (M3D4R) was used to model CFRP fabric (Figure 7.2 (b)) [98].

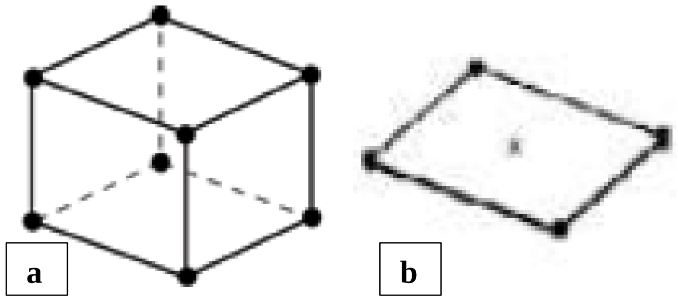

Figure 7.2 – (a) C3D8R element (b) M3D4R [98]

7.3.3 Mesh Size Analysis

Mesh convergence analysis was carried out to determine the optimal mesh size. According to the results, the element size of 2 mm was used for the ECC adhesive layer and CFRP fabric meshed with 2.5 mm elements were used. The concrete block was meshed using 10 mm x 10 mm elements. The aspect ratio of elements was kept between 0.5 and 1. Figure 7.3 (a) shows the developed mesh of the model.

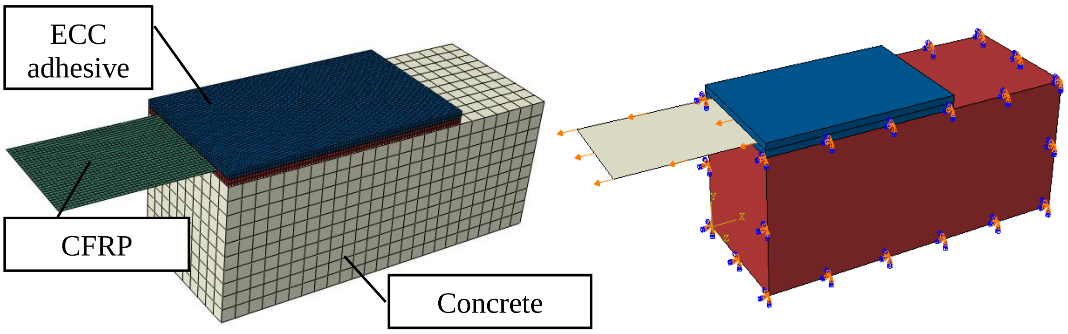

Figure 7.3 - (a) Meshed model (b) Boundary conditions and loading

7.3.4 Boundary conditions

All the moments and translations of the concrete block were restricted in the FE model as in the experimental setup. Loading was simulated as a gradual displacement in CFRP fabric. Figure 7.3 (b) presents the applied boundary conditions and loading.

7.3.5 Material models

The Concrete Damage Plasticity (CDP) model was used to assign the nonlinear behaviour of concrete [99]. The CDP model developed assumes that the two main failure mechanisms in concrete are the tensile cracking and the compressive crushing

[99]. Therefore both tensile and compressive behaviours need to be defined. To define the stress-strain relationship under tension, young's modulus (E_0), total strain (ε_t) and tensile strength (σ_t) of concrete were used [99]. Young's modulus was calculated using the Equation 7.7. Equations 7.1 and 7.2 gives the cracking strain and plastic strain values.

$$\tilde{\varepsilon}_t^{ck} = \varepsilon_t - \varepsilon_{ot}^{el} \quad \text{Eq (7.1)}$$

$$\tilde{\varepsilon}_t^{pl} = \tilde{\varepsilon}_t^{ck} - \frac{d_t}{(1-d_t)}\frac{\sigma_t}{E_0} \quad \text{Eq (7.2)}$$

Where,

ε_{ot}^{el} = Elastic strain = σ_t / E_0

ε_t = Total tensile strain

$\tilde{\varepsilon}_t^{ck}$ = Cracking strain

d_t = Tensile damage parameter = cracking strain/total strain

$\tilde{\varepsilon}_t^{pl}$ = Plastic strain

The tensile stress-strain curve was developed as shown in Figure 7.4. Developed tensile stress vs. strain curve for Grade 30 concrete is given in Figure 7.5.

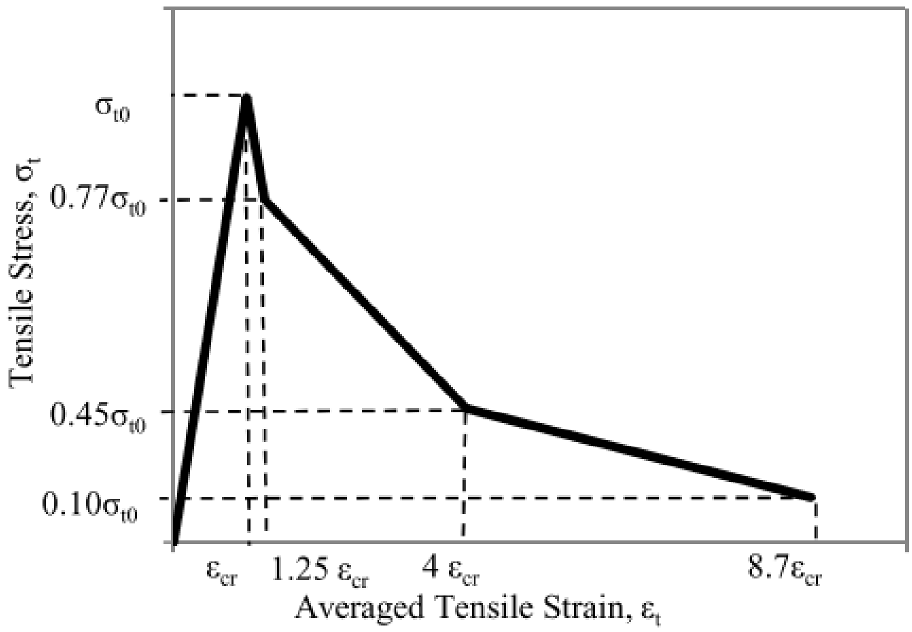

Figure 7.4 – Modified tension stiffening model for ABAQUS [99]

In the same manner, to develop the compressive stress-strain relationship, both compressive strength and compressive strain are required (Equation 7.3-7.8). Equation 7.5 was used to develop the graph between $0.5\sigma_{cu}$ and $0.3\sigma_{cu}$ (Figure 7.6). Developed compressive stress vs. strain graph for Grade 30 concrete is given in Figure 7.7.

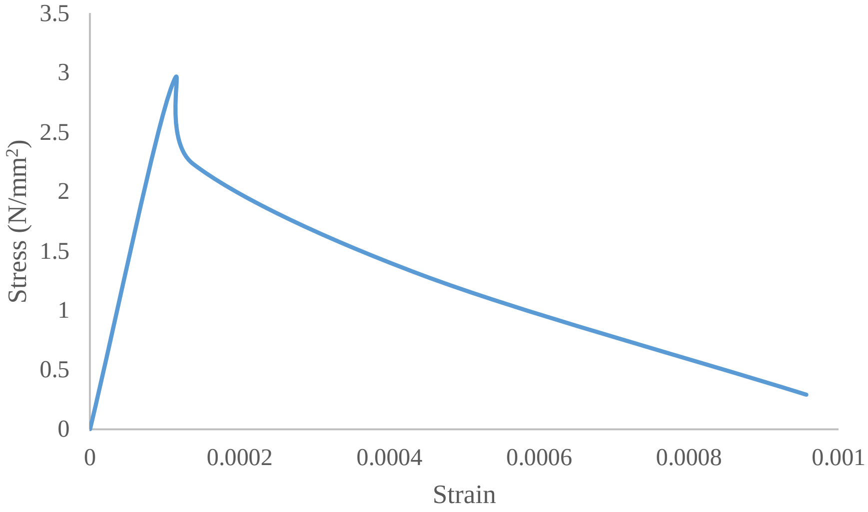

Figure 7.5 – Tensile stress vs. strain graph of Grade 30 concrete

$$\tilde{\varepsilon}_c^{in} = \varepsilon_c - \varepsilon_{oc}^{el} \qquad \text{Eq (7.3)}$$

$$\tilde{\varepsilon}_c^{pl} = \tilde{\varepsilon}_c^{in} - \frac{d_c}{(1-d_c)} \frac{\sigma_c}{E_0} \qquad \text{Eq (7.4)}$$

$$\sigma_c = \frac{\beta(\frac{\varepsilon_c}{\varepsilon_0})}{\beta - 1 + \left(\frac{\varepsilon_c}{\varepsilon_0}\right)^{\beta}} \sigma_{cu} \qquad \text{Eq (7.5)}$$

$$\beta = \frac{1}{1 - [\frac{\sigma_{cu}}{\varepsilon_0 E_0}]} \qquad \text{Eq (7.6)}$$

$$E_0 = 124.31\,\sigma_{cu} + 3283.12 \qquad \text{Eq (7.7)}$$

$$\varepsilon_0 = 8.9 \times 10^{-5}\sigma_{cu} + 2.114 \times 10^{-3} \qquad \text{Eq (7.8)}$$

Where,

ε_{oc}^{el} = σ_c / E_0

E_0 = Initial tangential modulus

$\tilde{\varepsilon}_c^{in}$ = Inelastic strain

ε_0 = Strain at peak stress

d_c = Compressive damage parameter = inelastic strain/total strain

In the above equations σ_c, σ_{cu} and E_0 are given in kip/in^2.

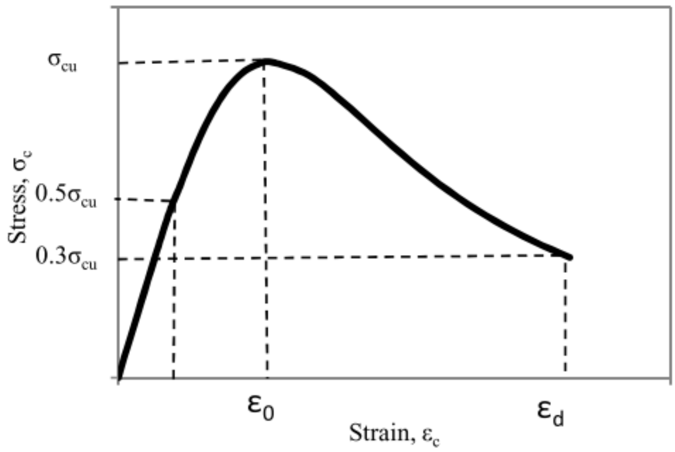

Figure 7.6 – Compressive stress-strain relationship for ABAQUS [99]

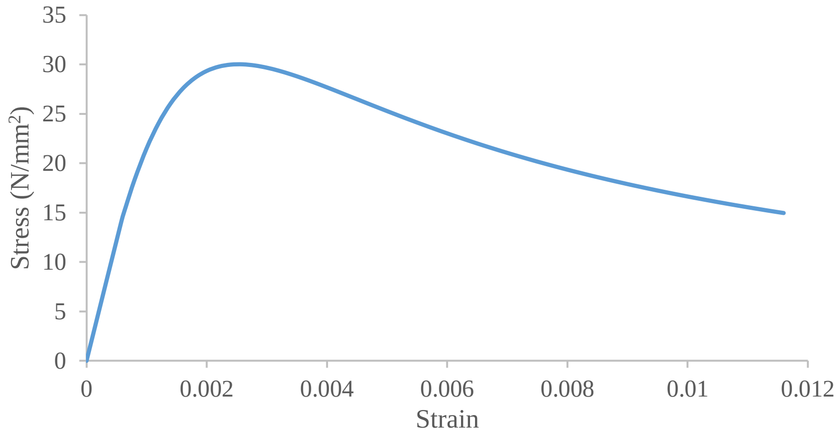

Figure 7.7 – Compressive stress vs. strain graph of Grade 30 concrete

Properties used for concrete are given in Table 7.2.

Table 7.2 – Properties for ECC and concrete

Properties	ECC	Concrete
Density (kg/m^3)	1895.04	2400
Dilation angle	37	37
Eccentricity	0.1	0.1
fbo/fco	1.16	1.16
K	0.667	0.667
Viscosity parameter	0	0

Nehdi and Ali [43] simulated ECC using both the CDP model and Drucker/Prager (DP) model. Li and Zhang [100] have highlighted the effectiveness of modelling dynamic actions of cementitious materials using the CDP model. Therefore the CDP model was used in modelling ECC. Properties used for the material model of ECC adhesive are given Table 7.2. Figures 7.8 and 7.9 show the tensile and compressive stress vs. strain graphs of ECC, respectively. CFRP fabric was modelled as a Lamina [98]. Table 7.3 gives the parameters used to define the material model of CFRP fabric [101].

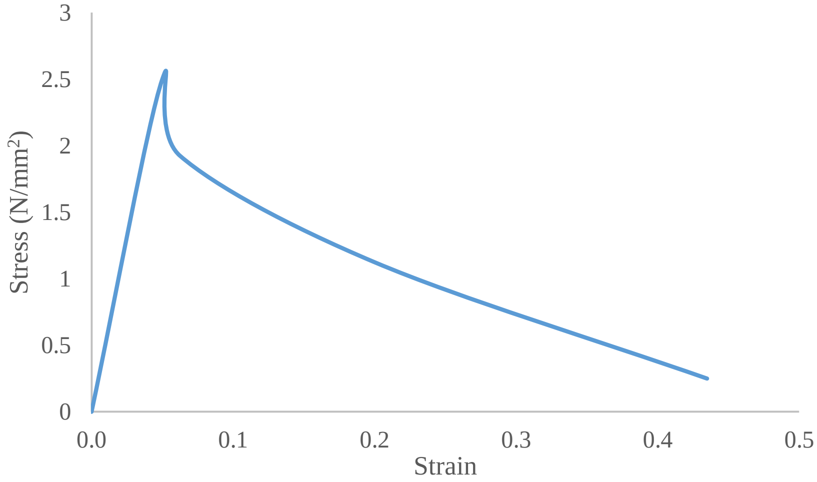

Figure 7.8 – Tensile stress vs. strain graph of ECC

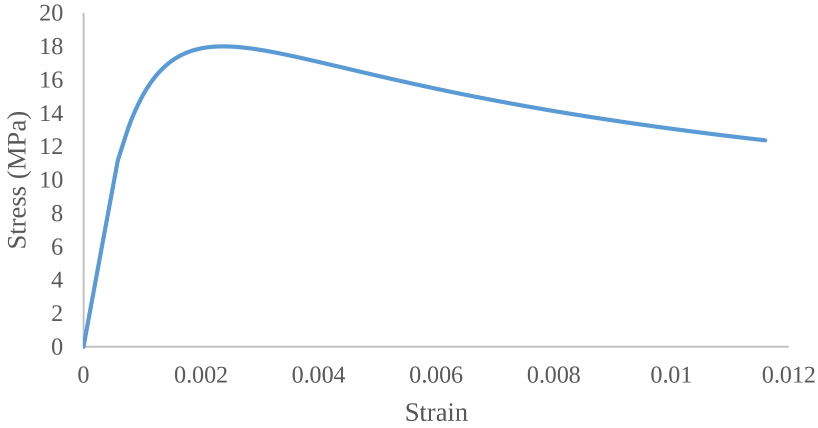

Figure 7.9 – Compressive stress vs. strain graph of ECC

Table 7.3 – Material properties of CFRP fabric [101]

Parameter	Value
E1 (N/m^2)	2.3E+11
E2 (N/m^2)	23000000000
Nu12	0.3
G12 (N/m^2)	6894000000
G13 (N/m^2)	6894000000
G23 (N/m^2)	4136000000
Density (kg/m^3)	0.3

7.3.6 Bond slip behaviour

A considerable bond-slip was observed in ECC – CFRP interface. Therefore, it was necessary to accompany the bond-slip behaviour with the adhering properties of ECC adhesive. This was stimulated by introducing a cohesive contact interaction for the contact surfaces along with damage initiation and damage evolution criteria. It follows the traction-separation law proposed by Camanho et al. [102] which defines that once the damage initiation is reached, the bond will undergo progressive damage. The elastic uncoupled traction-separation behaviour is defined by Equation (7.9).

$$T = \begin{Bmatrix} t_n \\ t_s \\ t_t \end{Bmatrix} = \begin{bmatrix} K_{nn} & 0 & 0 \\ 0 & K_{ss} & 0 \\ 0 & 0 & K_{tt} \end{bmatrix} \begin{Bmatrix} \delta_n \\ \delta_s \\ \delta_t \end{Bmatrix} = K\delta \qquad \text{Eq.(7.9)}$$

Here, the nominal traction stress vector “T” consists of 3 components t_n, t_s, t_t which are the normal traction and 2 shear tractions, respectively. δ_n, δ_s and δ_n are the corresponding displacements. Henriques et al. [103] have defined K_{nn}, K_{ss} and K_{tt} as given in Equations (7.10) and (7.11).

$$K_{ss} = K_{tt} = \frac{\tau_m}{s_m} \qquad \text{Eq.(7.10)}$$

$$K_{nn} = 100K_{ss} = 100K_{tt} \qquad \text{Eq.(7.11)}$$

τ_m is the maximum bond strength and s_m is the corresponding displacement at maximum bond strength. Interface bonding between ECC adhesive and concrete block was modelled as a Tie constraint.

7.4 Validation

Figure 7.10 compares the experiment load vs displacement graph for 150 mm bonding length with the predicted one. In both instances, graphs follow a similar path. In between 1 mm to 1.5 mm displacement, there happens to be a sudden increment in load as can be seen in the measured data. This sudden load increment is also evident in the FE model graph. Failure load predicted by the FE model was 2.87 kN and the corresponding displacement was 3.4 mm. Experiment failure load was 2.8 kN and the corresponding displacement was 3.3 mm. Therefore, the deviation of the predicted failure load from the actual failure load is about 2.5%. In the same manner, the deviation of predicted displacement at failure load from actual displacement is 3%. Therefore it can be deduced that the developed FE model has a good agreement with the actual experimental setup.

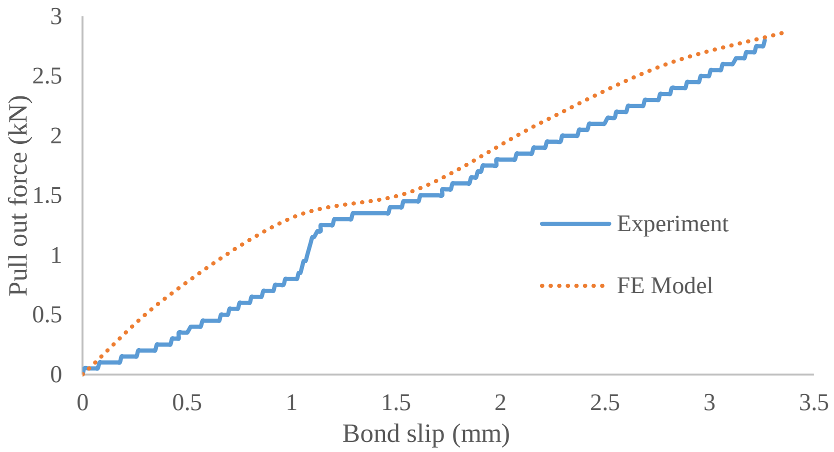

Figure 7.10 - Load vs. Displacement graph for the effective bond length 150 mm

Figure 7.11 shows the crack initiation of specimens. Figure 7.12 shows how cohesive interaction has damaged. In other words, it is how the debonding has occurred in ECC-CFRP interface. As per the predicted model, cohesion between bottom ECC adhesive layer and CFRP has greatly deteriorated. But this is comparatively less between CFRP and top ECC adhesive layer. This mechanism can be further explained with the resultant movement of the top ECC adhesive layer along with the CFRP fabric. The resultant movement of the top ECC adhesive layer is shown in Figure 7.13. So as per the model, both top ECC adhesive layer and CFRP fabric together show an upward inclined movement. This movement needs to be the reason behind the crack initiation occurred as given in Figure 7.12.

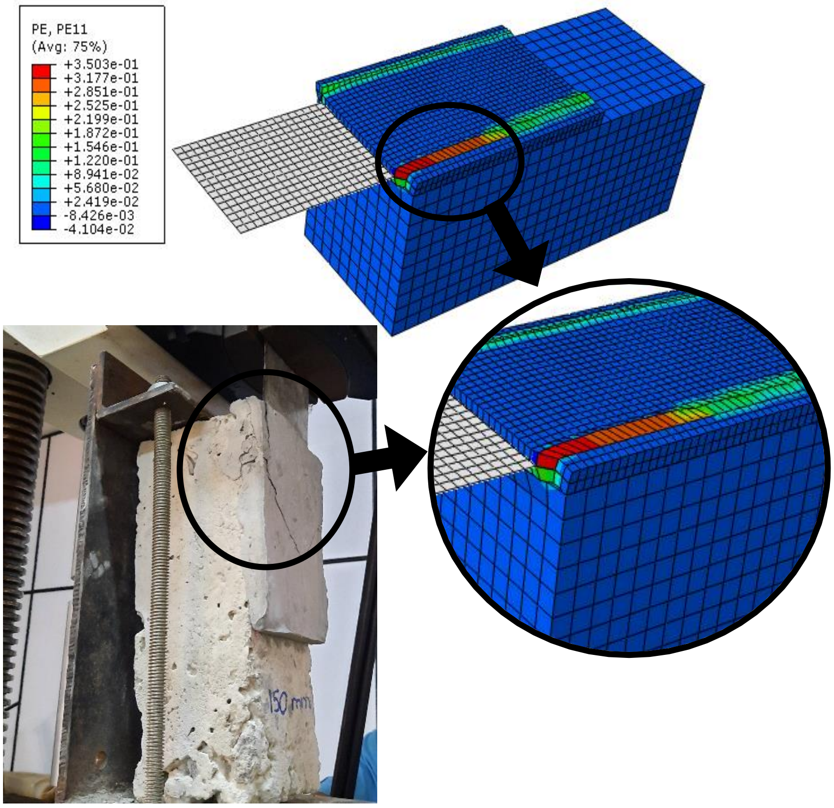

Figure 7.11 - Crack initiation in the test setup

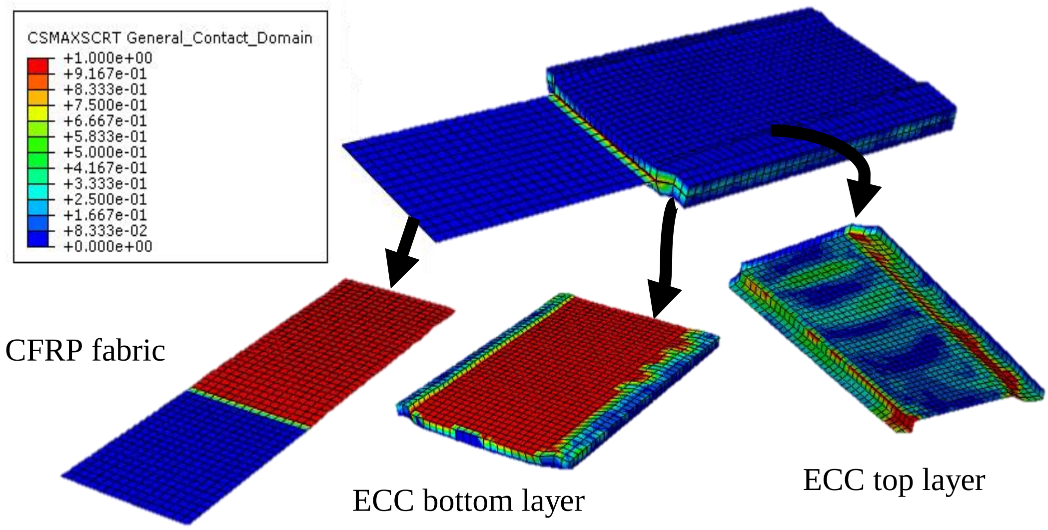

Figure 7.12 - CFRP-ECC interface debonding

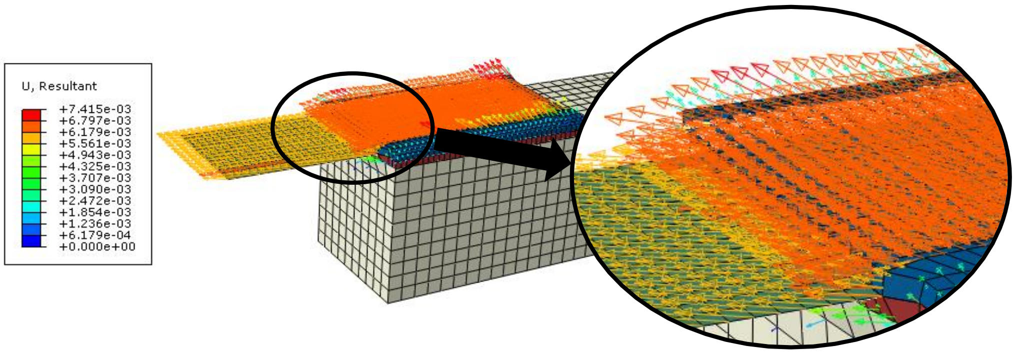

Figure 7.13 - Resultant movement of the top ECC adhesive layer

The same model was modified and used in predicting the performance of bond characteristics of composite with ECC adhesive system. The bond between ECC and concrete was changed from a tie constraint to a cohesive interaction. Figure 7.14 compares the experiment load vs displacement graph with the predicted one. Both graphs follow a comparatively similar path. However, the predicted pull out forces are slightly higher than the experiment pull out force values throughout the graph for a particular displacement.

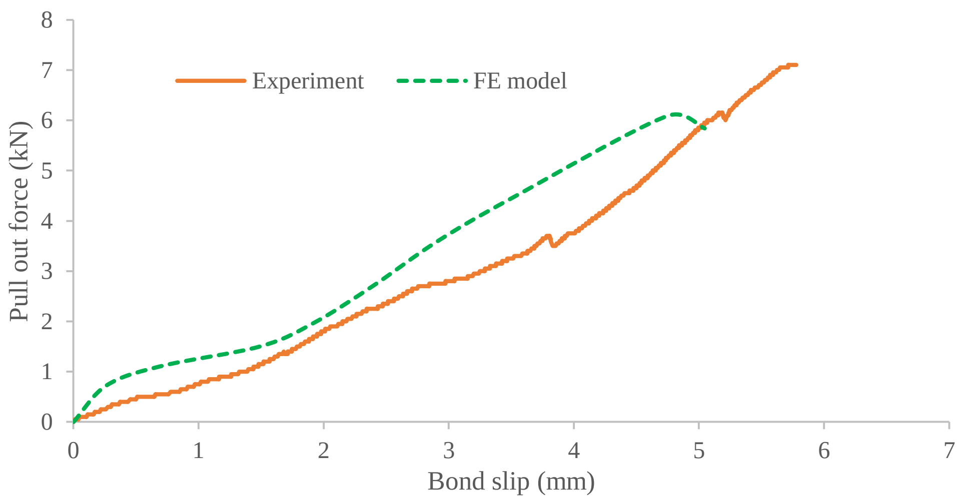

Figure 7.14 – Load vs. displacement graph for bond strength enhanced setup

However, the ultimate failure load of the FE model is 6.08 kN whereas the failure load of the experimental setup is 7.1 kN. Therefore, the predicted value shows a 14.37% deviation from the actual value. Displacement at failure load in the experimental setup is 5.78 mm while it is 4.75 mm in the FE model. Therefore the predicted displacement shows a 17.82% of increment from the actual displacement. This is fairly a good prediction for the actual scenario.

Figure 7.15 shows how bond failure occurred between ECC adhesive and concrete. Predicted results are similar to the actual scenario.

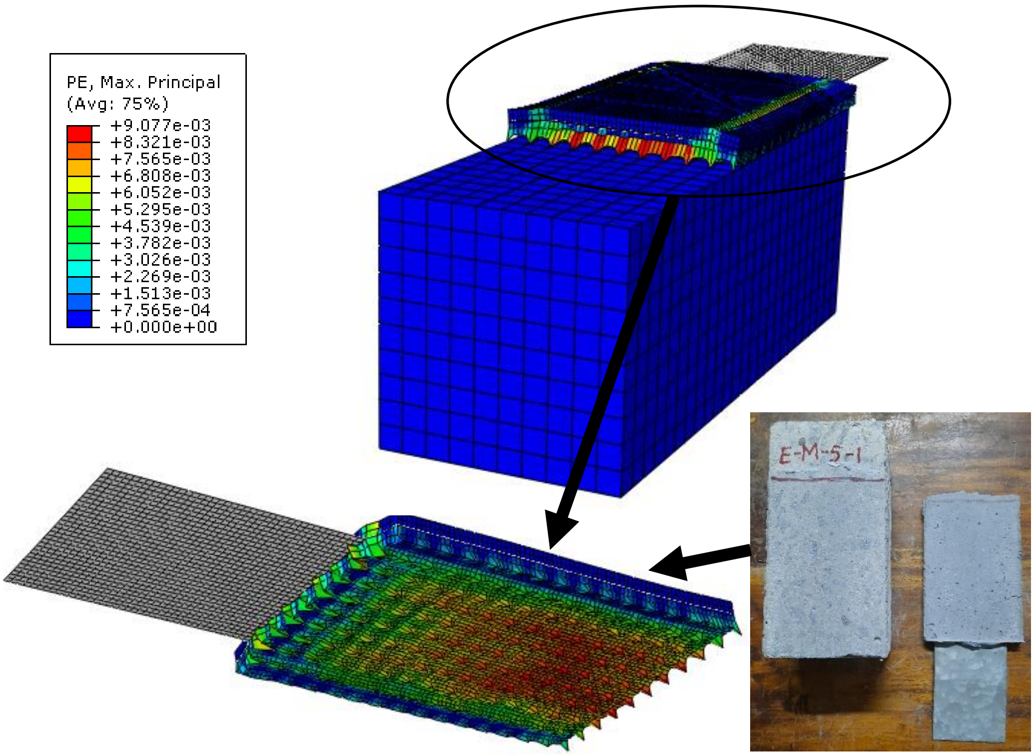

Figure 7.15 – ECC – Concrete interface surface bonding failure

Therefore, it can be concluded that this is a valid model to predict the behaviour of the actual scenario.

7.5 Parametric studies

7.5.1 Effect of bondline thickness of ECC adhesive

For the experimental study, the bondline thickness of the ECC adhesive used was 5 mm. Therefore, a parametric study was carried out to determine how the bondline thickness of the adhesive layer influences the bond strength between developed ECC adhesive and CFRP fabric (Figure 7.16). The thickness of the ECC layer applied on top of CFRP fabric was maintained constant as 5 mm throughout the study. Failure loads for adhesive bondline thicknesses of 2.5 mm, 5 mm, 10 mm and 15 mm were 5.39 kN, 6.58 kN, 2.08 kN and 4.31 kN, respectively. The corresponding displacements at failure loads were 3.76 mm, 5.25 mm, 5.45 mm and 5.01 mm. The failure load at 5 mm adhesive bondline thickness is nearly equivalent to 1.2 times the failure load corresponding to 2.5 mm adhesive bondline thickness. Thus, the failure load enhancement is 22.1% of the failure load for 2.5 mm adhesive bondline thickness. In the sample with adhesive bondline thickness of 2.5 mm, failure tends to occur in CFRP-ECC bottom layer interface. In the sample with 5 mm bondline thickness, failure occurred in concrete-ECC bottom layer interface. Therefore, the increase of bondline thickness has incremented the bond failure load. During these two instances, ECC bondline thickness was below or equal to the ECC layer on top of CFRP. However, during next instances where bondline thickness was higher than the top ECC layer thickness, a considerable drop was observed in bond strength.

When the bondline thickness was further incremented up to 10 mm, the failure load showed a drastic drop down to 2.08 kN. The FE model indicated that the failure was more likely to happen as an interface failure between CFRP and bottom ECC layer. In this case, the thickness of the bondline was 10 mm while the ECC layer thickness on top of CFRP was 5 mm. Therefore, it can be deduced that the thickness of both the bottom and top layers of ECC affect the bond strength of CFRP. For better bonding, the thickness of the top and bottom layers at least need to be maintained equally. This can be further proved by the predicted results of the sample with 15 mm adhesive bondline thickness. When the bondline thickness was incremented up to 15 mm from 10 mm, the bond failure load showed an increment. Yet the failure mode predicted was the interface failure between CFRP and ECC bottom layer and the failure load was below the corresponding failure loads of samples with 2.5 mm and 5 mm bondline thicknesses.

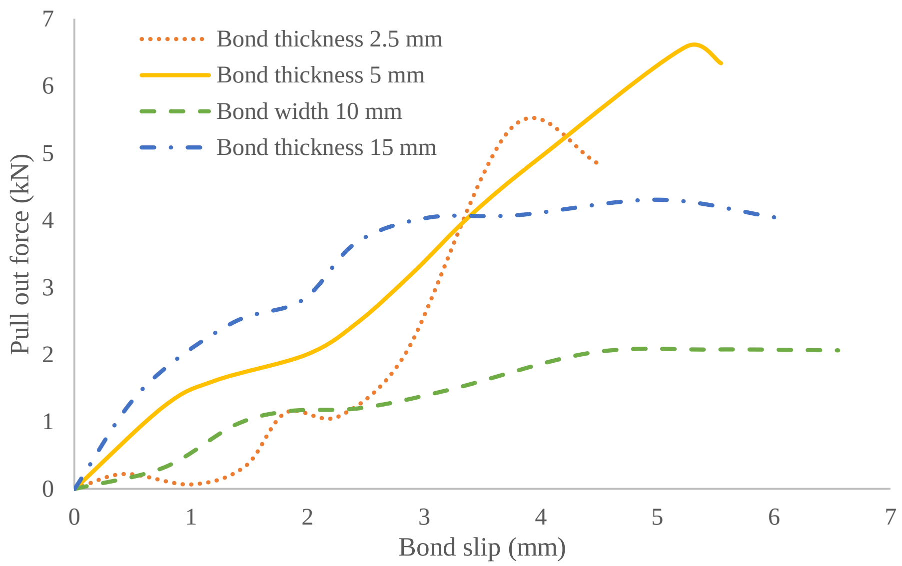

Figure 7.16 - Effect of ECC adhesive thickness

7.5.2 Effect of bond width of CFRP

A parametric study was performed to understand the effect of CFRP bond width on the bond performance (Figure 7.17). This was done by changing the CFRP bond width to 25 mm, 50 mm and 90 mm. For a 25 mm wide CFRP bond width, failure load was 1.18 kN. As per the simulation, CFRP strip tends to pull out with part of the ECC layer on top of it during the failure (7.18 (a)). The corresponding bond-slip at failure was 3.31 mm. This failure load further increased up to 2.10 kN, when the CFRP bond width was incremented to 50 mm. The corresponding bond-slip predicted was 5.10 mm. Therefore, the bond failure load enhancement from 25 mm bond width to 50 mm bond width is 78%. However, in both cases, samples were more likely to fail in CFRP-ECC interface as per the predicted model (7.18 (a) and (b)). The predicted pull out load for 75 mm wide bond was 6.58 kN and the respective bond-slip was 5.25 mm. In the experimental setup, the failure occurred in ECC-concrete interface. This was evident in the predicted model.

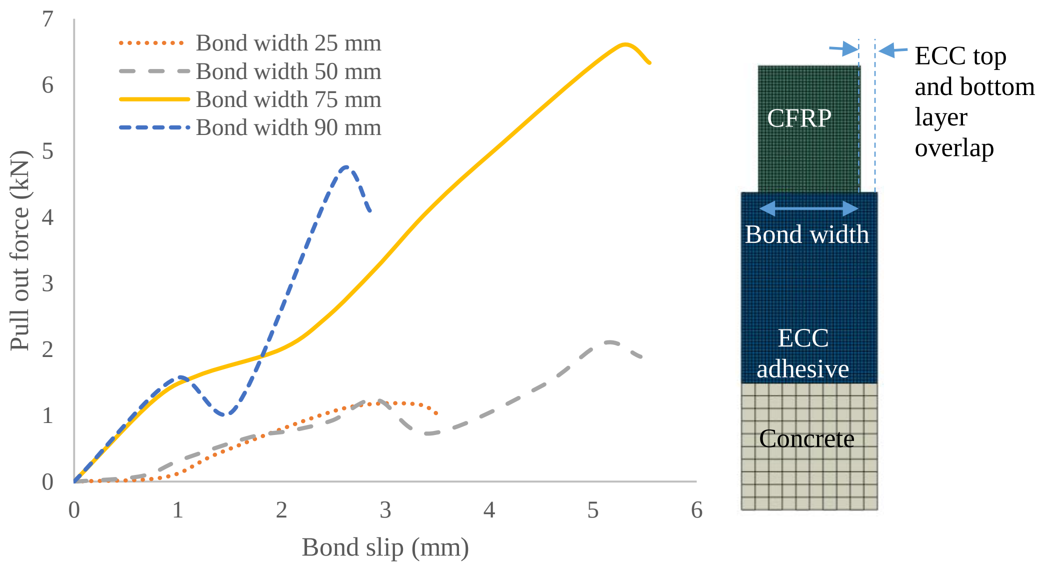

Figure 7.17 – Effect of CFRP bond width

When the bond width was further incremented up to 90 mm, failure load decreased to 4.68 kN. Therefore the predicted failure load reduction from 75 mm bond width to 90 mm bond width was 29%. The crucial observation in the predicted model for 90 mm bond width was the bond failure. Due to the reduction of ECC layer overlap from either side of CFRP fabric in 90 mm bond width sample, failure tends to occur in the bottom ECC layer-CFRP interface. As per the simulation, CFRP fabric got pulled out with the whole top ECC layer (7.18 (c)). The corresponding bond-slip was 2.56 mm. Therefore, it can be concluded that a considerable ECC top and bottom layer overlap of 12.5 mm should be maintained from either side of CFRP fabric for a good bond performance. Moreover, a bond width of more than 75 mm should be maintained in CFRP strengthening using ECC adhesive.

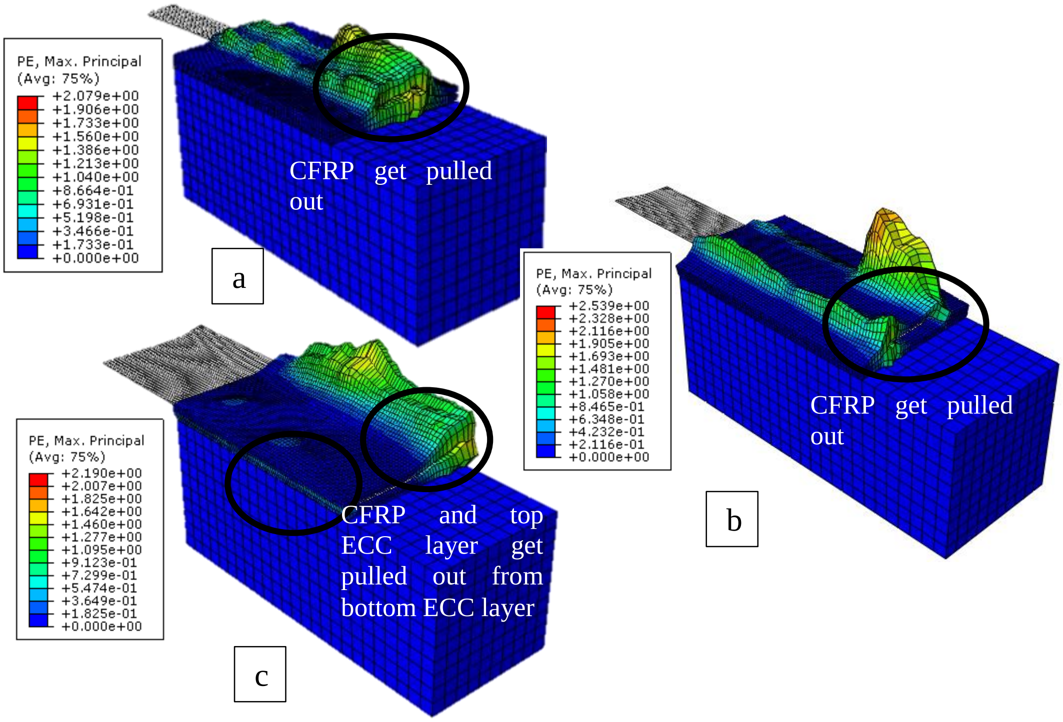

Figure 7.18 – Bond failure modes predicted by FE models

7.5.3 Bond stress along the bondline at different load levels

The bond stress deviation along a bondline parallel to the direction of the force applied was analyzed for different load levels (Figure 7.19). The bondline along the midpoint of 75 mm wide CFRP fabric was selected for the analysis. The bondline distance was measured from the bond edge closer to the grip of the CFRP. The bond stress showed a higher value within the initial 20 mm distance along the bondline at 1kN load. This distance gradually increased with the increment of load level. At the failure, higher bond stresses were present within the first 40 mm distance along the bondline. The highest positive bond stress was present at 10 mm distance for all the load levels. The bond stress was below 17 N/mm^2 within the bondline length 40 mm to 160 mm for all the load levels. Therefore, less stress is applied along the mid-region of the bond. However, the bond stress showed a slight increment towards the end of the bondline.

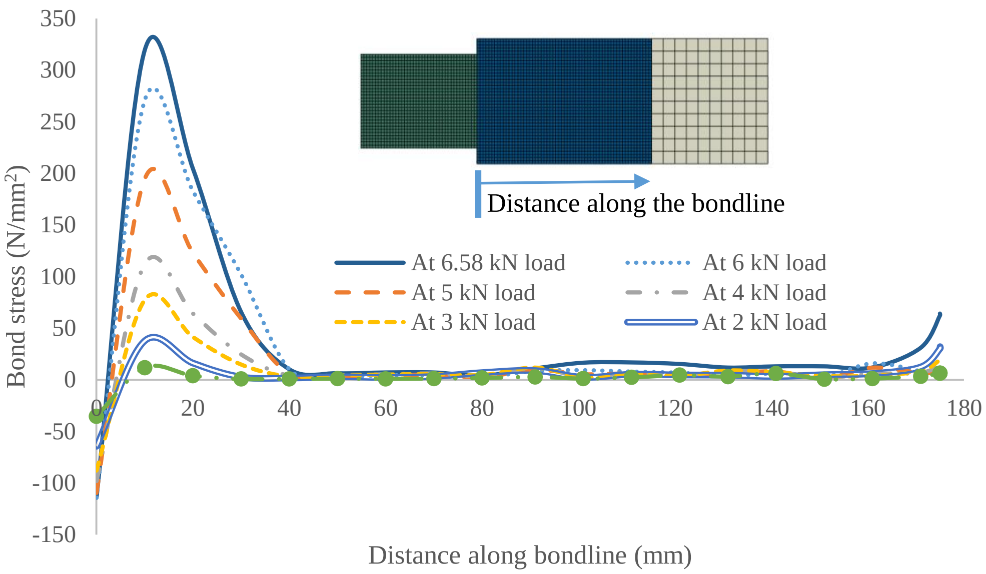

Figure 7.19 – Bond stress along bondline for different load levels

7.5.4 Bond shear stress along the bondline at different load levels

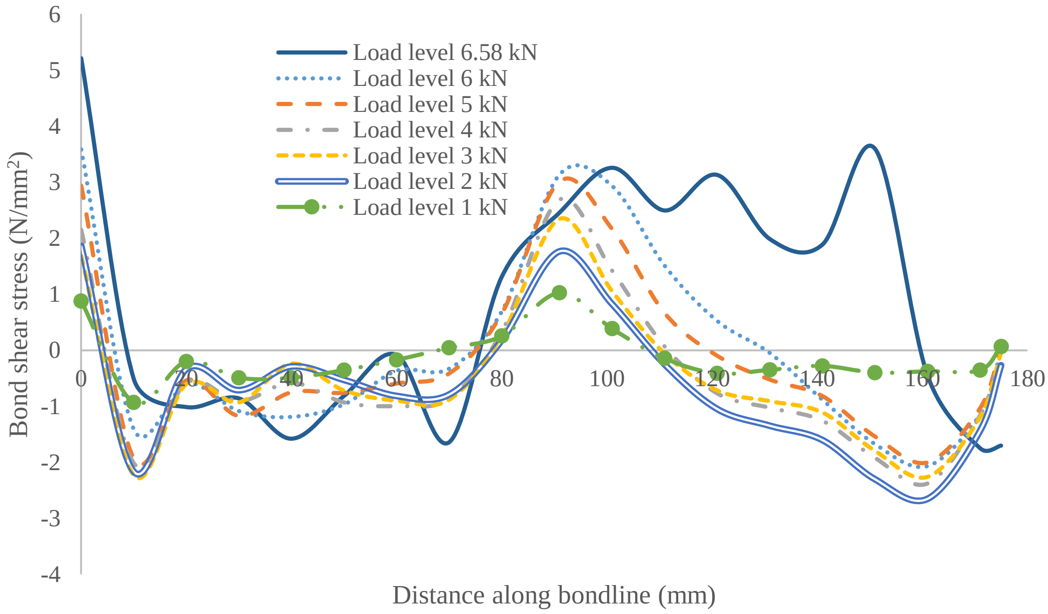

Figure 7.20 – Shear stress along bondline for different load levels

The bond shear stress deviation along a bondline parallel to the direction of the force applied was analyzed for different load levels. According to Figure 7.20, higher shear stress values are present at the bond edge closer to the loading region. Within the first 10 mm along the bondline, the shear stress undergoes a steep drop. Up to the mid-region of the bondline, shear stresses deviate in lower values. Around the mid-region of the bondline, shear stresses rise and gradually reach the lower values. The behaviour is fairly similar at all load levels. To the latter part of the bondline, shear stresses have undergone an increment in shear stresses at failure load.

7.5.5 Bond stress contours on CFRP fabric at different load levels

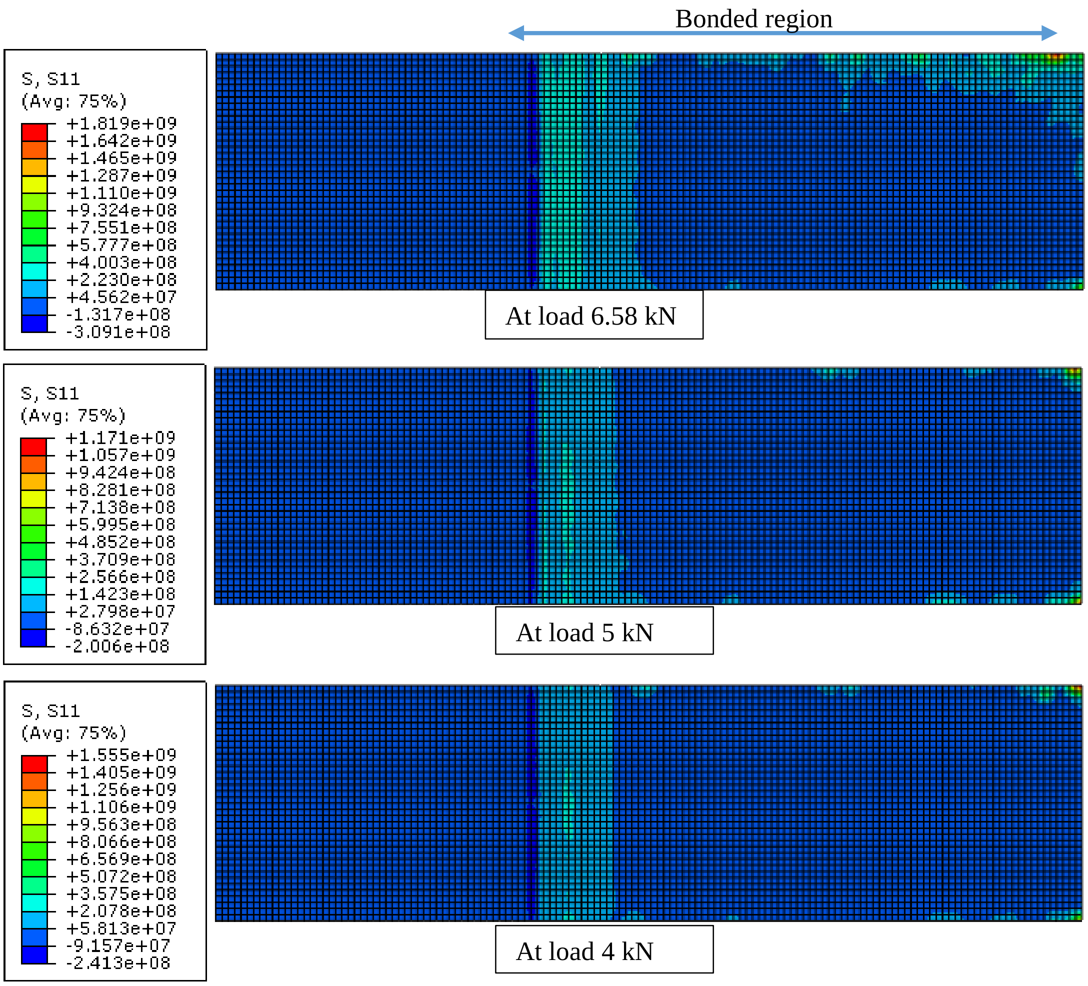

Figure 7.21 – Stress contours on CFRP for loads 6.58 kN, 5 kN and 4 kN

The stress contours of CFRP fabric at different load levels were compared to get an idea about the locations where stress concentrations are likely to be seen (Figure 7.21 and 7.22). During all the load levels, high-stress concentrations are seen near the end edge of CFRP bonded to the concrete. According to these results, it can be deduced that the interface failure between ECC and concrete initiated closer to this end edge.

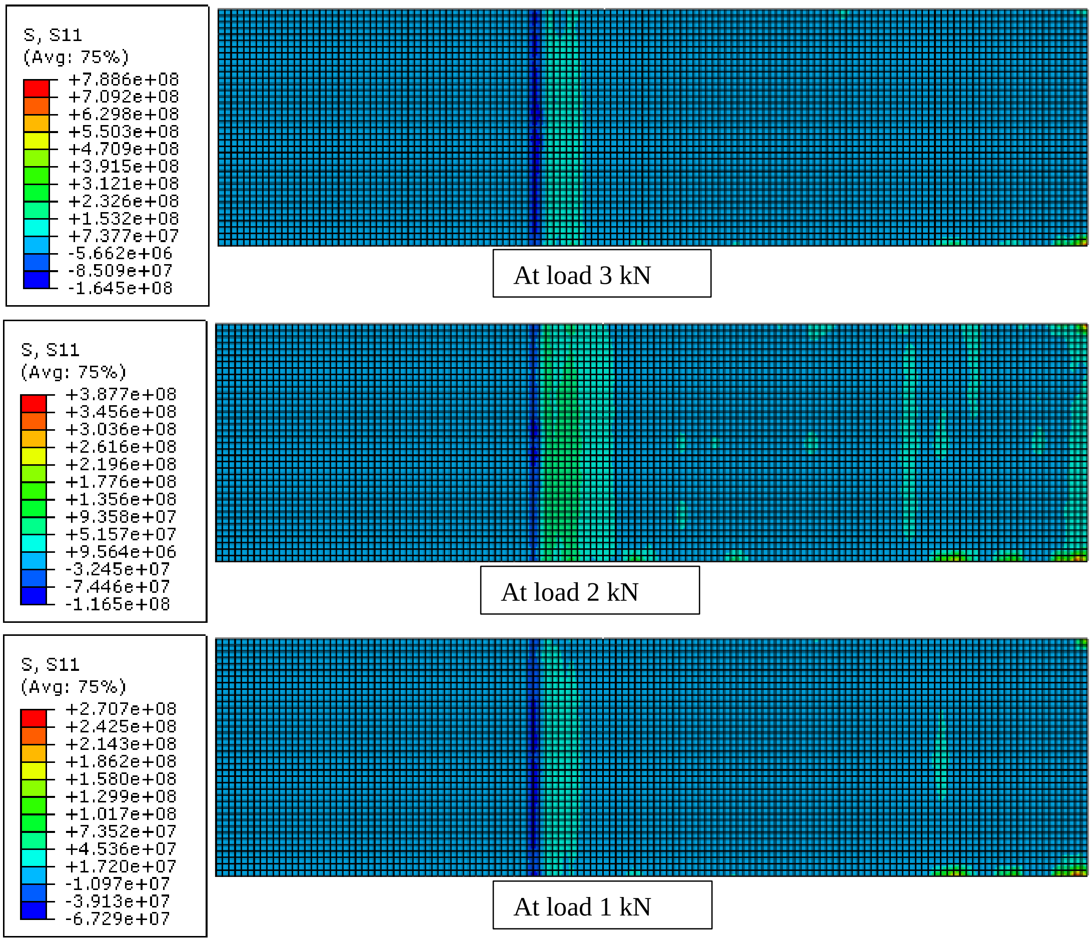

Figure 7.22 – Stress contours on CFRP for loads 3 kN, 2 kN and 1 kN

7.6 Chapter summary

This chapter includes the details of the FE model developed to predict the behaviour of direct pull-out test experimental results. The developed models behave similarly to the actual experimental setup. The developed model is in good agreement with the test results. Different parametric studies were carried out to analyze the behaviour of developed adhesive under different circumstances. The parametric study carried out by change of bondline thickness showed that both top and bottom layers affect the bond strength. Bond strength cannot be incremented by increasing only the thickness of the adhesive layer in the bondline. Further, the study carried out by changing the CFRP bond width showed that a considerable overlap of ECC top and bottom layers should be present for a better bond. However, very low bond strengths were shown by samples with CFRP bond width below 50 mm, even though a considerable ECC layer overlap was present. Moreover, bond strength and bond shear strength deviation along the bondline at different load levels were analyzed. The FE model showed that the bond strength gradually reaches a higher value with the increase of loading at the region 10 mm away from the bond edge closer to the loading. Highest bond shear stresses are present at the bond edge closer to the loading for all the load levels. But unlike in bond strength, the shear strength deviated in a greater range around the mid-region of the bonded area. The stress contours on the CFRP at different load levels showed that the ECC-concrete interface failure initiated at the bond edge away from the loading.

8 CONCLUSIONS AND RECOMMENDATIONS

8.1 Development of a cementitious adhesive

An experimental approach was taken to develop a cementitious adhesive to bond CFRP fabric to a concrete surface. Further, a FE model was developed to predict bond behaviour. The following conclusions were made using the results obtained.

1. In both mix proportions used to develop ECC adhesive, lower thermal conductivities were obtained when the PET fibre content is low
2. The thermal conductivity of ECC increased with the increase of fibre content
3. Fibre content as 2% of cement content is taken as the ideal fibre content to develop the cementitious adhesive depending on both thermal conductivity results and literature provided details
4. Both proportions showed similar thermal conductivities. However, MP-2 which was modified from ECC-M45 mix proportion showed lower thermal conductivity values for 2% fibre content
5. The mix proportion MP-2 with fibre content as 2% of cement content was selected as the best design mix proportion to develop the cementitious adhesive for CFRP fabric depending on both experimental results and literature. The weight proportion of cement: silica sand: fly ash: water is 1: 0.8: 1.2: 0.85
6. The thermal conductivity of the selected ECC mix proportion ranged between 0.145 - 0.18 W/mK. Therefore, this adhesive mix shows good insulating properties
7. The developed ECC adhesive shows a compressive strength of 52.77 N/mm^2 (28 days), tensile strength of 3.83 N/mm^2 (28 days) and a 14 days flexural strength of 7.1 N/mm^2
8. The effective bond length was obtained as 150 mm. The corresponding bond strength was 224.9 N/mm^2. The failure occurred between the CFRP-ECC adhesive interfaces
9. Attempts were taken to enhance surface free energy needs to incremented in contact surface by introducing a technique to develop friction

10. Bond was further enhanced to 570.28 N/mm^2 by sticking sand on top of CFRP fabric using epoxy adhesive before bonding it to a concrete substrate using developed ECC adhesive. The percentage bond strength enhancement achieved was 158%
11. The bond glass transition temperature of ECC adhesive ranges between 100 ^{0}C to 120 ^{0}C while it range between 60 ^{0}C to 80 ^{0}C for pure epoxy adhesive. Therefore, ECC adhesive performs better than epoxy adhesive in elevated temperature.
12. When the cementitious adhesive was used to bond CFRP to a column prototype, compressive strength of the concrete cylinder was enhanced by 34%. However, this strength enhancement is lower than that of the strength enhancement acquired by epoxy adhesive
13. The developed FE model for the direct pull out test and actual experiment show showed a good agreement with each other
14. The parametric study carried out by changing bondline thickness of ECC showed that the bond strength cannot be incremented by only increasing the bondline thickness. Both ECC bondline thickness and ECC top layer affect the bond strength
15. Very low bond strengths were achieved by bonding CFRP fabric below 50 mm width
16. A considerable top and bottom ECC layer overlap should be kept from either side of CFRP fabric for a better bond strength
17. Higher bond stresses were present in a region along the bondline which is 10 mm away from the bond edge closer to the loading

8.2 Modified epoxy adhesive

1. Epoxy adhesive modified by adding PET fibres showed a higher bond strength than pure epoxy adhesive
2. When the fibre content was incremented from 0% to 50%, the modified epoxy adhesive achieved the highest bond strength when the PET content is 10% of the volume of epoxy adhesive. It was 1168.67 N/mm^2. Compared to the

strength of the pure epoxy bond, the strength enhancement achieved by the modification is 91%.

3. The percentage of strength enhancement reduces when the PET fibre content increases gradually up to 50%.
4. When the bond temperature was increased up to 150 ^{0}C, the sample which showed the highest bond strength at room temperature showed a bond strength reduction of 62%. Lower strength reduction was shown by sample with fibre content 30% of epoxy volume. It was 49%.
5. The fibre content as 30% of epoxy volume selected as the ideal proportion to develop the modified epoxy adhesive depending on the overall bond performance at ambient and elevated temperature conditions
6. The average 7 days tensile, compressive and flexural strengths of the modified epoxy adhesive were 63.24 N/mm^2, 21.59 N/mm^2 and 49.05 N/mm^2, respectively (at 30 ^{0}C)
7. The effective bond length of the modified epoxy adhesive is 100 mm and it is 125 mm for pure epoxy adhesive
8. In modified epoxy adhesive, bond strength reduced relatively in a linear manner under elevated temperature up to 120 ^{0}C.
9. Bond strength achieved by modified epoxy was higher than pure epoxy adhesive even under the exposure to elevated temperature. The strength enhancement of modified epoxy compared to pure epoxy range between 20%-25% when the exposed temperature was below 60 ^{0}C.
10. Within the temperature range 80 ^{0}C - 120 ^{0}C, strength enhancement of modified epoxy compared with pure epoxy adhesive for a specific temperature reached beyond 180%. At 120 ^{0}C, strength enhancement in modified epoxy was 339% with respect to pure epoxy bond strength. This is because the bond glass transition temperature of epoxy adhesive ranged in between 60 ^{0}C – 80 ^{0}C.
11. The modified epoxy adhesive bond did not reach its glass transition temperature till 120 ^{0}C

12. By bonding CFRP using modified epoxy to a column prototype, a strength enhancement of 165% was achieved whereas the strength enhancement recorded in CFRP bonded using pure epoxy adhesive was 147%
13. Therefore, the modified epoxy performs well in strengthening columns when compared with pure epoxy adhesive.

8.3 Recommendations

1. Authors recommend using a suitable anchoring technique to enhance the bond between ECC adhesive (ECO-ECC) and concrete since the bond failure occurred in ECC-concrete interface
2. A convenient application method need to be implemented when applying the ECC cementitious adhesive (ECO-ECC) in curved surfaces

REFERENCES

[1] A. H. Al-abdwais and R. S. Al-mahaidi, "Bond properties between carbon fibre reinforced polymer (CFRP) textile and concrete using modified cement-based adhesive," *Construction and Building Materials*, vol. 154, pp. 983–992, 2017.

[2] D. Petkova, T. Donchev, and J. Wen, "Experimental study of the performance of CFRP strengthened small scale beams after heating to high temperatures," *Construction and Building Materials*, vol. 68, pp. 55–61, 2014.

[3] J. C. P. H. Gamage, R. Al-Mahaidi, and M. B. Wong, "Bond characteristics of CFRP plated concrete members under elevated temperatures," *Composite Structures*, vol. 75, pp. 199–205, 2006.

[4] R. Barnes and J. Fidell, "Performance in Fire of Small-Scale CFRP Strengthened Concrete Beams," *Journal of Composites for Construction*, vol. 10, no. December, pp. 503–508, 2006.

[5] B. B. Koisch, "Carbon Fiber Cement Matrix (CFCM) overlay system for Masonry Strengthening," *Journal of Composites for Construction*, vol. 2, no. May, pp. 105–109, 1998.

[6] B. Täljsten and T. Blanksvärd, "Mineral-Based Bonding of Carbon FRP to Strengthen Concrete Structures," *Journal of Composites for Construction*, vol. 11, no. April, pp. 120–128, 2007.

[7] N. Saba, M. Jawaid, and O. Y. Alothman, "Recent advances in epoxy resin , natural fiber-reinforced epoxy composites and their applications," *Journal of Reinforced Plastics and Composites*, 2015.

[8] A. V. Pocius, "Elastomer Modification of Structural Adhesives.," *Rubber Chemistry and Technology*, vol. 58, no. 3. pp. 622–636, 1985.

[9] R. Bagheri and R. A. Pearson, "Interfacial studies in CTBN- modified epoxies," *Journal of Applied Polymer Science*, vol. 58, no. 2, pp. 427–437, 1995.

[10] A. B. B. Saleh, Z. A. M. Ishak, A. S. Hashim, W. A. Kamil, and U. S. Ishiaku, "Synthesis and characterization of liquid natural rubber as impact modifier for epoxy resin," *Physics Procedia*, vol. 55, pp. 129–137, 2014.

[11] D. Ratna, "Modification of epoxy resins for improvement of adhesion: A critical review," *Journal of Adhesion Science and Technology*, vol. 17, no. 12, pp. 1655–1668, 2003.

[12] S. Pujari, A. Ramakrishna, and K. T. Balaram Padal, "Investigations on Thermal Conductivities of Jute and Banana Fiber Reinforced Epoxy Composites," *Journal of The Institution of Engineers (India): Series D*, vol. 98, no. 1, pp. 79–83, 2017.

[13] R. N. Manjunath, V. Khatkar, and B. K. Behera, "Comparative assessment of

static and dynamic mechanical properties of glass and PET fiber reinforced epoxy composites," *Materials Today: Proceedings*, vol. 18, pp. 4048–4057, 2019.

[14] Y. S. Bagrecha, R. B. Tailor, M. Ramachandran, and P. P. Raichurkar, "An effect of banana fiber size on banana fiber reinforced epoxy composites with coconut shell powder as filler," *International Journal of Mechanical and Production Engineering Research and Development*, vol. 2018, no. December, pp. 150–155, 2018.

[15] G. Raghavendra, S. Ojha, S. K. Acharya, and S. K. Pal, "Jute fiber reinforced epoxy composites and comparison with the glass and neat epoxy composites," *Journal of Composite Materials*, vol. 48, no. 20, pp. 2537–2547, 2014.

[16] S. Rocca, N. Galati, and A. Nanni, "Review of Design Guidelines for FRP Confinement of Reinforced Concrete Columns of Noncircular Cross Sections," *Journal of Composites for Construction*, vol. 12, no. 1, pp. 80–92, 2008.

[17] V. Alecci, S. Briccoli, and G. Ranocchiai, "Concrete columns confined with CFRP wraps," *Materials and Structures*, vol. 47, pp. 397–410, 2013.

[18] P. Fernandes, J. Sena-cruz, J. Xavier, P. Silva, E. Pereira, and J. Cruz, "Durability of bond in NSM CFRP-concrete systems under di ff erent environmental conditions," *Composites Part B*, vol. 138, no. March 2017, pp. 19–34, 2018.

[19] S. M. Soliman, E. El-salakawy, and B. Benmokrane, "Bond Performance of Near-Surface-Mounted FRP Bars," no. February, pp. 103–111, 2011.

[20] H. M. Diab and O. A. Farghal, "Composites : Part B Bond strength and effective bond length of FRP sheets / plates bonded to concrete considering the type of adhesive layer," *COMPOSITES PART B*, vol. 58, pp. 618–624, 2014.

[21] A. Wiberg, "Strengthening of Concrete Beams Using Cementitious Carbon Fibre Composites," Royal Institute of Technology, 2003.

[22] S. Hashemi and R. Al-mahaidi, "Cement based bonding material for FRP," in *11th International Inorganic Bonded Fiber Composites Conference*, 2008, no. January, pp. 267–271.

[23] S. Hashemi and R. Al-mahaidi, "Experimental and finite element analysis of flexural behavior of FRP-strengthened RC beams using cement-based adhesives," *Construction and Building Materials*, vol. 26, no. 1, pp. 268–273, 2012.

[24] A. Badanoiu and J. Holmgren, "Cementitious composites reinforced with continuous carbon fibres for strengthening of concrete structures," *Cement & Concrete Composites*, vol. 25, no. 3, pp. 387–394, 2003.

[25] H. Pham and R. Al-mahaidi, "Experimental investigation into flexural retrofitting of reinforced concrete bridge beams using FRP composites,"

Composite Structures, vol. 66, pp. 617–625, 2004.

[26] C. Wu and V. C. Li, "Thermal-mechanical behaviors of CFRP-ECC hybrid under elevated temperatures," *Composites Part B: Engineering*, vol. 110, pp. 255–266, 2017.

[27] A. Al-abdwais and R. Al-mahaidi, "Modified cement-based adhesive for near-surface mounted CFRP strengthening system," *Construction and Building Materials*, vol. 124, pp. 794–800, 2016.

[28] A. Mohammed, N. T. K. Al-Saadi, and R. Al-Mahaidi, "Assessment of bond strength of NSM CFRP strips embedded in concrete using cementitious adhesive made with graphene oxide," *Construction and Building Materials*, vol. 154, pp. 504–513, 2017.

[29] Z. Pan *et al.*, "Mechanical properties and microstructure of a graphene oxide-cement composite," *Cement and Concrete Composites*, vol. 58, pp. 140–147, 2015.

[30] A. Mohammed, J. G. Sanjayan, W. H. Duan, and A. Nazari, "Incorporating graphene oxide in cement composites : A study of transport properties," *Construction and Building Materials*, vol. 84, pp. 341–347, 2015.

[31] A. Mohammed, N. T. K. Al-Saadi, R. Al-Mahaidi, and M. Asce, "Utilization of Graphene Oxide to Synthesize High-Strength Cement-Based Adhesive," *Journal of Materials in Civil Engineering*, pp. 1–7, 2016.

[32] M. S. Konsta-gdoutos, Z. S. Metaxa, and S. P. Shah, "Cement & Concrete Composites Multi-scale mechanical and fracture characteristics and early-age strain capacity of high performance carbon nanotube / cement nanocomposites," *Cement and Concrete Composites*, vol. 32, no. 2, pp. 110–115, 2010.

[33] L. Yue and C. Bing, "Factors that affect the properties of magnesium phosphate cement," *Construction and Building Materials*, vol. 47, pp. 977–983, 2013.

[34] L. Yue, S. Tongfei, C. Bing, and L. Yaqiang, "Performance of magnesium phosphate cement at elevated temperatures," *Construction and Building Materials*, vol. 91, pp. 126–132, 2015.

[35] L. Yue, B. Weiliang, S. Tongfei, and L. Xiongfei, "Research on Axial Compression Test of CFRP Confined Concrete Column With MPC," *Journal of Beijing University of Technology*, vol. 43, no. 3, pp. 3–8, 2017.

[36] C. Zhao, Y. Li, Z. Wang, and Z. Li, "Study on Axial Compression Test of Corroded Reinforced Concrete Columns Reinforced by MPC Bonding CFRP," in *The 3rd International Conference on Manufacturing, Material and Metallurgical Engineering*, 2018.

[37] J. J. Makwana and D. J. D. Rathod, "Interface Characterization of Different Types of Fibers in Engineered Cementitious Composites (ECC)," *IOSR Journal*

of Mechanical and Civil Engineering, vol. 14, no. 01, pp. 08–14, 2017.

[38] P. Sathishkumar, P. Sampathkumar, M. Karthik, and C. Vignesh, "Significance of Various Fibres on Engineered Cementitious Concrete," *International Journal of Science, Engineering and Technology*, vol. 4, no. 1, pp. 284–290, 2016.

[39] S. Hashemi and R. Al-mahaidi, "Flexural performance of CFRP textile-retrofitted RC beams using cement-based adhesives at high temperature," *Construction and Building Materials*, vol. 28, no. 1, pp. 791–797, 2012.

[40] C. Wu and V. C. Li, "CFRP-ECC hybrid for strengthening of the concrete structures," *Composite Structures*, vol. 178, pp. 372–382, 2017.

[41] M. Sahmaran and V. C. Li, "Durability of mechanically loaded engineered cementitious composites under highly alkaline environments," *Cement & Concrete Composites*, vol. 30, pp. 72–81, 2008.

[42] V. C. Li, "Tailoring ECC for Special Attributes : A Review," *International Journal of Concrete Structures and Materials*, vol. 6, no. 3, pp. 135–144, 2012.

[43] M. L. Nehdi and M. A. E. M. Ali, "Experimental and Numerical Study of Engineered Cementitious Composite with Strain Recovery under Impact Loading," *Applied Sciences*, vol. 9, no. 5, p. 994, 2019.

[44] X. Huang, R. Ranade, Q. Zhang, W. Ni, and V. C. Li, "Mechanical and thermal properties of green lightweight engineered cementitious composites," *Construction and Building Materials*, vol. 48, pp. 954–960, 2013.

[45] J. Yu, J. Lin, Z. Zhang, and V. C. Li, "Mechanical performance of ECC with high-volume fly ash after sub-elevated temperatures," *Construction and Building Materials*, vol. 99, pp. 82–89, 2015.

[46] E. H. Yang, Y. Yang, and V. C. Li, "Use of high volumes of fly ash to improve ECC mechanical properties and material greenness," *ACI Materials Journal*, vol. 104, no. 6, pp. 620–628, 2007.

[47] G. Yang, J. Yu, and Y. Luo, "Development and Mechanical Performance of Fire-Resistive Engineered Cementitious Composites," *Journal of Materials in Civil Engineering*, vol. 31, no. 5, pp. 1–10, 2019.

[48] X. Yang, W. Y. Gao, J. G. Dai, Z. D. Lu, and K. Q. Yu, "Flexural strengthening of RC beams with CFRP grid-reinforced ECC matrix," *Composite Structures*, vol. 189, no. January, pp. 9–26, 2018.

[49] P. S. Bhat, V. Chang, and M. Li, "Effect of elevated temperature on strain-hardening engineered cementitious composites," *constructio*, vol. 69, pp. 370–380, 2014.

[50] American Society for Testing and Materials, "ASTM C 109/C 109M - Standard Test Method for Compressive Strength of Hydraulic Cement Mortars," *ASTM International*, pp. 29–31, 2009.

[51] Japan Society of Civil Engineers, *Recommendations for Design and Construction of High Performance Fiber Reinforced Cement Composites with Multiple Fine Cracks (HPFRCC)*. Tokyo, 2008.

[52] A. Katz, V. C. Li, and A. Kazmer, “Bond properties of carbon fibers in cementitious matrix,” *Journal of Materials in Civil Engineering*, vol. 7, no. 2, pp. 125–128, 1995.

[53] J. Yu and C. K. Y. Leung, “Strength improvement of strain-hardening cementitious composites with ultrahigh-volume fly ash,” *Journal of Materials in Civil Engineering*, vol. 29, no. 9, p. 5017003, 2017.

[54] V. Li, S. Wang, and C. Wu, “Tensile strain-hardening behavior of PVA-ECC,” *ACI Materials Journal*, vol. 98, no. June 2011, pp. 483–492, 2019.

[55] X. Lin *et al.*, “Recycling polyethylene terephthalate wastes as short fibers in Strain-Hardening Cementitious Composites (SHCC),” *Journal of Hazardous Materials*, vol. 357, no. May, pp. 40–52, 2018.

[56] M. Tajvidi, R. H. Falk, and J. C. Hermanson, “Effect of natural fibers on thermal and mechanical properties of natural fiber polypropylene composites studied by dynamic mechanical analysis,” *Journal of Applied Polymer Science*, vol. 101, no. 6, pp. 4341–4349, 2006.

[57] S. Budhe, M. D. Banea, and S. de Barros, “Bonded repair of composite structures in aerospace application: a review on environmental issues,” *Applied Adhesion Science*, vol. 6, no. 1, 2018.

[58] S. Black, “Structural Adhesives, Part II: Aerospace,” *Composites World*, 2016. [Online]. Available: https://www.compositesworld.com/articles/structural-adhesives-part-ii-aerospace.

[59] M. D. Banea and L. F. M. Da Silva, “Adhesively bonded joints in composite materials : an,” *Journal of Materials Design and Applications*, vol. 223, pp. 1–18, 2009.

[60] R. D. Adams, J. Coppendale, V. Mallick, and H. Al-Hamdan, “The effect of temperature on the strength of adhesive joints,” *International Journal of Adhesion and Adhesives*, vol. 12, no. 3, pp. 185–190, 1992.

[61] I. A. Ashcroft, D. J. Hughes, and S. J. Shaw, “Mode I fracture of epoxy bonded composite joints : 1 . Quasi-static loading,” *International Journal of Adhesion and Adhesives*, vol. 21, pp. 87–99, 2001.

[62] M. D. Banea and L. F. M. Da Silva, “The effect of temperature on the mechanical properties of adhesives for the automotive industry,” *Journal of Materials Design and Applications*, vol. 224, pp. 51–62, 2010.

[63] R. Frassine, M. Rink, and A. Pavan, “Viscoelasticeffects on the interlaminar fracture behaviour of thermoplastic matrix composites : II . Rate and temperature dependence in unidirectional peek / carbon-fibre laminates,”

Composites Science and Technology, vol. 56, pp. 1253–1260, 1996.

[64] Z. Jia, D. Hui, G. Yuan, J. Lair, K. Lau, and F. Xu, "Mechanical Properties of an Epoxy-based Adhesive under High Strain Rate Loadings at Low Temperature Environment," *Composites Part B*, vol. 105, pp. 132–137, 2016.

[65] M. D. Banea, F. S. M. De Sousa, L. F. M. Da Silva, R. D. S. G. Campilho, and A. M. B. De Pereira, "Effects of temperature and loading rate on the mechanical properties of a high temperature epoxy adhesive," *Journal of Adhesion Science and Technology*, vol. 25, no. 18, pp. 2461–2474, 2011.

[66] L. F. M. Da Silva and R. D. Adams, "Measurement of the mechanical properties of structural adhesives in tension and shear over a wide range of temperatures," *Journal of Adhesion Science and Technology*, vol. 19, no. 2, pp. 109–141, 2005.

[67] A. N. Rider, C. H. Wang, and P. Chang, "Bonded repairs for carbon/BMI composite at high operating temperatures," *Composites Part A: Applied Science and Manufacturing*, vol. 41, no. 7, pp. 902–912, 2010.

[68] A. Sánchez Cebrián, R. Basler, F. Klunker, and M. Zogg, "Acceleration of the curing process of a paste adhesive for aerospace applications considering cure dependent void formations," *International Journal of Adhesion and Adhesives*, vol. 48, pp. 51–58, 2014.

[69] Solvay, "Aerospace - Our Composite Material Solutions," 2020. [Online]. Available: https://www.solvay.com/en/solutions-market/aerospace.

[70] Henkel Corporation, "Aerospace - Henkel Adhesives," 2020. [Online]. Available: https://www.henkel-adhesives.com/us/en/industries/aerospace/aerospace-structural-adhesives.html. [Accessed: 13-Jan-2020].

[71] Hexcel Corporation, "HexBond™ Adhesives," 2020. [Online]. Available: https://www.hexcel.com/Products/Adhesives/.

[72] Permabond Engineering Adhesives, "Aerospace Adhesives," 2020.

[73] Renegade Materials Corporation, "Adhesives for Aerospace Applications," 2020. [Online]. Available: http://www.renegadematerials.com/products/.

[74] Nations Online Project, "Administrative Map of Nepal - Nations Online Project." 2014.

[75] X-Calibur Structural Systems, "X-Wrap C300 Technical Data Sheet," 2020.

[76] X-Calibur Structural Systems, "X-Wrap Lamination Adhesive Technical Data Sheet," 2020.

[77] American Society for Testing and Materials, "ASTM C618 - 19 - Standard Specification for Coal Fly Ash and Raw or Calcined Natural Pozzolan for Use in Concrete," *ASTM International*, 2005.

[78] L. Ćojbašić, G. Stefanović, and Ž. Sekulić, “Influence of the fly ash chemical composition on the portland cement and fly ash mixture hydration mechanism,” *FACTA UNIVERSITATIS Series: Mechanical Engineering,* vol. 3, no. 1, pp. 117–125, 2005.

[79] P. Chindaprasirt, P. De Silva, K. Sagoe-Crentsil, and S. Hanjitsuwan, “Effect of SiO 2 and Al 2 O 3 on the setting and hardening of high calcium fly ash-based geopolymer systems,” *Journal of Materials Scienece,* vol. 47, no. 12, pp. 4876–4883, 2012.

[80] F. Awaja and D. Pavel, “Review - Recycling of PET,” *European Polymer Journal,* vol. 41, no. July, pp. 1453–1477, 2005.

[81] B. Bapat, “Measurement of Thermal Conductivity by Lee ’ s method,” 2020.

[82] American Society for Testing and Materials, “ASTM D7340 - 07(2018) Standard Practice for Thermal Conductivity of Leather,” *ASTM International,* vol. 15.04, 2018.

[83] M. A. Issa, M. Rahman, and R. Alrousan, “Prediction of Ultimate Load at the CFRP-Concrete Interface under Pure Shear Mode,” vol. 6, no. 6, pp. 183–195, 2016.

[84] J. C. P. H. Gamage, M. B. Wong, and R. Al-Mahadi, “Performance of CFRP strengthened concrete members under elevated temperatures,” *Proceeding of the International Sysposium on Bond Behaviour of FRP in Structures (BBFS 2005),* no. Bbfs, pp. 113–118, 2005.

[85] S. Soares, J. Sena-Cruz, J. R. Cruz, and P. Fernandes, “Influence of surface preparation method on the bond behavior of externally bonded CFRP reinforcements in concrete,” *Materials,* vol. 12, no. 3, pp. 20–24, 2019.

[86] American Society for Testing and Materials, “D638-14 - Standard Test Method for Tensile Properties of Plastics,” *ASTM International,* vol. 82, no. C, pp. 1–15, 2016.

[87] American Society for Testing and Materials, “ASTM - D 695-02a : Standard Test Method for Compressive Properties of Rigid Plastics,” *ASTM International,* vol. i, pp. 74–80, 2008.

[88] American Society for Testing and Materials, “ASTM - D790-03-Standard Test Method for Flexural Properties of Unreinforced and Reinforced Plastics and Electrical Insulation Materials,” *ASTM International,* pp. 1–11, 2015.

[89] Epoxy Technology Inc., “Pot Life , Working Life and Gel Time of Epoxies,” Billerica, Massachusetts, 2014.

[90] S. H. Ali, A. A. D. Al-Zuky, A. H. Al-Saleh, and H. J. Mohamad, “Measure liquid viscosity by tracking falling ball Automatically depending on image processing algorithm,” *Journal of Physics: Conference Series,* vol. 1294, no. 2, 2019.

[91] V. C. Li, “Engineered Cementitious Composites (ECC) – Material , Structural , and Durability Performance,” in *Concrete Construction Engineering Handbook*, E. Nawy, Ed. CRC Press, 2007.

[92] V. Li, “Engineered Cementitious Composites (ECC) – Material , Structural , and Durability Performance Engineered Cementitious Composites (ECC) – Material , Structural , and Durability Performance,” in *Concrete Construction Engineering Handbook*, CRC Press, 2008.

[93] American Society for Testing and Materials, “ASTM C190-85 - Method of Test for Tensile Strength of Hydraulic Cement Mortars,” *ASTM International*, 1985.

[94] American Society for Testing and Materials, “ASTM C305-14 - Standard Practice for Mechanical Mixing of Hydraulic Cement Pastes and Mortars of Plastic Consistency,” *ASTM International*, vol. 04, p. 3, 2009.

[95] European Committee for Standardization, “EN 1015-11 - Methods of test for mortar for masonry,” *European Standard*, vol. 3, no. 1, 2006.

[96] A. Yerramala, R. C, and B. D. V, “Influence of Fly ash replacement on strength properties of cement mortar,” *International Journal of Engineering Science and Technology*, vol. 4, no. 08, pp. 3657–3665, 2012.

[97] M. M. Islam, M. S. Islam, M. A. Rahman, and A. Das, “Strength Behavior of Mortar using Fly Ash as Partial Replacement of Cement,” *Concrete Research Letters*, vol. 1(3), no. September 2010, pp. 98–106, 2010.

[98] Dassault Systemes Simulia and Corporation, “ABAQUS Standard User’s Manual, Version 6.14,” *ABAQUS*, 2014.

[99] B. L. Wahalathantri, D. P. Thambiratnam, T. H. T. Chan, and S. Fawzia, “A material model for flexural crack simulation in reinforced concrete elements using Abaqus,” in *First International Conference on Engineering, Designing and Developing the Built Environment for Sustainable Wellbeing*, 2011, pp. 260–264.

[100] J. Li and Y. X. Zhang, “Evaluation of constitutive models of hybrid-fibre engineered cementitious composites under dynamic loadings,” *Construction and Building Materials*, vol. 30, pp. 149–160, 2012.

[101] R. Daud, L. Cunningham, and Y. Wang, “Non-linear FE Modelling of CFRP-strengthened RC Slabs under Cyclic Loading,” *Athens Journal of Technology & Engineering*, vol. 2, no. 3, pp. 161–180, 2015.

[102] P. P. Camanho, C. G. Dávila, and M. F. De Moura, “Mixed-mode Progressive Delamination in Composite Materials,” *Journal of Composite Materials*, vol. 37, no. May 2014, pp. 1415–1438, 2003.

[103] J. Henriques, L. Simões, and I. B. Valente, “Numerical modeling of composite beam to reinforced concrete wall joints Part I : Calibration of joint components,” *Engineering Structures*, vol. 52, pp. 747–761, 2013.

ANNEXES

Annex A - Technical specification of ECC-ECO adhesive

Data sheet is attached in the following page.

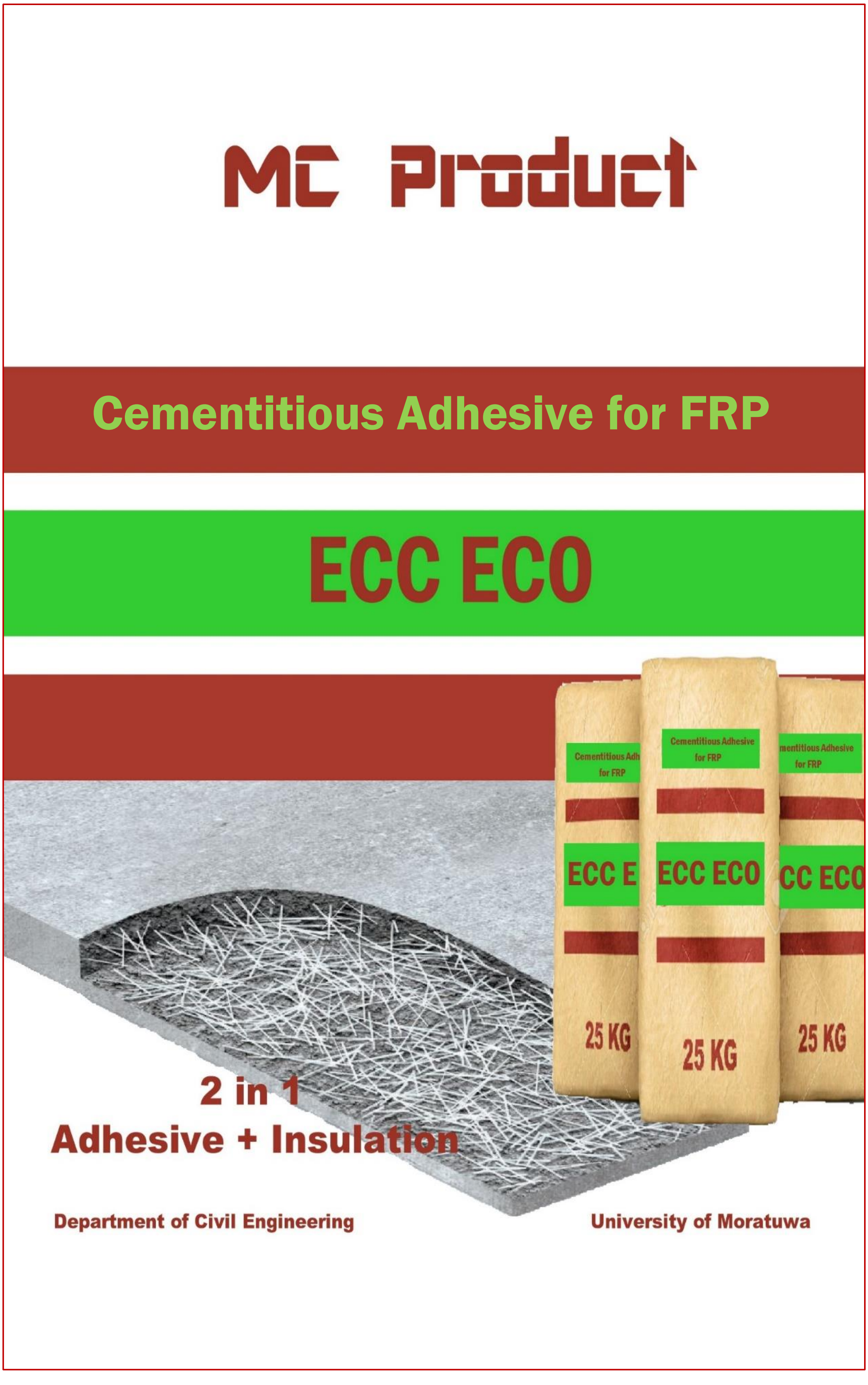
MC Product
Cementitious Adhesive for FRP
ECC ECO
Cementitious Adhesive for FRP
ECC ECO
25 KG
2 in 1
Adhesive + Insulation
Department of Civil Engineering
University of Moratuwa

ECC-ECO

PET Fibre Reinforced Cementitious Adhesive

MC Product

DESCRIPTION

ECC ECO is a fibre reinforced cementitious adhesive designed to adhere Fibre Reinforced Polymer (FRP) fabrics to concrete elements. It is also a thermal resisting adhesive which provides insulation to the structure.

ADVANTAGES

- Good workability
- Low thermal conductivity

PROPERTIES

Compressive strength (MPa) (30 ^{0}C)	53 (28 days)
Tensile strength (MPa) (30 ^{0}C)	3.83 (28 days)
Tensile strain	5.86%
Flexural strength (MPa) (30 ^{0}C)	7.10 (14 days)
Glass transition temperature (^{0}C)	100 - 120
Density (kg/m^3)	1895
Thermal conductivity (W/mK)	0.145 – 0.18
Color	Light gray

APPLICATION

Surface preparation

Concrete substrate should be free from dust, dirt, oil, sealer or old coatings before applying the ECC ECO adhesive. The surface needs to be grinded and then the dust should be wiped out using a wet cloth. Then the wet surface should be kept to dry before applying the adhesive.

Adhesive preparation

Mix proportion

ECC ECO adhesive: Water = 1: 0.425

Mix the mortar in a mechanical mixer until a homogeneous mixture is made. For best results, apply the **ECC ECO** adhesive within 45 minutes after the preparation.

FRP fabric preparation

For a better bond, adhere sand on top of FRP fabric using a polymeric adhesive before adhering it to the concrete substrate using **ECC ECO** adhesive.

Surface application

- Apply a 5 mm thick layer of **ECC ECO** adhesive on top of concrete substrate
- Lay the FRP fabric on top of adhesive layer and gently press it for better bonding
- Apply another 5 mm thick layer of **ECC ECO** adhesive on top of bonded FRP fabric
- For better bonding stick sand on top of FRP fabric using a polymeric glue before bonding it to concrete substrate using **ECC ECO** adhesive.

PACKAGING

ECC ECO adhesive is supplied in 25 kg bags

STORAGE

ECC ECO adhesive has a shelf life of 12 months when stored in a dry place. Discard any open or damaged packages.

HEALTH AND SAFETY

Protective methods should be followed to avoid the adhesive get contact with eyes. Contact with eyes shall be washed immediately with clean water followed by medical attention.

MC Products (Pvt) Ltd.
University of Moratuwa,
Katubedda,
SRI LANKA
Tel : +94771234567

Annex B - Technical specification of PETCO-Epoxy adhesive

Data sheet is attached in the following page.

MC Product

PETCO Epoxy

Department of Civil Engineering

University of Moratuwa

PETCO Epoxy

PET Fibre Reinforced Epoxy Adhesive

MC Product

DESCRIPTION

PETCO Epoxy is a fibre reinforced epoxy adhesive designed to adhere Fibre Reinforced Polymer (FRP) fabrics to concrete elements. It is a modified epoxy adhesive which has a better thermal resistance than typical epoxy adhesive.

ADVANTAGES

- High strength
- Strong adhesion
- Can be used in both vertical and horizontal application
- Solvent free

PROPERTIES

Tensile strength (7 days)	63.24 MPa (30 ^{0}C)
Compressive strength (7 days)	21.59 MPa (30 ^{0}C)
Flexural strength (7 days)	49.05 MPa (30 ^{0}C)
Coverage	0.5 – 06 kg/m^2
Color	Light gray
Pot life	25 mins at 30 ^{0}C
Glass transition temperature	> 120 ^{0}C

APPLICATION

Surface preparation

Concrete substrate should be free from dust, dirt, oil, sealer or old coatings before applying the PETCO Epoxy adhesive. The surface needs to be grinded and then the dust should be wiped out using a wet cloth. Then the wet surface should be kept to dry before applying the adhesive.

Adhesive preparation

Mix 2 parts of Base (with fibre) with one part of Hardener well until a homogeneous mixture is obtained.

Surface application

- Apply a coating of **PETCO Epoxy** adhesive mix on top of concrete substrate surface
- Wrap the FRP fabric on it
- Press the FRP fabric gently until air trapped voids are removed
- Apply another coating of **PETCO Epoxy** adhesive on top of FRP fabric

PACKAGING

2 kg Hardener + 3 kg Base (With fibre)

STORAGE

PETCO Epoxy adhesive has a shelf life of 18 months when stored in a dry place. Keep the bottles tightly closed after each use.

HEALTH AND SAFETY

Protective methods should be followed to avoid the adhesive get contact with eyes. Contact with eyes shall be washed immediately with clean water followed by medical attention.

MC Products (Pvt) Ltd.
University of Moratuwa,
Katubedda,
SRI LANKA
Tel : +94771234567

Annex C – Publications

Publications are attached in the following pages.

Modification of Engineered Cementitious Composite Mortar to use as an adhesive for CFRP/Concrete bond

4 authors, including:

M.W.Chamodi Himasha
University of Moratuwa
3 PUBLICATIONS 0 CITATIONS

JCPH Gamage
University of Moratuwa
53 PUBLICATIONS 292 CITATIONS

Vajira Attanayaka
University of Moratuwa
2 PUBLICATIONS 2 CITATIONS

ISBN:
Paper ID: ICSBE2020-145

MODIFICATION OF ENGINEERED CEMENTITIOUS COMPOSITE MORTAR TO USE AS AN ADHESIVE FOR CFRP/CONCRETE BOND

M.W.C. Himasha[1*], J.C.P.H. Gamage[2], G.I.P. De Silva[3], V. Attanayaka[4]
[1]*Postgraduate researcher, Department of Civil Engineering, University of Moratuwa, SRI LANKA*
[2]*Senior Lecturer, Department of Civil Engineering, University of Moratuwa, SRI LANKA*
[3]*Senior Lecturer, Department of Material Science and Engineering, University of Moratuwa, SRI LANKA*
[4]*Airow Solutions (Pvt) Ltd, SRI LANKA*
**Correspondence E-mail: mvchimasha@gmail.com, TP: +94774008602*

Abstract: This study focuses on the development of a thermally insulative cementitious adhesive for bonding Carbon Fiber Reinforced Polymer (CFRP) fabrics with concrete using Engineered Cementitious Composite (ECC) mortar. The poor thermal performance of epoxy adhesive encouraged the development of a new cementitious adhesive which could resist elevated temperature. The ECC adhesive was developed using locally available materials. The developed adhesive has a low thermal conductivity between 0.145 - 0.18 W/(mK) which shows its resistance to elevated temperature. The developed adhesive showed an average bond strength of 570.28 N/mm^2 for an effective bond length of 150 mm. When compared with epoxy adhesive, ECC adhesive showed a 15% reduction in bond strength. However, under elevated temperature, the bond strength reduction in ECC adhesive is very low compared to the bond strength reduction in epoxy. When the bondline temperature was incremented up to 100 ^{0}C, the strength reduction evident in modified ECC adhesive was 5.21%, while it was 69% for epoxy adhesive. It shows that the developed ECC adhesive resist high temperature better than epoxy. The average 28 days tensile strength of the adhesive was 3.83 N/mm^2 and the average 28 days compressive strength was 52.77 N/mm^2. A finite element model was developed and validated for the pullout test to predict the bond performance of ECC adhesive. The parametric study conducted varying the adhesive thickness concluded that the bond strength enhanced with the increment of adhesive thickness up to 20 mm.

Keywords: Engineered Cementitious Composite; Cementitious adhesive; Carbon Fibre Reinforced Polymer; Thermal performance; Finite Element Modelling

1. Introduction

Carbon Fiber Reinforced Polymer (CFRP) is a generally used retrofitting material in structural applications. The epoxy is a commonly used commercially available polymeric adhesive which is used to bond CFRP with concrete. It is used widely due to its higher bonding strength. However, the bond strength of epoxy is susceptible to deteriorate when exposed to a higher temperature beyond its glass transition temperature (Hashemi and Al-mahaidi, 2012). The glass transition temperature is the temperature around which a polymeric adhesive undergoes a sudden drop in its adhering properties (Barnes and Fidell, 2006). For epoxy adhesive, the glass transition temperature is around 60 ^{0}C – 70 ^{0}C (Gamage, Al-Mahaidi and Wong, 2006). The high cost of materials (Koisch, 1998), emission of toxic fumes (Täljsten and Blanksvärd, 2007) and flammability (Täljsten and Blanksvärd, 2007) are other disadvantages of epoxy adhesives. Therefore, a lot of researchers suggested replacing epoxy with a cementitious adhesive to resist high temperature (Hashemi and Al-mahaidi, 2012; Himasha and Gamage, 2019). Cementitious adhesives show better performance under elevated temperatures and good consistency with concrete (Koisch, 1998). Researches have been conducted on introducing cementitious insulations to overcome this issue (Kahandawa Arachchi, Gamage and De Silva, 2019; Selvaranjan *et al.*, 2020). However, those attempts introduced an extra dead load to the structure and their bonding with CFRP/epoxy composite is questionable.

Most of the cementitious adhesives developed for CFRP-concrete bond are brittle in nature (Hashemi and Al-mahaidi, 2012; Wu and Li, 2017). Brittleness reduces the effective transferring of the load from concrete to CFRP (Hashemi and Al-mahaidi, 2012; Wu and Li, 2017). ECC is a cementitious mortar reinforced with dispersed multidirectional fibres. Fibres contribute to creating ductility in ECC (Makwana and Rathod, 2017). ECC comprises Portland cement, silica sand, fly ash, water and fibres. Higher fly ash content in ECC increases the ductility and reduces the compressive strength (Yang, Yang and Li, 2007). ECC can be developed by using different fibres such as Poly Vinyl Alcohol (PVA), Polyethylene terephthalate (PET), Polyethylene (PE) and Polypropylene (PP). Sathishkumar *et al.* (2016) conducted tests on ECC developed with the abovementioned fibre types to analyze changes in mechanical properties. Results suggested that PVA is the ideal fibre type among them (Sathishkumar *et al.*, 2016). PET fibres showed better results than PE

and PP fibres (Sathishkumar *et al.*, 2016). ECC with fibre content as 2% of cement content showed the highest tensile, compressive and flexural strengths for all the 4 types of fibres (Sathishkumar *et al.*, 2016). The 2% fibre content is the suggested fibre proportion to be used in developing ECC since it is closer to the critical fibre content needed to attain the strain hardening stage (Li, 2007). The microcracks develop in the strain hardening stage, further enhanced the ductile nature in ECC (Sahmaran and Li, 2008). Fly ash content lowers the thermal conductivity of ECC (Yang, Yang and Li, 2007; Huang *et al.*, 2013). The mix proportion defined as ECC-M45 is tailored to attain multiple cracking and to maintain a controlled crack width (Li, 2007).
Approximately 75% of the total cost of ECC developed with PVA fibres (ECC-PVA) is spent on PVA fibres (Yu and Leung, 2017). Therefore it is not an economically feasible product. PET is a solid waste and recycled PET fibres can be used to develop ECC with PET fibres (ECC-PET). ECC can be modified to use in a wide range of purposes (Li, 2008). Therefore, the authors focus on developing ECC-PET as a thermally insulative cementitious adhesive for CFRP-concrete bond. The ECC-M45 mix proportion was modified to develop the cementitious adhesive. The adhesive was developed using locally available materials. A lot of researchers have successfully developed the local versions of ECC (Boshoff and Zijl, 2007; Li, 2007). The developed adhesive was tested for its mechanical properties, bond performance and thermal effect on bond strength. A finite element model was developed and validated to perform a parametric study on the performance of ECC-PET adhesive.

2. Test program

The authors have used the locally available materials in developing ECC as a thermally insulative adhesive for CFRP-concrete bond. The initial phase of the test program was to decide a fibre proportion to develop the adhesive depending on its thermal conductivity. The next phase was to determine the mechanical properties of the developed cementitious adhesive. The feasibility of the adhesive was evaluated depending on its bond strength and thermal performance.

2.1 Material properties and ECC adhesive preparation

The materials used to develop ECC adhesive are Portland cement, silica sand, fly ash, water and Polyethylene Terephthalate (PET) fibres (Figure 1). The required silica sand was obtained from Piramal Glass Ceylon PLC, Naththandiya, Sri Lanka and fly ash was obtained from the Norochcholi power plant, Sri Lanka. A chemical analysis was conducted on fly ash at the Geological Survey and Mines Bureau of Sri Lanka to find the chemical composition of the material (Table 1). The chemical composition of fly ash drastically differs depending on the source from where it is obtained. This change can be seen when comparing with the chemical composition of fly ash used by Wu and Li (2017) to develop ECC as an adhesive (Table 1).

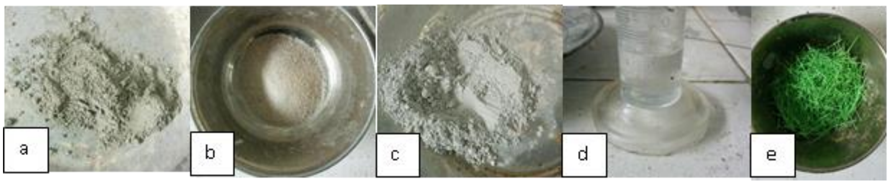

Figure 1: (a) Cement (b) Silica sand (c) Fly ash (d) Water (e) PET fibers

Table 1: Chemical composition of fly ash

	Norochcholai power plant, Sri Lanka	**DTE Monroe Power Plant, State of Michigan, USA** (Wu and Li, 2017)
SiO_2 (%)	46.89	42.20
Al_2O_3 (%)	30.69	22.51
MgO (%)	1.56	3.20
CaO (%)	7.56	15.66
Na_2O (%)	0.23	0.98
K_2O (%)	0.64	1.53
P_2O_5 (%)	2.67	-
Fe_2O_3 (%)	1.88	9.20
SO_3	-	1.85
Loss on ignition	5.59	1.34

The fly ash obtained from Norochcholai power plant can be categorized as class F type as per STM C618-19 (American Society for Testing and Materials, 2005). The CaO content in fly ash collected from Norochcholai plant is below 10%. The fly ash with a CaO content lower than 10% shows more pozzolanic characteristics (Ćojbašić, Stefanović and Sekulić, 2005). The pozzolanic materials need the presence of Calcium hydroxide for the formation of solid matter (Ćojbašić, Stefanović and Sekulić, 2005). Therefore water requirement might be high for hydration. The PET fibres have a thickness of 0.4 mm and a length of 10 mm. The manufacturer provided properties of CFRP fabric is given in Table 2 (X-Calibur Structural Systems, 2020).

Sample preparation was done in accordance with ASTM C305 (American Society for Testing and Materials, 2018). Portland cement, silica sand, fly ash and PET fibres were mixed in a mechanical mixer initially and then water was added to the paste gradually. The whole paste was kept for mixing in the mechanical mixer for 10 minutes with an angular velocity of 50 rpm, to get a homogenous mixture. The mix proportion of ECC-M45 self-consolidating mortar (Li, 2007) was used to develop the ECC adhesive. Water cement ratio of this particular mix design is 0.56 which resulted in a dry mortar with poor adhering qualities. Therefore, the water-cement ratio was increased to 0.85 to achieve the desired sticky nature. Cement: fly ash: silica sand: water mix proportion ratio of modified ECC adhesive is 1: 1.2: 0.8: 0.85.

Table 2: Manufacturer-provided material properties of CFRP fabric (X-Calibur Structural Systems, 2020)

Parameter	**Value**
Sheet weight	300 g/m^3
Carbon content	95%
Net effective thickness	0.166 mm
Modulus of elasticity	240 GPa
Tensile strength	4000 MPa
Elongation at break	2%

2.2 Thermal conductivity

The thermal conductivity test was conducted to check how the deviation of the fibre content affects the thermal conductivity of the mortar. Thermal conductivity is the property which indicates the ability of a material to conduct heat (Bapat, 2020). Lee's disc method is commonly used to determine the thermal conductivity of bad heat conductors (Bapat, 2020). Circular samples with a diameter of 60 mm and a thickness of 5 mm were cast to test for the thermal conductivity. Figure 2 shows Lee's disc apparatus and the samples. The samples were cast deviating the fibre volume in the mix proportion as 1%, 2%, 3%, 4% and 5% of cement volume and for each fibre volume, 3 circular samples were cast.

Prepared samples were demoulded after 1 day of curing and then the samples were cured in a water bath for 27 days. Then these samples were dried for a day in the air (27 ± 3 ^{0}C; 74 ± 5%) before testing for thermal conductivity. The silicone heat sink compound was applied on both sides of the sample to obtain an even surface. The test was conducted in accordance with ASTM D7340 - 07 (American Society for Testing and Materials, 2018). Figure 3 shows the test results.

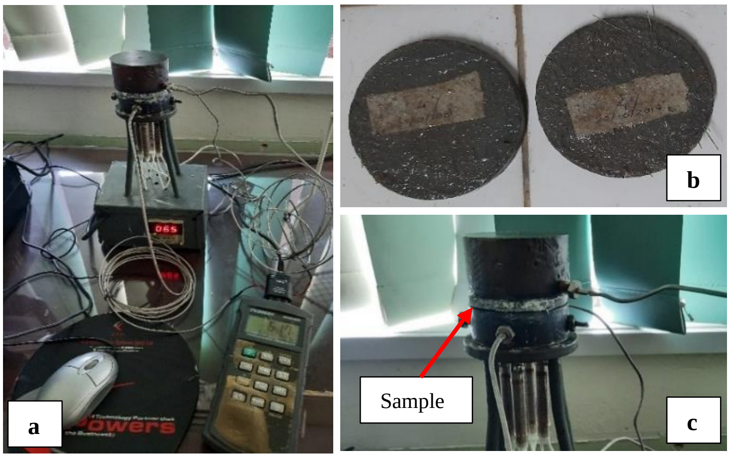

Figure 2: (a) Lee's disc apparatus (b) Samples (c) Sample mounted in the apparatus

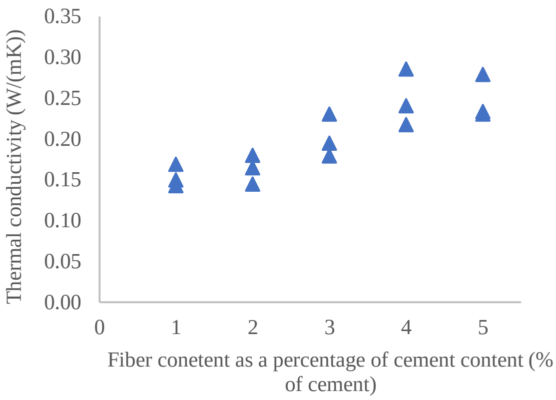

Figure 3: Thermal conductivity - fiber content graph

According to Figure 3, thermal conductivity increased with the increase of fibre content in a relatively linear manner. Thus, the mix designs with lower fibre contents show better resistance to elevated temperature. ECC achieves its optimum tensile ductility when the fibre content is 2% of cement content (Li, 2007). Further, the experiments conducted by Sathishkumar *et al.* (2016) highlighted the fact that ECC-PET reached its highest tensile, compressive and flexural strengths at 2% fibre content. The thermal conductivity corresponding to this fibre content ranged in between 0.145 -0.18 W/(mK). Therefore, depending on both experimental results and literature data, 2% of fibre content was selected as the optimum fibre content to develop ECC adhesive. The density of fly ash is less than one third of the cement. Since the lowering of density reduces the thermal conductivity, the fly ash content also affected in lower thermal conductivity in this adhesive (Bentz *et al.*, 2011).

2.3 Developed adhesive properties

The developed adhesive was tested for its mechanical properties. Samples with the dimensions of 70 mm x 70 mm x 70 mm were cast for compressive strength test in accordance with ASTM C109 (American Society for Testing and Materials, 2009). Average 7 days and 28 days compressive strengths of cementitious adhesive were 16.97 N/mm^2 and 52.77 N/mm^2, respectively. The dumbell shaped samples were cast to conduct the uniaxial tensile test in accordance with CRD-C 260-01(US Army Corps of Engineers, 2001). The average tensile strength was 3.83 N/mm^2 and the average tensile strain was 5.86%. The density of developed ECC adhesive was 1895.04 kg/m^3.

2.4 Bond strength and effective bond length

A series of direct pull out tests were conducted to find the effective bond length of the developed adhesive. Grade 25 concrete blocks with the dimension of 100 mm x 100 mm x 250 mm were used as the concrete substrate to bond CFRP fabric. The bond surface of the concrete block was grinded and wiped using a wet cloth to remove the week layer on top of the concrete block. After drying the surface, the developed ECC adhesive was applied on top of the bonding surface to a thickness of 5 mm. A CFRP fabric strip with a width of 75 mm was laid on top of ECC adhesive layer maintaining a part of CFRP fabric strip (100 mm length) outside the bonding region to fix the grip to pull the CFRP strip during testing. The grip was fabricated by fixing 2 aluminium sheets, each with the dimension 75 mm x 100 mm on either side of the CFRP fabric strip part left for the grip, using epoxy adhesive. Samples were fabricated with 6 different bond lengths; 50 mm, 75 mm, 100 mm, 125 mm, 150 mm and 175 mm. Samples were cured for 28 days before testing.

Samples were mounted on the universal testing machine using a set-up fabricated to conduct the pullout test (Figure 5). The CFRP strip was pulled with a rate of 2 mm/min. Figure 4 shows the test results.

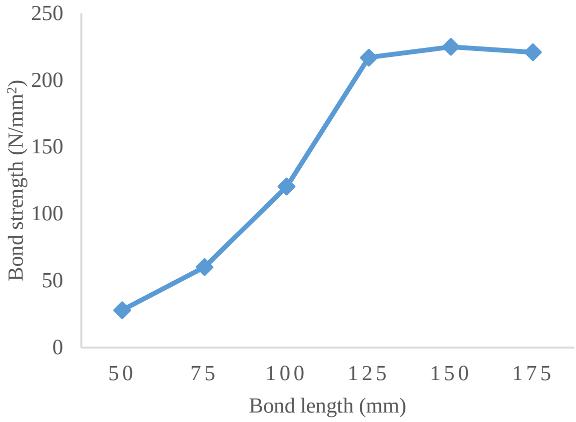

Figure 4: Bond strength - Bond length graph

Figure 5: Testing the sample

The bond strength increased up to 150 mm bond length. The bond strength deviation between two bond lengths; 150 mm and 175 mm was very low. Therefore, 150 mm was selected as the effective bond length for the developed ECC adhesive. The corresponding bond strength for effective bond length was 224.9 N/mm^2. However, the bond strength of epoxy-bonded sample for the same bond length is 670.68 N/mm^2. Therefore, the bond strength reduction in developed ECC adhesive compared with the epoxy-bonded sample was 66.47%. An interface bond between CFRP and ECC adhesive was evident in all the samples. Therefore, measures were taken to avoid this bond interface failure and to enhance the bond strength in the next phase of the test program.

2.5 Enhancement of bond strength

To avoid the interface failure between CFRP and ECC adhesive, approaches were taken to increase surface free energies. One approach was to increase the surface friction and the other approach was to change the nature of adhesive by using ECC slurry over ECC mortar. Therefore the first technique implemented was sticking silica sand on top of CFRP fabric using epoxy adhesive before bonding it using ECC adhesive (E-M-SS-1/2). The second technique was to replace the silica sand in the first technique with sand sieved through 1.7 mm sieve (E-M-S-1/2). The third option was to remove silica sand in ECC adhesive mix and produce the ECC slurry to use as the adhesive for CFRP (E-S-N-1/2). The fabricated samples were tested for their pull out strength and the obtained results are given in Table 3.

Table 3: Test results of bond strength enhancing techniques

Sample code	Average Failure load (kN)	Bond strength (N/mm^2)	Percentage strength enhancement compared to the sample without strength enhancement
E-M-SS-1	5.60	449.80	100%
E-M-SS-2			
E-M-S-1	7.10	570.28	158%
E-M-S-2			
E-S-N-1	1.55	124.50	-45%
E-S-N-2			

Apart from E-M-S-1/2, all the other approaches failed in the CFRP-ECC adhesive interface failure. Samples E-M-S-1 and E-M-S-2 failed due to interface failure between ECC adhesive and concrete substrate. Therefore, sticking sand on CFRP fabric have avoided the CFRP-ECC adhesive interface failure. Moreover, these samples achieved the highest bond strength of 570.25 N/mm^2 which showed a 158% of bond strength enhancement when compared with the previous bond strength of ECC adhesive without strength enhancement techniques. Further, it can be seen that the bond strength of ECC adhesive has reached a value closer to epoxy adhesive bond strength. In all these instances, the effective bond length was maintained. Hence, depending on these results it can be concluded that sticking sand on CFRP using epoxy is a successful method of enhancing surface free energy in CFRP-ECC adhesive interface.

2.7 Thermal performance of the ECC adhesive

Cementitious adhesives were suggested to use over epoxy adhesives because of their thermal resisting nature. Therefore, the developed ECC adhesive and epoxy adhesive were tested for their thermal performance by conducting the pullout test under elevated temperature. The bondline temperature of samples was elevated up to 100 ^{0}C using a 1000 W flashlight while conducting the pullout test. Two K-type stainless steel shield thermocouples were fixed to the bondline while fabricating the samples to monitor the temperature rise. A data logger was used to read the bondline temperature. Figure 6 shows how the bond strength has deviated when both adhesive types were exposed to 100 ^{0}C.

Bond strength reduction at elevated temperature was comparatively low in ECC adhesive compared to the epoxy adhesive. The failure occurred in the ECC adhesive-concrete interface, even under high-temperature exposure. It showed that the ECC adhesive-concrete interface is sensitive to temperature. The glass transition temperature of epoxy exceeded when exposing the sample to 100 ^{0}C. It resulted in a drastic bond strength drop as indicated in Figure 6.

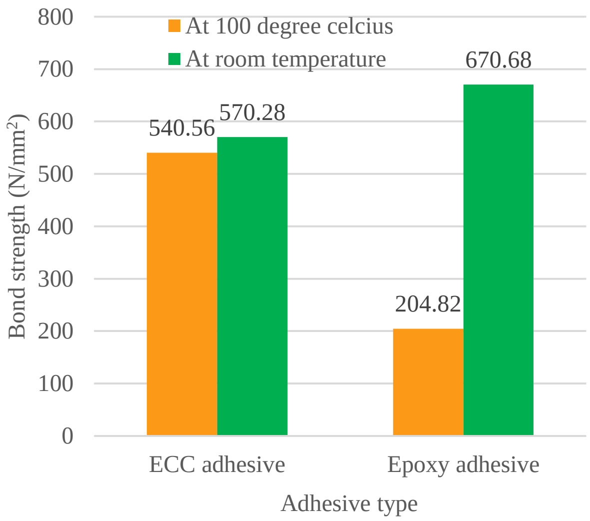

Figure 6: Effect of elevating bondline temperature

3. Numerical model

To assess the behaviour of direct pullout test, a three-dimensional Finite Element model was developed (Dassault Systemes Simulia and Corporation, 2014). The model was analysed in a computer with an Intel(R) Core(TM) i5-4200U processor and an 8 GB RAM.

3.1 Material models, defining of elements and mesh analysis

The Concrete Damage Plasticity (CDP) model was used to assign the nonlinear behaviour of concrete (Wahalathantri *et al.*, 2011). Nehdi and Ali (2019) simulated ECC using both the CDP model and Drucker/Prager (DP) model. Li and Zhang (2012) have highlighted the effectiveness of modelling dynamic actions of cementitious materials using the CDP model. Therefore the CDP model was used in damage modelling for both ECC adhesive and concrete block. CFRP fabric was modelled as a Lamina element.

The eight-node linear hexahedral solid element with reduced integration (C3D8R) was used to model both concrete block and ECC adhesive layers. The four-node quadrilateral membrane shell element with reduced integration (M3D4R) was used to model CFRP fabric. Mesh convergence analysis was carried out to determine the optimal mesh size. According to the results, the element size of 5 mm was used for ECC adhesive layer, 2.5 mm elements were used for meshing CFRP fabric and 10 mm elements were used for concrete block. The aspect ratio of elements was kept between 0.5 and 1. Figure 7(a) shows the meshed setup.

3.2 Boundary conditions and bond-slip behaviour

The same boundary conditions provided in the experimental setup were modelled. Loading was simulated as a displacement in CFRP fabric. Figure 7(b) presents the applied boundary conditions and loading. Bond-slip was observed in both ECC-concrete and ECC – CFRP interfaces. Therefore, it was necessary to accompany the bond-slip behaviour with the adhering properties of ECC adhesive. This was simulated by defining a cohesive contact interaction for the mentioned contact surfaces along with damage initiation and damage evolution criteria. It follows the traction-separation law proposed by Camanho et al. (2003) which defines that once the damage initiation is reached the bond will undergo progressive damage.

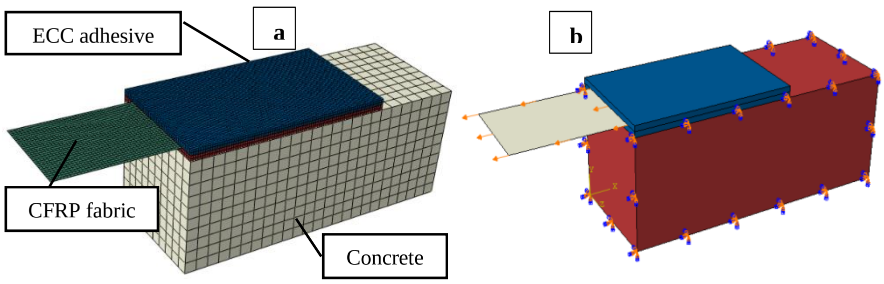

Figure 7: (a) Meshed model (b) Boundary conditions and loading

3.3 Validation of the model

The experiment and predicted load vs displacement graphs are given in Figure 8. Both graphs follow a comparatively similar path. But the predicted load vs. displacement graph showed slightly higher loading values compared to the experiment loading values for a particular displacement. The ultimate failure load of the FE model was 6.81 kN whereas the failure load of the

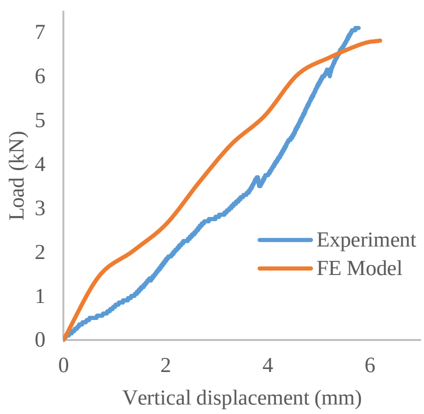

Figure 8: Load – Vertical displacement graph

experimental setup was 7.1 kN. Therefore, the predicted value showed a 4.08% deviation from the actual value. Displacement at failure load in the experimental setup was 5.78 mm while it was 6.2 mm in the FE model. Thus, the predicted displacement showed 7.27% of increment from the actual displacement. This is fairly a good prediction for the actual scenario. Figure 9 shows how the evolved ECC adhesive-concrete interface failure was predicted in the FE model.

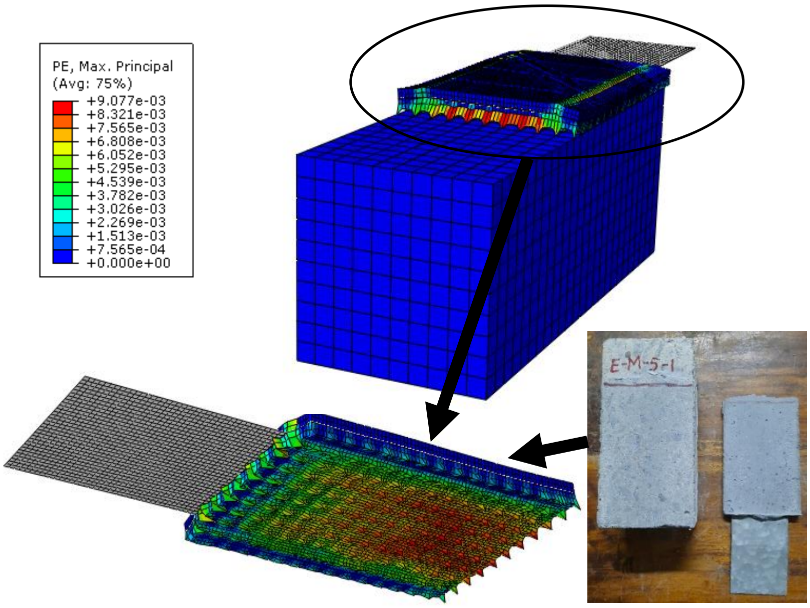

Figure 9: ECC – Concrete interface bond failure

3.4 Parametric study

A parametric study was performed to check the effect of adhesive thickness on bond strength. Therefore, models were developed for different adhesive thicknesses where two equivalent adhesive layers are applied on the top and bottom of CFRP fabric. Hence, the adhesive thickness is the overall thickness which includes both top and bottom adhesive layers. Failure loads for adhesive thickness 2.5 mm, 5 mm, 10 mm and 20 mm were 0.37 kN, 2.45 kN, 7.10 kN and 9.40 kN respectively (Figure 10). The corresponding bond slip at failure loads were 1.87 mm, 2.90 mm, 5.71 mm and 9.55 mm (Figure 10).

Failure load at 5 mm adhesive thickness is nearly equivalent to 7 times the failure load corresponding to 2.5 mm adhesive thickness. Thus, the failure load enhancement is 562% of the failure load for 2.5

mm adhesive thickness. Percentage failure load enhancement for 10 mm adhesive thickness is 190% of the failure load for 5 mm adhesive thickness. This percentage increment further reduces to 32%, when the adhesive thickness increment from 10 mm to 20 mm. Therefore it is clear that the percentage increment of failure load gradually decreases with the increment of adhesive thickness, even though failure load keeps on increasing gradually.

When bond-slip at failure load is concerned, with the increment of adhesive layer thickness, bond-slip at failure increases gradually. But unlike the behaviour in failure load, here the percentage increment of failure load bond-slip between two consecutive adhesive thicknesses keeps on increasing as 55% of bond-slip enhancement from adhesive thickness 2.5 mm to 5 mm, 97% for adhesive thickness from 5mm to 10 mm. But this slightly reduced to 67% when adhesive thickness incremented from 10 mm to 20 mm. Hence, it is clear that the enhancement of ECC adhesive layer thickness will enhance the bond strength. But this enhancement gradually decreases as the percentage increment between 2 consecutive adhesive thicknesses.

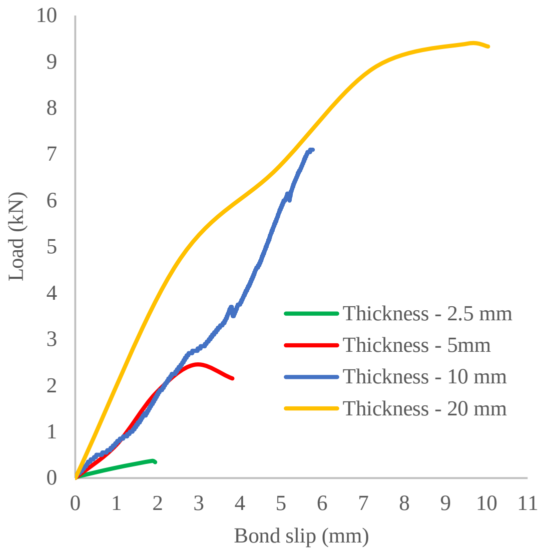

Figure 10: Effect of ECC adhesive thickness

4. Conclusions

The following conclusions were made from the experimental and numerical study.

1. Thermal conductivity of ECC-PET adhesive with PET fibre content as 2% of cement content ranged between 0.145 - 0.18 W/mK. Thus, the adhesive shows thermal resisting nature
2. The developed ECC-PET adhesive showed 7 days compressive strength of 16.97 N/mm^2, 28 days compressive strength of 52.77 N/mm^2 and tensile strength of 3.83 N/mm^2

3. The effective bond length of developed adhesive is 150 mm and the corresponding average bond strength is 224.9 N/mm^2. The failure occurred in CFRP-ECC interface
4. The CFRP-ECC interface failure can be avoided by sticking sand on top of CFRP fabric using epoxy adhesive before adhering it to a concrete substrate using ECC-PET adhesive
5. This approach enhanced the average bond strength to 570.28 N/mm^2. The percentage of bond strength enhancement was 158%. The failure occurred in ECC-concrete bond interface
6. The average bond strength was reduced by 5.21% when the bondline temperature of samples adhered using ECC-PET adhesive was incremented to 100^{0}C, whereas for epoxy adhesive this reduction was around 69%
7. The ECC-concrete bond is sensitive to temperature increment
8. From the parametric study, it was found that the increment of developed ECC adhesive thickness increases the failure load. However, the percentage failure load enhancement between 2 consecutive adhesive thicknesses reduces gradually

Acknowledgements

Authors would like to highly acknowledge the financial support provided by the National Research Council grant No: PPP 18-01 and Airow Solutions (Pvt) Ltd. Furthermore, the help given by the laboratory technicians in the Department of Civil Engineering, University of Moratuwa during the experimental work is highly appreciated.

References

American Society for Testing and Materials (2005) 'ASTM C618 - 19 - Standard Specification for Coal Fly Ash and Raw or Calcined Natural Pozzolan for Use in Concrete', *ASTM International*.

American Society for Testing and Materials (2009) 'ASTM C 109/C 109M - Standard Test Method for Compressive Strength of Hydraulic Cement Mortars', *ASTM International*, pp. 29–31. doi: 10.1201/9781420091175-c5.

American Society for Testing and Materials (2018) 'ASTM D7340 - 07(2018) Standard Practice for Thermal Conductivity of Leather', *ASTM International*. West Conshohocken, PA, 15.04. doi: 10.1520/D7340-07R18.

Bapat, B. (2020) *Measurement of Thermal Conductivity by Lee ' s method*. Available at: http://www.iiserpune.ac.in/~bhasbapat/phy221_files/Lee%27s Method.pdf.

Barnes, R. and Fidell, J. (2006) ‘Performance in Fire of Small-Scale CFRP Strengthened Concrete Beams’, *Journal of Composites for Construction*, 10(December), pp. 503–508. doi: 10.1061/(ASCE)1090-0268(2006)10:6(503).

Bentz, D. P., Peltz, M., Dura´n-Herrera, A., Valdez, P. and Jua´rez, C. (2011) ‘Thermal properties of high-volume fly ash mortars and concretes’, *Journal of Building Physics*, 34(3), pp. 263–275. doi: 10.1177/1744259110376613.

Boshoff, W. P. and Zijl, G. Van (2007) ‘Tensile creep of SHCC’, in *Fifth International RILEM Conference on High performance fibre reinforced cement composites (HPFRCC)*. Mainz, pp. 87–96.

Camanho, P. P., Dávila, C. G. and Moura, M. F. De (2003) ‘Mixed-mode Progressive Delamination in Composite Materials’, *Journal of Composite Materials*, 37(May 2014), pp. 1415–1438. doi: 10.1177/002199803034505.

Ćojbašić, L., Stefanović, G. and Sekulić, Ž. (2005) ‘Influence of the fly ash chemical composition on the portland cement and fly ash mixture hydration mechanism’, *FACTA UNIVERSITATIS Series: Mechanical Engineering*, 3(1), pp. 117–125.

Dassault Systemes Simulia and Corporation (2014) ‘ABAQUS Standard User’s Manual, Version 6.14’, *ABAQUS*. Rhode Island, USA.

Gamage, J. C. P. H., Al-Mahaidi, R. and Wong, M. B. (2006) ‘Bond characteristics of CFRP plated concrete members under elevated temperatures’, *Composite Structures*, 75, pp. 199–205. doi: 10.1016/j.compstruct.2006.04.068.

Hashemi, S. and Al-mahaidi, R. (2012) ‘Flexural performance of CFRP textile-retrofitted RC beams using cement-based adhesives at high temperature’, *Construction and Building Materials*. Elsevier Ltd, 28(1), pp. 791–797. doi: 10.1016/j.conbuildmat.2011.09.015.

Himasha, M. W. C. and Gamage, J. C. P. H. (2019) ‘A Review on Cementitious Adhesives used to bond CFRP with Concrete’, in *10th International Conference on Structural Engineering and Construction Management*. Kandy, p. 93.

Huang, X., Ranade, R., Zhang, Q., Ni, W. and Li, V. C. (2013) ‘Mechanical and thermal properties of green lightweight engineered cementitious composites’, *Construction and Building Materials*. Elsevier Ltd, 48, pp. 954–960. doi: 10.1016/j.conbuildmat.2013.07.104.

Kahandawa Arachchi, K. A. D. Y. T., Gamage, J. C. P. H. and De Silva, G. I. P. (2019) ‘Thermal insulation systems for CFRP/concrete composites: A review’, in *10th International Conference on Structural Engineering and Construction Management*, p. 94.

Koisch, B. B. (1998) ‘Carbon Fiber Cement Matrix (CFCM) overlay system for Masonry Strengthening’, *Journal of Composites for Construction*, 2(May), pp. 105–109. doi: 10.1061/(ASCE)1090-0268(1998)2:2(105).

Li, J. and Zhang, Y. X. (2012) ‘Evaluation of constitutive models of hybrid-fibre engineered cementitious composites under dynamic loadings’, *Construction and Building Materials*, 30, pp. 149–160. doi: 10.1016/j.conbuildmat.2011.11.031.

Li, V. (2008) ‘Engineered Cementitious Composites (ECC) – Material , Structural , and Durability Performance Engineered Cementitious Composites (ECC) – Material , Structural , and Durability Performance’, in *Concrete Construction Engineering Handbook*. CRC Press.

Li, V. C. (2007) ‘Engineered Cementitious Composites (ECC) – Material , Structural , and Durability Performance’, in Nawy, E. (ed.) *Concrete Construction Engineering Handbook*. CRC Press.

Makwana, J. J. and Rathod, D. J. D. (2017) ‘Interface Characterization of Different Types of Fibers in Engineered Cementitious Composites (ECC)’, *IOSR Journal of Mechanical and Civil Engineering*, 14(01), pp. 08–14. doi: 10.9790/1684-1401020814.

Nehdi, M. L. and Ali, M. A. E. M. (2019) ‘Experimental and Numerical Study of Engineered Cementitious Composite with Strain Recovery under Impact Loading’, *Applied Sciences*, 9(5), p. 994. doi: 10.3390/app9050994.

Sahmaran, M. and Li, V. C. (2008) ‘Durability of mechanically loaded engineered cementitious composites under highly alkaline environments’, *Cement & Concrete Composites*, 30, pp. 72–81. doi: 10.1016/j.cemconcomp.2007.09.004.

Sathishkumar, P., Sampathkumar, P., Karthik, M. and Vignesh, C. (2016) ‘Significance of Various Fibres on Engineered Cementitious Concrete’, *International Journal of Science, Engineering and Technology*, 4(1), pp. 284–290. Available at: http://www.ijset.in/wp-content/uploads/2016/02/10.2348.ijset0116284.pdf.

Selvaranjan, K., Gamage, J. C. P. H., De Silva, G. I. P. and Attanayaka, V. (2020) ‘Thermal performance of rice husk ash mixed mortar in concrete and masonry buildings’, *Budownictwo i Architektura*, 19(4), pp. 43–52. doi: 10.35784/bud-arch.2121.

Täljsten, B. and Blanksvärd, T. (2007) ‘Mineral-Based Bonding of Carbon FRP to Strengthen Concrete Structures’, *Journal of Composites for Construction*, 11(April), pp. 120–128. doi: 10.1061/(ASCE)1090-0268(2007)11:2(120).

US Army Corps of Engineers (2001) 'CRD-C260-01 Standard Test Method for Tensile Strength of Hydraulic Cement Mortars', *COE Standards*, pp. 1–8. Available at: https://www.wbdg.org/FFC/ARMYCOE/STANDARDS/crd_c260.pdf.

Wahalathantri, B. L., Thambiratnam, D. P., Chan, T. H. T. and Fawzia, S. (2011) 'A material model for flexural crack simulation in reinforced concrete elements using Abaqus', in *First International Conference on Engineering, Designing and Developing the Built Environment for Sustainable Wellbeing*, pp. 260–264. Available at: http://eprints.qut.edu.au/41712/.

Wu, C. and Li, V. C. (2017) 'CFRP-ECC hybrid for strengthening of the concrete structures', *Composite Structures*. Elsevier Ltd, 178, pp. 372–382. doi: 10.1016/j.compstruct.2017.07.034.

X-Calibur Structural Systems (2020) *X-Wrap C300 Technical Data Sheet*. Available at: https://www.x-calibur.us/files/X-Wrap C300.pdf.

Yang, E. H., Yang, Y. and Li, V. C. (2007) 'Use of high volumes of fly ash to improve ECC mechanical properties and material greenness', *ACI Materials Journal*, 104(6), pp. 620–628. doi: 10.14359/18966.

Yu, J. and Leung, C. K. Y. (2017) 'Strength improvement of strain-hardening cementitious composites with ultrahigh-volume fly ash', *Journal of Materials in Civil Engineering*. American Society of Civil Engineers, 29(9), p. 5017003. doi: 10.1061/(ASCE)MT.1943-5533.0001987.

A REVIEW ON CEMENTITIOUS ADHESIVES USED TO BOND CFRP WITH CONCRETE

Conference Paper · December 2019

2 authors:

M.W.Chamodi Himasha
University of Moratuwa

JCPH Gamage
University of Moratuwa

A REVIEW ON CEMENTITIOUS ADHESIVES USED TO BOND CFRP WITH CONCRETE

M.W.C.Himasha[1*], J.C.P.H,Gamage [1]
[1]Department of Civil Engineering, University of Moratuwa, Katubedda, Moratuwa, Sri Lanka.
**Correspondence E-mail: mvchimasha@gmail.com, TP: +94774008602*

Abstract: Carbon Fiber Reinforced Polymer (CFRP) strengthening which is generally used in retrofitting works of concrete structures demonstrates a major drawback when the fire performance of the bonding agent is concerned. Even though CFRP itself shows a good resistance over fire, epoxy adhesive used for all these years as the bonding agent lags in its performance under elevated temperature. At elevated temperatures, bond deteriorates gradually causing failure in the strengthening system. To overcome this negative impact, research has been carried out on cementitious adhesives which show a better resistance over thermal effect. This paper reviews the suitability and applicability of a polymer based cementitious adhesive and a non-polymer based cementitious adhesive used to bond CFRP with concrete.

Keywords: Carbon Fiber Reinforced Polymer; Cementitious adhesive; Engineered Cementitious Composite; Graphene oxide

1. Introduction

CFRP strengthening has been one of the widely used retrofitting methods in the present world. Type of adhesive used as the bonding agent plays a major role in the long term performance of the strengthening setup(Al-abdwais and Al-mahaidi, 2017). Performance of strengthening system under elevated temperature needs to be given a huge concern. CFRP strengthened concrete can reduce its strength by 65% at 300 ^{0}C(Petkova, Donchev and Wen, 2014). Generally epoxy (organic) adhesives are used as the bonding agent for fibre composites. But they have several disadvantages apart from its suitability with respect to better bonding behaviour. Strength of epoxy adhesive deteriorates rapidly with elevated temperature higher than the glass transition, Tg (60 ^{0}C –70 ^{0}C) (Gamage and Wong, 2006). The glass transition temperature (Tg) is the temperature around which a sudden drop in properties of the adhesive occurs and adhesive changes from a relatively stiff material to a viscous material(Barnes and Fidell, 2006). Apart from that, it possesses other disadvantages like high cost of material(Koisch, 1998), toxic fumes(Täljsten and Blanksvärd, 2007). To overcome these issues, cementitious adhesives are developed. Usually cement-based adhesives have lower strength than organic adhesives. There is a possibility to apply the cement-based bonding agent at temperatures as low as 0 °C, meaning that if the epoxy adhesive is replaced with a mineral-based bonding agent it would be more environmental friendly. These cementitious adhesives are of two types; polymer based cementitious adhesives and non-polymer based cementitious adhesives. When developing a new adhesive, several properties need to be checked to assess its compatibility to the purpose. Setting time and flowability evaluates the suitability of the adhesive for practical application. Apart from that mechanical properties like tensile strength, compressive strength and pull-off strength need to be checked.

The literature review below is a comprehensive study on two cement-based adhesives which can be used as the bonding agent for CFRP strengthening of a concrete element. The first section focuses on the Engineered Cementitious Composite (ECC) which is a polymer-based cementitious adhesive where polymer fibers are being used. Next section includes a detailed study on Graphene oxide-based cementitious adhesive which is a non-polymer based cementitious adhesive. The last section presents an overall conclusion about the comprehensive study.

2. Engineered Cementitious Composite as a cementitious adhesive

ECC is a cement-based composite mortar which is systematically engineered to behave in a ductile manner under tension. The composite mortar contains cement, sand, fly ash, water, superplasticizer and fibers. Even though other cementitious adhesives perform well under elevated temperature, they show low ductility. This creates a negative effect on the load transferring from the concrete substrate to CFRP(Hashemi and Al-mahaidi, 2012; Wu and Li, 2017a) and lacks prior failure warning. ECC achieves the desired ductility by microcracking in strain hardening stage(Li, 2008). In a study done on retrofitting a beam using basalt FRP and mortar system, it was recommended to use polymer-modified cementitious mortar rather than using cementitious mortar for better bonding(Elsanadedy *et al.*, 2013).

An experimental study done by strengthening concrete beams using CFRP-ECC hybrid showed premature debonding at the interface. Thus the flexural performance of the beam was not enhanced(Yu *et al.*, 2015). Compressive test on cubes (50 mm x 50 mm x 50 mm) cast by ECC was done as per ASTM C190/C190M (ASTM, 2013). Dog bone shaped specimen test was used to test for tensile strength as per recommended by Japan Society of Civil Engineers (JSCE) (JSCE, 2008).Average compressive strength of samples using PVA fiber as the fiber component in ECC was 50.9 MPa (Wu and Li, 2017a). Peak pull out stress is proportional to the embedded length(Wu and Li, 2017a). For 170 mm embedded length, stress reached to 174.2 MPa(Wu and Li, 2017a). The tensile strain capacity of ECC was found as 2.8% (average), which is closer to 252 times higher than that of the cement mortar(Wu and Li, 2017a).

Mix design of ECC is solely a trial and error process. Different reference mix design ratios have been developed, so as to achieve certain properties within appropriate ranges depending on the application. ECC M45 is one such widely used mix design proportion where Poly Vinyl Alcohol (PVA) fibers are used. The fiber content of 2% by volume is used in the mix to achieve strain hardening effect(Li, 2007) as fibers act as the reinforcement. A research study done on effect of various fibers on the performance of ECC has suggested the use of PVA over the use of Polyethylene, Polypropylene and Polyester fibers as it depending on the mechanical properties of ECC developed with each fiber type. Further the authors suggest using PVA fiber content of 2% by volume in the mix since it produces the mortar mix which achieves the highest compressive, tensile and flexural strengths with regard to all other trial mixes(Sathishkumar *et al.*, 2016).

Explosive spalling is a common catastrophic failure mode of normal mortars in a fire. One of the major reasons for concrete spalling under elevated temperature is the increment in internal pressure induce as a result of water vapour(Kalifa, Menneteau and Quenard, 2000). Due to the melting of PVA fibers in ECC, it resists spalling failure up to 800 ^{0}C(Sahmaran, Lachemi and Li, 2010). Channels created by melting the fiber create paths for moisture to escape without creating high internal pressure within the mixture(Sahmaran, Lachemi and Li, 2010). Another experimental study proves that ECC does not crack or spall up even when the temperature reaches up to 500 ^{0}C(Wu and Li, 2017b). Scanning electron microscope images taken before and after temperature treatment proves the formation of interconnected channels(Wu and Li, 2017b).

In an experimental approach initiated to investigate residual compressive strength of ECC under elevated temperature, it was found that compressive strength of ECC reduced by 4.8% when exposed to 300 ^{0}C and it reaches to 31.3% at 500 ^{0}C. But in normal mortar compressive strength reduction at 300 ^{0}C is 13.8%, while there is no residual compressive strength at 400 ^{0}C(Wu and Li, 2017b). Up to 200 ^{0}C, the tensile strength of ECC was around 4.9 MPa - 5.2 MPa. It dropped by 69.4% at 500 ^{0}C(Wu and Li, 2017b). The interface between ECC and the concrete substrate is more sensitive to the temperature than the ECC – CFRP interface. ECC – CFRP system was debonded from the concrete substrate when temperature reached 300 ^{0}C(Wu and Li, 2017b)

Researchers investigated the enhancement in the deflection capacity by replacing of ductile ECC around main flexural reinforcement(Maalej and Leong, 2005). In casting Reinforced Concrete (RC) beam, they have used concrete for 2/3 of the depth of the beam and remaining 1/3 of the depth of the beam is filled with ECC. Experimental results show that the finer cracks form in ECC delay the crack induced stress concentration and ultimately result in effective stress distribution along with FRP layer(Maalej and Leong, 2005). Further suggestions were made to investigate bonding ability between ECC and FRP laminate.

PVA fiber which is 2% of the total volume of the typical PVA-ECC M45 mix account for 80% of the total material cost(Yu and Leung, 2017). Cost of PE fibers is 8 times the cost of PVA fibers(Li *et al.*, 2001). So it is a necessity to find a cost-effective alternative instead of PE and PVA fibers. As a solution recycled Polyethylene terephthalate (PET) fibers can be used over PE and PVA fibers(Lin *et al.*, 2018). But virgin PET fiber degrade in an alkaline environment(Silva *et al.*, 2005). Therefore an appropriate surface treatment method should be adopted. Smaller diameter PET fibers exhibit effective crack-bridging but show poor workability and poor fiber dispersion too. Thicker PET fibers exhibit better resistance over alkaline environment(Lin *et al.*, 2018).

3. Graphene oxide-based cementitious adhesive

Graphene oxide is a nanomaterial. Graphene oxide (GO) is an important precursor for the production of graphene by chemical reduction of graphene oxide. Researchers have highlighted the advantages of GO addition to cement-based materials (Mohammed *et al.*, 2015; Rhee *et al.*, 2015). Several pieces of research have been carried out on cement mixed with graphene and its derivatives such as graphene oxide, reduced graphene oxide to investigate its compressive, tensile and flexural performance. Higher thermal integrity and crack propagation resistance have encouraged its use as a cementitious adhesive for CFRP.

Cement based adhesive with GO (GM) and Control mix without GO (CM) was prepared using an automatic mortar mixer in compliance with the BS EN 196-1 (BSI 2005a), BS EN 196-3 (BSI 2005b), and BS EN 480-1 (BSI 2014) specifications. Several tests were performed on the material; Consistency of the cement-based adhesive mortars (CM and GM) was tested by adopting ASTM C1437 (ASTM 2015),Time of initial and final setting of CM and GM was measured according to ASTM C191 (ASTM 2013a) at a temperature of 23°C and relative humidity of 60%, Pull-off testing was performed according to ASTM C1583 (ASTM 2013b), Chemical composition of GO was examined using X-ray photoelectron spectroscopy (XPS) analysis, Particle-size distribution of the GO was examined using a CILAS 1190 laser particle-size analyzer. The developed adhesive mixture gained a pot life up to 120 min with a flow of 7.5%, tensile strength of 13.8 MPa, compressive strength of 101 MPa and pull-off strength of 1.2 MPa(Mohammed *et al.*, 2016).

The innovative high-strength self-compacting non-polymer cementitious adhesive (IHSSC-CA) developed using GO was recommended to use over polymer-based cementitious adhesives and epoxy adhesives in NSM CFRP application due to its self-compacting behavior, flowability and workability(Mohammed *et al.*, 2018). Use of IHSSC-CA as the bonding agent for CFRP in RC beam strengthening has enhanced the deflection and ultimate flexural capacity when compared with the control RC beam. In the case of epoxy adhesive, deflection has been reduced and ultimate flexural capacity has been increased(Tareq *et al.*, 2017b). CFRP strengthened RC beams using epoxy as bonding agent does not maintain any residual strength after reaching the peak load. But using IHSSC-CA as bonding agent helps to sustain a residual strength of 87% of ultimate capacity after reaching peak load(Tareq *et al.*, 2017b). CFRP strengthened post-fatigue RC beams failed in rupturing of CFRP strip after the yielding of steel reinforcement and concrete crushing in compression region. This proves that the bond between

CFRP and concrete substrate does not degrade under fatigue loading(Tareq *et al.*, 2017a).

To avoid the exposure of CFRP to elevated temperature it was suggested to introduce a cover layer of 20 mm over CFRP layer if the exposed temperature reaches up to 600 ^{0}C and introduce a layer of 25 mm if the exposed temperature reaches up to 800 ^{0}C(Mohammed, Al-saadi and Al-mahaidi, 2016). Results have proved that this approach has increased the bond strength between CFRP and concrete substrate when compared with an instance where a protective layer is not laid(Mohammed, Al-saadi and Al-mahaidi, 2016).

Since non-homogeneity or segregation was not observed, this indicates adequate cohesion stability in the adhesive mix. Initial setting and final setting times are slightly more than CM in GM. A higher amount of plasticizer increases setting time. Surrounding environment also affects the setting time of cementitious. Hence, superplasticizer content needs to be reduced in wet conditions or increase it in a dry environment(Mohammed *et al.*, 2016).

GM shows an increase in tensile strength up to 45% compared with CM. It was found that GM exhibits a higher compressive strength compared to CM, showing about a 13.5% increase. Increased strength of GM may be due to the modification of the pore size structure of cementitious materials by increasing the small pores and densifying the microstructure of cementitious materials(Mohammed *et al.*, 2016). Failure patterns of CM and GM indicate GM can arrest and restrict crack propagation(Mohammed *et al.*, 2016). Some researchers have also reported that GO has the potential to arrest cracks by preventing crack propagation (Pan et al. 2015; Han et al. 2015). It is said that nanomaterials delay the initiation of nano cracks, thus requiring higher loads to start cracking, which improves the weak tensile strength of the cementitious matrix (Metaxa et al. 2010).

An experimental study was carried out to assess the bond strength of graphene oxide-based cementitious adhesive when applied on NSM technique. Pull out test results revealed that developed cementitious adhesive shows a better bonding ability than epoxy adhesive since the CFRP laminate ruptured when the developed cementitious adhesive was used as the bonding agent while it got debonded at presence of epoxy adhesive(Mohammed, Al-Saadi and Al-Mahaidi, 2017; Tareq *et al.*, 2018; Mohammed *et al.*, 2018). Furthermore, the graphene-based cementitious adhesive was successful in achieving 84% of the bond strength of epoxy adhesive(Mohammed, Al-Saadi and Al-Mahaidi, 2017). Liquid nature and self-compacting nature of the developed adhesive accounts for effective coating around the CFRP strip eliminating the formation of air voids(Mohammed, Al-Saadi and Al-

Mahaidi, 2017). This was further proved by performing Burnauer-Emmett-Teller (BET) isotherm analysis which demonstrates that the adsorption of the material is high after performing pull out test when compared with the unloaded state(Mohammed, Al-Saadi and Al-Mahaidi, 2017). From topographic images and roughness parameters obtained by Three-dimensional laser profilometery analysis it was deduced that graphene-based cementitious adhesive was able to apply uniform stress over the CFRP strip where epoxy adhesives showed stress concentrations at random locations(Mohammed, Al-Saadi and Al-Mahaidi, 2017). This adhesive depicts a ductile behaviour where a gradual decrement occurred in residual pullout strength after attaining peak strength(Mohammed, Al-Saadi and Al-Mahaidi, 2017; Tareq *et al.*, 2018).

Graphene oxide added high strength concrete shows resistance to spalling giving a 40% compressive and tensile strength reduction at 800 ^{0}C while after 400 ^{0}C, high strength concrete started spalling and 28.7% of its compressive strength was reduced(Mohammed, Sanjayan and Nazari, 2017). The pore structure of a mortar mix is a crucial factor which affects strength-related properties of the mix. Experimental results show that addition of graphene oxide refine the pore structure and improve mechanical properties(Mohammed, Sanjayan and Nazari, 2017).

There exists a strong adhesion between the GO and cement matrix. Interaction between GO and cement matrix form a strong covalent bond in between thus increases the load transfer efficiency between two materials enhancing the mechanical properties of the composite(Jamal *et al.*, 2016). When the presence of GO in the paste is 0.05% of the total weight of the paste, the compressive strength of the composite enhanced by 15% to 33% and flexural strength enhanced by 41% to 59%(Pan *et al.*, 2015). Composite also shows a 6.3% increment (from 3.48 GPa to 3.70 GPa) in the elastic modulus. GO increases the strain capacity of the composite and delay the propagation of micro cracks(Pan *et al.*, 2015). As per Table 1, when the weight percentage of GO in the cementitious mortar increases, the fluidity of the mortar paste decreases and the viscosity increases. Moreover, when GO addition is incremented up to 0.03%, paste shows a significantly low fluidity and a high viscosity(Wang *et al.*, 2015).

Table 1: Effect of GO content in the mortar mix(Wang *et al.*, 2015)

Dosage of GO (w %)	**0**	**0.01**	**0.02**	**0.03**	**0.04**	**0.05**
Cement paste fluidity (mm)	236	17	201	92	81	70
Apparent viscosity (mPa.s)	988.5	1200.7	2268.8	5154.4	12788.4	19284
Initial setting time (min)	170	170	165	155	140	130
Final setting time (min)	330	325	320	305	310	300

Thermal diffusivity of the cementitious paste is increased with the increase of GO content. This reduces the thermal gradient in the paste resulting in higher thermal integrity(Sedaghat *et al.*, 2014).

4. Conclusion

By reviewing the literature following conclusions were made regarding the two cementitious adhesives.

- ECC achieves required ductility by microcracking in the strain hardening stage.
- Fiber content of 2% by volume is the optimum fiber content required to prepare ECC as a polymer based cementitious adhesive.
- ECC mix prepared using PVA fibers resist spalling failure up to 800 ^{0}C.
- Self-compacting behavior of GO based cementitious adhesive shows its suitability as a bonding agent.
- Protective cover layer of GO based cementitious over CFRP layer enhances the bond strength between CFRP and concrete substrate.
- GO based cementitious adhesive resists crack propagation improving tensile strength of the mix
- With the increase of GO content in the mortar, it reaches a higher thermal integrity while lowering the fluidity of mortar.

5. Acknowledgement

Authors would like to acknowledge Dr.G.I.P.de Silva for his guidance. Furthermore, the financial support provided by National Research Council of Sri Lanka and Airow Solutions (Pvt) Ltd is highly acknowledged.

6. References

Al-abdwais, A. H. and Al-mahaidi, R. S. (2017) 'Bond properties between carbon fibre reinforced polymer (CFRP) textile and concrete using modified cement-based adhesive', *Construction and Building Materials*. Elsevier Ltd, 154, pp. 983–992. doi: 10.1016/j.conbuildmat.2017.08.027.

Barnes, R. and Fidell, J. (2006) 'Performance in Fire of Small-Scale CFRP Strengthened Concrete Beams', (December), pp. 503–508.

Elsanadedy, H. M. *et al.* (2013) 'Flexural strengthening of RC beams using textile reinforced mortar - Experimental and numerical study', *Composite Structures*. Elsevier Ltd, 97, pp. 40–55. doi: 10.1016/j.compstruct.2012.09.053.

Gamage, J. C. P. H. and Wong, M. B. (2006) 'Bond characteristics of CFRP plated concrete members under elevated temperatures', 75, pp. 199–205. doi: 10.1016/j.compstruct.2006.04.068.

Hashemi, S. and Al-mahaidi, R. (2012) 'Flexural performance of CFRP textile-retrofitted RC beams using cement-based adhesives at high temperature', *Construction and Building Materials*. Elsevier Ltd, 28(1), pp. 791–797. doi: 10.1016/j.conbuildmat.2011.09.015.

Jamal, T. B. *et al.* (2016) 'A Review Paper on Graphene Modified Cement A Review Paper on Graphene Modified Cement', *BUET-ANWAR ISPAT 1st Bangladesh Civil Engineering SUMMIT*, (November), pp. 146–153.

Kalifa, P., Menneteau, F. D. and Quenard, D. (2000) 'Spalling and pore pressure in HPC at high temperatures', *Cement and Concrete Research*, 30(12), pp. 1915–1927. doi: 10.1016/S0008-8846(00)00384-7.

Koisch, B. B. (1998) 'Carbon Fiber Cement Matrix (CFCM) Overlay System For Masonary StrenghteninG', (May), pp. 105–109.

Li, V. C. *et al.* (2001) 'Tensile strain-hardening behavior of polyvinyl alcohol engineered cementitious composite (PVA-ECC)', *ACI*

Materials Journal-American Concrete Institute. Detroit, Mich.: American Concrete Institute,[c1987-, 98(6), pp. 483–492.

Li, V. C. (2007) 'Engineered Cementitious Composites (ECC) – Material , Structural , and Durability Performance'.

Li, V. C. (2008) 'Durability of mechanically loaded engineered cementitious composites under highly alkaline environments', 30, pp. 72–81. doi: 10.1016/j.cemconcomp.2007.09.004.

Lin, X. *et al.* (2018) 'Recycling polyethylene terephthalate wastes as short fibers in Strain-Hardening Cementitious Composites (SHCC)', *Journal of Hazardous Materials*, 357(May), pp. 40–52. doi: 10.1016/j.jhazmat.2018.05.046.

Maalej, M. and Leong, K. S. (2005) 'Engineered cementitious composites for effective FRP-strengthening of RC beams', *Composites Science and Technology*, 65(7–8), pp. 1120–1128. doi: 10.1016/j.compscitech.2004.11.007.

Mohammed, A. *et al.* (2015) 'Incorporating graphene oxide in cement composites : A study of transport properties', *Construction and Building Materials*. Elsevier Ltd, 84, pp. 341–347. doi: 10.1016/j.conbuildmat.2015.01.083.

Mohammed, A. *et al.* (2016) 'Utilization of Graphene Oxide to Synthesize High-Strength Cement-Based Adhesive', pp. 1–7. doi: 10.1061/(ASCE)MT.1943-5533.0001705.

Mohammed, A. *et al.* (2018) 'The role of graphene oxide in limited long-term carbonation of cement-based matrix', *Construction and Building Materials*. Elsevier Ltd, 168, pp. 858–866. doi: 10.1016/j.conbuildmat.2018.02.082.

Mohammed, A., Al-saadi, N. T. K. and Al-mahaidi, R. (2016) 'Bond behaviour between NSM CFRP strips and concrete at high temperature using innovative high-strength self-compacting cementitious adhesive (IHSSC-CA) made with graphene oxide', *Construction and Building Materials*. Elsevier Ltd, 127, pp. 872–883. doi: 10.1016/j.conbuildmat.2016.10.066.

Mohammed, A., Al-Saadi, N. T. K. and Al-Mahaidi, R. (2017) 'Assessment of bond strength of NSM CFRP strips embedded in concrete using cementitious adhesive made with graphene oxide', *Construction and Building Materials*. Elsevier Ltd, 154, pp. 504–513. doi: 10.1016/j.conbuildmat.2017.07.238.

Mohammed, A., Sanjayan, J. G. and Nazari, A. (2017) 'Effects of graphene oxide in enhancing the performance of concrete exposed to high-temperature', *Australian Journal of Civil Engineering*. Taylor & Francis, 8353(September), pp. 1–10. doi: 10.1080/14488353.2017.1372849.

Pan, Z. *et al.* (2015) 'Mechanical properties and microstructure of a graphene oxide-cement composite', *Cement and Concrete Composites,* 58, pp. 140–147. doi: 10.1016/j.cemconcomp.2015.02.001.

Petkova, D., Donchev, T. and Wen, J. (2014) 'Experimental study of the performance of CFRP strengthened small scale beams after heating to high temperatures', *Construction and Building Materials*. Elsevier Ltd, 68, pp. 55–61. doi: 10.1016/j.conbuildmat.2014.06.014.

Rhee, I. *et al.* (2015) 'Compressive strength sensitivity of cement mortar using rice husk-derived graphene with a high specific surface area', *Construction and Building Materials*. Elsevier Ltd, 96, pp. 189–197. doi: 10.1016/j.conbuildmat.2015.08.016.

Sahmaran, M., Lachemi, M. and Li, V. C. (2010) 'Assessing mechanical properties and microstructure of fire-damaged engineered cementitious composites', *ACI Materials Journal*. American Concrete Institute, 107(3), p. 297.

Sathishkumar, P. *et al.* (2016) 'Significance of Various Fibres on Engineered Cementitious Concrete', 4(1), pp. 284–290.

Sedaghat, A. *et al.* (2014) 'Investigation of Physical Properties of Graphene-Cement Composite for Structural Applications', *Open Journal of Composite Materials*, 04(01), pp. 12–21. doi: 10.4236/ojcm.2014.41002.

Silva, D. A. da *et al.* (2005) 'Degradation of recycled PET fibers in Portland cement-based materials', *Cement and Concrete Research*. Elsevier, 35(9), pp. 1741–1746.

Täljsten, B. and Blanksvärd, T. (2007) 'Mineral-Based Bonding of Carbon FRP to Strengthen Concrete Structures', (April), pp. 120–128.

Tareq, N. *et al.* (2017a) 'Assessment of residual strength of concrete girders rehabilitated using NSM CFRP with cementitious adhesive made with graphene oxide after exposure to fatigue loading', *Construction and Building Materials*. Elsevier Ltd, 153, pp. 402–422. doi: 10.1016/j.conbuildmat.2017.07.121.

Tareq, N. *et al.* (2017b) 'Performance of RC beams rehabilitated with NSM CFRP strips using innovative high-strength self-compacting cementitious adhesive (IHSSC-CA) made with graphene oxide', *Composite Structures,* 160, pp. 392–407. doi: 10.1016/j.compstruct.2016.10.084.

Tareq, N. *et al.* (2018) 'Bond performance of NSM CFRP strips embedded in concrete using direct pull-out testing with cementitious adhesive made with graphene oxide', *Construction and Building Materials*. Elsevier Ltd, 162, pp. 523–533. doi: 10.1016/j.conbuildmat.2017.12.050.

Wang, Q. *et al.* (2015) 'Influence of graphene oxide additions on the microstructure and mechanical strength of cement', *Xinxing Tan Cailiao/New Carbon Materials*. Institute of Coal Chemistry, Chinese Academy of Sciences, 30(4), pp. 349–356. doi: 10.1016/S1872-5805(15)60194-9.

Wu, C. and Li, V. C. (2017a) 'CFRP-ECC hybrid for strengthening of the concrete structures', *Composite Structures*. Elsevier Ltd, 178, pp. 372–382. doi: 10.1016/j.compstruct.2017.07.034.

Wu, C. and Li, V. C. (2017b) 'Thermal-mechanical behaviors of CFRP-ECC hybrid under elevated temperatures', *Composites Part B: Engineering*. Elsevier Ltd, 110, pp. 255–266. doi: 10.1016/j.compositesb.2016.11.037.

Yu, J. *et al.* (2015) 'Mechanical performance of ECC with high-volume fly ash after sub-elevated temperatures', *Construction and Building Materials*. Elsevier Ltd, 99, pp. 82–89. doi: 10.1016/j.conbuildmat.2015.09.002.

Yu, J. and Leung, C. K. Y. (2017) 'Strength improvement of strain-hardening cementitious composites with ultrahigh-volume fly ash', *Journal of Materials in Civil Engineering*. American Society of Civil Engineers, 29(9), p. 5017003.

Finite Element Modelling of Reinforced Concrete Horizontally Curved Beams strengthened for shear using Carbon Fiber Reinforced Polymer

Conference Paper · October 2019

2 authors:

M.W.Chamodi Himasha
University of Moratuwa

JCPH Gamage
University of Moratuwa

Proceedings of the 7th International Symposium on

Advances in Civil and Environmental Engineering Practices for Sustainable Development

ACEPS - 2019

Finite Element Modelling of Reinforced Concrete Horizontally Curved Beams strengthened for shear using Carbon Fiber Reinforced Polymer

M.W.C.Himasha[1] and J.C.P.H.Gamage[1]

[1]Department of Civil Engineering, Faculty of Engineering, University of Moratuwa, Katubedda, Moratuwa, SRI LANKA

A R T I C L E I N F O

Article history:
Received
Revised
Accepted
Available online

Keywords:
Horizontally curved concrete beams
CFRP
Shear strengthening
Finite Element Modelling (FEM)

A B S T R A C T

In the current world with the trend of constructing architecturally complex structures, the use of horizontally curved beams has been popular. Strengthening of shear deficient such curved beams to improve performance is an important aspect. Since Carbon Fiber Reinforced Polymer (CFRP) materials have been used for strengthening straight beams for shear successfully, assessing the application of this technology on curved beams is an innovative approach. A numerical model was developed using a finite element analysis technique. The predicted results are in good agreement with test results. More than 23% strength gain in shear was noted from strengthened beams.

1. INTRODUCTION

Reinforced concrete (RC) curved beams can currently be seen in many applications such as highway intersections, bridges, curved buildings and ring shaft conveying vaults. Apart from bending and shear, curved beams subject to torsion. With the increasing applications of RC curved beams in structural work, the importance of strengthening methods on such elements are getting highlighted.

Concrete beams fail in different mechanisms. Shear failure is a one such mechanism. Shear failure has a tendency to occur prior to flexural failure when the shear strength of beam is inadequate to develop its flexural capacity. Such beams are known to be shear critical beams (Balakrishnan et al., 1988).

RC beams are usually strengthened by CFRP laminates fixed to the bottom of the beam. But often they fail due to the debonding of the CFRP laminate from the concrete substrate (Rvendran et al., 2016). Most of the researches have conducted focusing on the suggestion of a better bonding technique to avoid the debonding of CFRP from the concrete substrate in the enhancement of flexural performance of strengthened RC beams (Ariyachandra et al., 2017; Premarathne & Gamage, 2013; Amarasinghe & Gamage, 2015).

Chaallal et al. (1998) have investigated external shear strengthening of RC beams using CFRP. They suggest the use of diagonal CFRP side strips over vertical CFRP side strips as they perform well in terms of shear strength, crack propagation and stiffness. But all those studies are done on straight RC beams, whereas this particular research accounts for horizontally curved RC beams. Abating of strength due to debonding issue can be avoided by wrapping CFRP fabrics around the RC beam. Therefore, this study is focused on shear strengthening of curved RC beams using CFRP wraps in shear region.

2. THE TEST PROGRAM

Two configurations; non-strengthened and strengthened with CFRP were tested as given in Table 1. Beams prepared for the experimental process are shown in Figure 1(a) and 1(b). Since the study was focused on the shear behaviour, stirrups were removed within the region 450 mm (1/4 of beam arc length) from both ends to allow the beams to fail in shear failure mode.

Table 1 Test setup

Specimen number	Type	Section dimensions	Radius	Curve length
		mm^2	m	m
1-1-2-CO	Control	200 x 200	2	1.8
1-2-2-CO	Control	200 x 200	2	1.8
2-1-2-FA	CFRP wrapped	200 x 200	2	1.8
2-2-2-FA	CFRP wrapped	200 x 200	2	1.8
3-1-4-FA	CFRP wrapped	200 x 200	4	1.8
3-2-4-FA	CFRP wrapped	200 x 200	4	1.8

3. NUMERICAL MODELLING

A three dimensional (3D) model was developed for two configurations as shown in Figure 2(a) and 2(b).

Figure 1(a) Non-strengthened control beam

Figure 1(b) CFRP strengthened beam

Figure 2(a) Numerical model of control beam

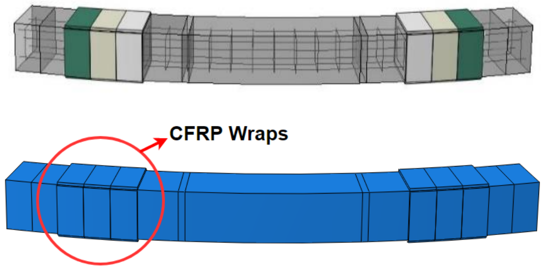

Figure 2(b) Numerical model of CFRP strengthened beam

FEM of the beams was developed using ABAQUS software (Sharcnet.ca, 2018). An initial model was developed to validate experimental results found in literature. Then this model was further developed to validate the obtained experimental results accordingly. This validated model was used in predicting the behavioural patterns of CFRP strengthened curved beams under varying parameters.

3.1. Material properties

Grade 30 concrete was used. Mechanical properties were assigned based on the previous research studies (Tamura & Murata, 2010; Muralidharan et al., 2017).

Table 2 Properties of concrete

Properties	Units	Value
Density	kg/m^3	2400
Young's modulus, E_{cm}	MPa	31000
Compressive yield stress, f_{ck}	N/mm^2	34
Poisson's ratio		0.2
Dilation angle		5
Eccentricity		0.1
fbo/fco		1.16
K		0.667
Viscosity parameter		0.0001

The concrete damaged plasticity model is used in modelling the nonlinear behaviour of concrete (Wahalathantri et al., 2011). Table 2 presents the properties of concrete used for modelling the substrate behaviour.

CFRP fabric was modelled as an orthotropic elastic material of thickness 1.2 mm. For such material, stress- strain relationship is defined as follows (Sharcnet.ca, 2018):

$$\begin{bmatrix} \sigma_{11} \\ \sigma_{22} \\ \sigma_{33} \\ \sigma_{12} \\ \sigma_{13} \\ \sigma_{23} \end{bmatrix} = \begin{bmatrix} D_{1111} & D_{1122} & D_{1133} & 0 & 0 & 0 \\ & D_{2222} & D_{1212} & 0 & 0 & 0 \\ & & D_{3333} & 0 & 0 & 0 \\ & & & D_{1212} & 0 & 0 \\ & Sym. & & & D_{1313} & 0 \\ & & & & & D_{2323} \end{bmatrix} \begin{bmatrix} \varepsilon_{11} \\ \varepsilon_{22} \\ \varepsilon_{33} \\ \gamma_{12} \\ \gamma_{13} \\ \gamma_{23} \end{bmatrix} \quad (1)$$

Where;

σ_{11}, σ_{22} and σ_{33} are direct stresses in x, y and z directions, respectively while σ_{12}, σ_{13} and σ_{23} are shear stresses. $\varepsilon_{11}, \varepsilon_{22}, \varepsilon_{33}, \gamma_{12}, \gamma_{13}$ and γ_{23} are strains in corresponding directions.

Each stiffness parameter in the matrix is defined as equations shown below (Sharcnet.ca, 2018):

$$D_{1111} = E_1(1 - v_{23}v_{32})\beta \quad (2)$$

$$D_{2222} = E_2(1 - v_{13}v_{31})\beta \quad (3)$$

$$D_{3333} = E_3(1 - v_{12}v_{21})\beta \quad (4)$$

$$D_{1133} = E_1(v_{31} - v_{21}v_{32})\beta \quad (5)$$

$$D_{2233} = E_2(v_{32} - v_{12}v_{31})\beta \quad (6)$$

$$D_{1122} = E_1(v_{21} - v_{31}v_{23})\beta \quad (7)$$

$$D_{1212} = G_{12} \quad (8)$$

$$D_{1313} = G_{13} \quad (9)$$

$$D_{1212} = G_{12} \quad (10)$$

$$\beta = 1 \Big/ 1 - v_{12}v_{21} - v_{23}v_{32} - v_{13}v_{31} - 2v_{21}v_{32}v_{13} \quad (11)$$

$$v_{ij} = \frac{E_i}{E_j} v_{ji} \quad (12)$$

The material properties found in the literature to calculate stiffness parameters for modelling CFRP fabric is listed in Table 3 (Daud et al., 2015).

Table 4 shows the stiffness parameters calculated using Eq. (2) to (12), to define the material properties of the CFRP fabric in FE model.

Table 3 Properties of CFRP (Daud et al., 2015)

Property	Values found from literature	
	Value	Unit
E_1	230	GPa
E_2	23	GPa
E_3	23	GPa
G_{12}	6.894	GPa
G_{23}	4.136	GPa
G_{13}	6.894	GPa
v_{12}	0.3	
v_{23}	0.25	
v_{13}	0.25	
Tensile strength	3400	MPa

The manufacturer provided material properties are listed in Table 5. These values satisfy the Tensile strength and Modulus of Elasticity found in literature (Table 3).

Deformed steel bars were used to reinforce the concrete beams. Properties are given in Table 6.

Table 4 Calculated stiffness parameters (Sharcnet.ca, 2018)

Data	Value
D1111	2.88E+11
D2222	3.06E+10
D3333	3.05E+10
D1122	7.31E+09
D1133	5.38E+09
D2233	7.46E+09
D1212	6.89E+09
D1313	6.89E+09
D2323	4.14E+09
γ	1.337793

Table 5 Properties of CFRP provided by the manufacturer (X-Calibur Construction Chemistry Inc., 2018)

Properties	Unit	Value
Density	g/cm^3	1.6
Tensile Strength	MPa	4000
Modulus of Elasticity	GPa	240

Table 6 Properties of steel rebars (British Standards Institution, 2005; British Standards Institution, 2004)

Properties	Units	Value
Density	kg/m^3	7850
Young's modulus	MPa	210000
Shear modulus	MPa	81000
Poisson's ratio		0.3
Coefficient of linear thermal expansion	/K	12×10^{-6}
Yield strength (f_y)	MPa	460
Ultimate strength (f_u)	MPa	540

3.2. Finite element mesh, Boundary conditions and loading

In meshing of RC beam, Hex element shape- C3D8R elements were used (Daud et al., 2015). This element has 8 nodes with 3 degrees of freedom at each node and capable of predicting cracking in three orthogonal directions, plastic deformation and crushing (Tejaswini & Raju, 2015).

Reinforcing bars were modelled using B31 beam elements (Tejaswini & Raju, 2015). CFRP fabric was modelled as a skin reinforcement for the concrete beam. This tool defines a skin that perfectly bonds to the surface of an existing part (Pereira, 2005) which simulate the bonding of CFRP fabric with epoxy adhesive. Figure 3 presents the Finite element mesh of the beam.

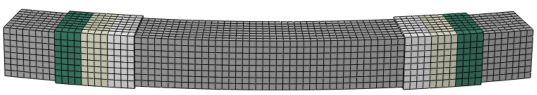

Figure 3 Finite Element Mesh of the Horizontally Curved RC beam (Curvature Radius = 4 m)

So as to select the optimum mesh size, a mesh sensitivity analysis was carried out with mesh sizes of 40 mm, 35 mm, 30 mm, 25 mm, 20 mm and 15 mm. Results started converging at 25 mm mesh size. Hence, the typical mesh size selected in this analysis is 25 mm. Clamp used in the experimental setup, the torsion along the beam was restrained with the vertical and horizontal translations. So the same support conditions were assigned in the model as shown in Fig. 4.

Beam was loaded at two points. Loading was done at 650 mm from the beam edge. In FE model simulation, load was modelled as a displacement with an amplitude of uniformly increasing displacement (0.001 m/s).

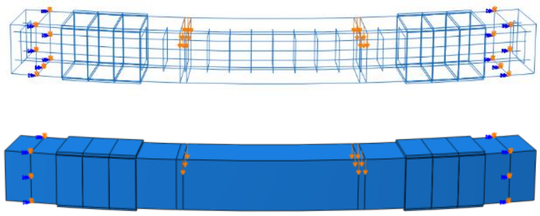

Figure 4 Boundary conditions and loading applied on the beam

The bond between RC beam and the reinforcing bars is defined using embedded constraint. With this constraint reinforcement is hosted inside RC beam. Aspect ratio of 1 was selected for the FE model to increase the accuracy of the results.

4. MODEL RESULTS

4.1. Model validation

As an initial attempt, the experimental setup in Tamura & Murata (2010) was used to evaluate the behaviour of horizontally curved RC beams. Table 7 gives the details of the corresponding beam. All attributes, geometry and material properties assigned were the same as in the test programme. Figure 5 shows the comparison between predicted and tested load - deflection relationship.

Table 7 Details of the beam (Tamura & Murata, 2010)

Beam	Shear span/ Depth	Curvature Radius	Curved Length	Cross Sectional Dimensions
		mm	mm	mm^2
B2-3.2	3.2	4000	1800	200 x 200

Following are the results obtained.

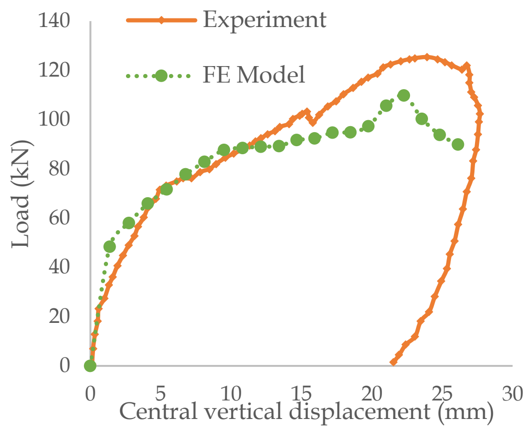

Figure 5 Predicted and tested (Tamura & Murata, 2010) Load vs. Displacement curves

Initially, both tested and predicted behaviours indicated a similar behaviour up to 89 kN load. Then a slight deviation from the experimental results was noted in the predicted results. Average discrepancy between predicted and experimented values within this region is 12%.

Table 8 Comparison of failure loads and deflection tested (Tamura & Murata, 2010)

Parameter	Experiment	FE Model	Deviation
Failure Load	125.42 kN	109.8 kN	12%
Corresponding Deflection	23.9 mm	22.3 mm	7%

The predicted failure load shows a 12% deviation from the tested load. A 7% deviation was noted from the corresponding mid-span displacement (Table 8). These figures clearly indicate the accuracy of the model.

Further, this model was used to predict the performance of tested beams in the currently ongoing research. Figure 6 shows the comparison of the experimental results in the current study with the model predicted results.

In this case, the FE model gives an ultimate load capacity of 39.65 kN while in experimental results show 43.52 kN capacity. This is about an 8% difference. In FE model, displacement at ultimate load is 8.77 mm while it is 10.81 in the tested sample which indicates 18% difference. Even though this indicates a large discrepancy, the deviation observed was 13%. These results also indicate the evidence for the accuracy of the model.

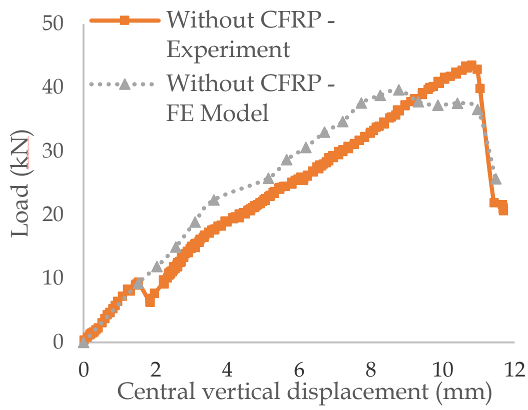

Figure 6 Load vs. Displacement graph with 2 m out of plane curvature

Table 9 Comparison of failure loads and deflection of the control beam

Parameter	Experimental Data	FEM Results	Deviation
Failure Load	43.52 kN	39.65 kN	8%
Corresponding Deflection	10.81 mm	8.77 mm	18%

4.2. CFRP strengthened curved beam with 2 m curvature

The load vs. deflection relationships are shown in Figure 7. It is clearly observed that the predicted results follow a path similar to the experimental curve of specimen 2-1-2-FA.

As indicated in Table 10, FE model gives an ultimate load capacity of 52.82 kN. This is about a 1% difference from the average failure load of experimental data. In FE model, the displacement at the ultimate load is 9.79 mm which indicates 39% difference from the average displacements observed during testing. Readings of beam 2-2-2-FA here follow a bit absurd behaviour due to a failure occurred in the fixture used to obtain displacement readings. Therefore, those results are not much accurate and the average displacement obtained for corresponding experimental displacement lacks accuracy. As a result, the corresponding displacement of the

FE model shows a considerable deviation from the average experimental failure displacement.

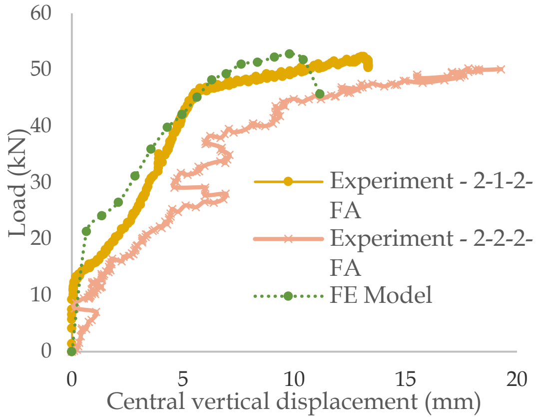

Figure 7 Load vs. Displacement – CFRP retrofitted out of plane curved beam with 2 m curvature

Table 10 Comparison of failure loads and deflection CFRP strengthened curved beam with 2 m curvature

Parameter	**Experiment (2-1-2-FA)**	**Experiment (2-2-2-FA)**	**FEM Results**	**Deviation**
Failure Load	54.40 kN	52.32 kN	52.82 kN	1%
Corresponding Deflection	19.29 mm	13.02 mm	9.79 mm	39%

4.3. The behavior of CFRP retrofitted curved beam with 4 m curvature

The load vs. deflection curves are shown in Figure 8. Graphs follow a similar path until the load increment up to 30 kN. From 30 kN to 50 kN, predicted results show slightly higher values than experimental results. Beyond 50 kN, both predicted and experimental (3-1-4-FA) results follow a similar behaviour until failure.

As indicated in Table 11, FE model predictions give an ultimate load capacity of 69.27 kN. This is about 8.6% difference from the average failure load of tested samples. In FE model, displacement noted at ultimate load is 29.21 mm which indicate 1.6% difference from the average displacements observed during testing.

All these results indicate the accuracy of the developed numerical model. Hence this model can be used to predict the effects of bond parameters.

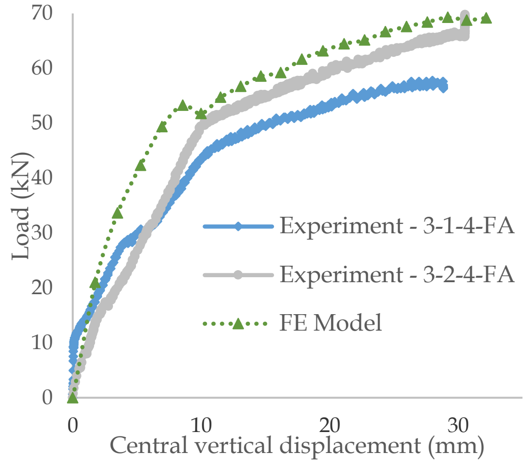

Figure 8 Load vs. Displacement – CFRP retrofitted beam with 4 m curvature

Table 11 Comparison of failure loads and deflection CFRP strengthened curved beam with 4 m curvature

Parameter	**Experiment (3-1-4-FA)**	**Experiment (3-2-4-FA)**	**FEM Results**	**Deviation**
Failure Load	57.76 kN	69.76 kN	69.27 kN	8.6%
Correspon ding Deflection	28.86 mm	30.53 mm	29.21 mm	1.6%

5. PARAMETRIC ANALYSIS

The parametric analysis was carried out to evaluate the behaviour of CFRP wrapped horizontally curved beams with varying parameters.

5.1. Effects of beam curvature

Figure 9 shows the comparison of load vs deflection behaviour of CFRP wrapped beams to enhance the shear performance. Failure loads of beams with curvature radius for 1 m, 2 m, 3 m and 4 m are 31.16 kN, 52.82 kN, 54.32 kN and 69.27 kN, respectively.

Graphs clearly depict an enhancement in the failure load under the increased curvature. From shear strengthened beam with curvature radius 1 m to 2 m, a 69.51% of strength enhancement is noted. This lowers to 2% from beam with curvature radius 2 m to 3 m. Again the strength enhancement increases up to 27.5% from the beam with curvature radius 3 m to curvature radius 4 m. So the increment is uneven. Further, a clear increment in beam displacement at failure is shown. This provides evidence of on improved ductility with increasing curvature of shear strengthened out of plane curved beams.

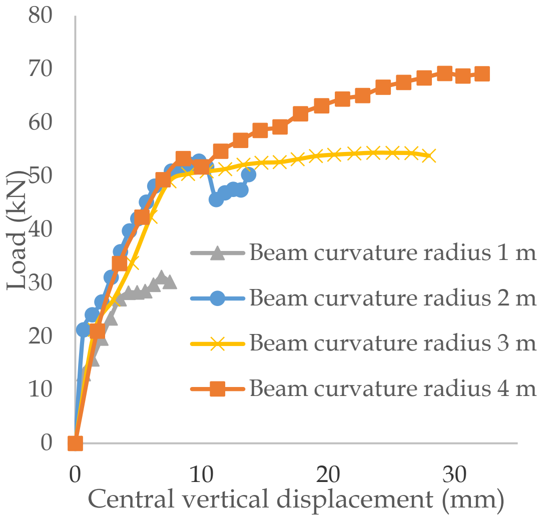

Figure 9 Effects of beam curvature of CFRP retrofitted beam for shear

5.2. Effects of support condition

When the support condition changes from partially fixed to totally fixed condition, the failure load increases from 69.27 kN to 75.88 kN. In here, the partially fixed condition is the support condition provided in the experimental setup. At simply supported condition, the failure load is 53.97 kN while it is 93.93 kN under pinned support condition. When one side of the beam is pinned while other is simply supported, analysis shows a failure load of 76.28 kN (Figure 10). This failure load is closer to the failure load of the fixed support condition. Even the load paths follow slightly similar routes. Hence it can be concluded that under these two conditions, beams behave in a similar manner. Moreover, both fixed and pinned condition and pinned support condition follows a similar loading path and coincide each other on the graph.

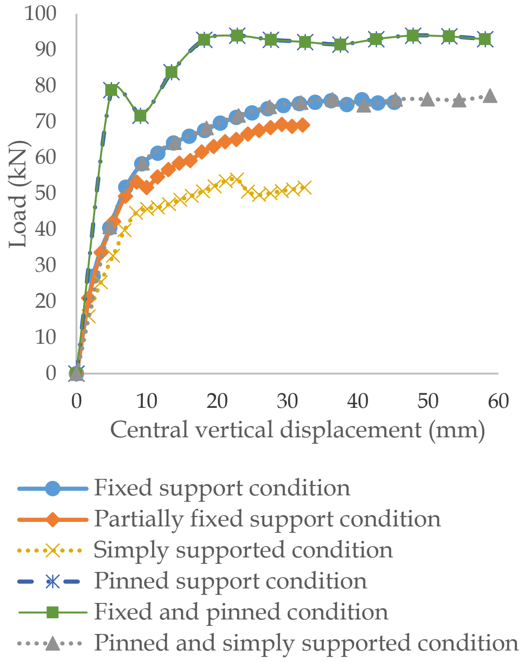

Figure 10 Effects of support condition

All these instances provide clear evidence to prove that if at least one support condition is a pinned support, it highly affects the enhancement of failure load of the CFRP strengthened curved RC beams. In a non-strengthened RC straight beam, pinned support condition does not restrain the vertical downward deflection of the beam at its mid-span as it allows the moment about the supports. Same condition applies here and it enables the beam reach a higher deflection while resisting a higher load than fixed support condition.

5.3. Effects of number of CFRP layers

Referring to Figure 11, it can be clearly concluded that the enhancement of failure load of horizontally curved RC beams depends on the number of CFRP wraps.

Here the failure loads in the ascending order of a number of CFRP wraps are 69.27 kN, 85.29 kN and 88.02 kN. Further, these results depict that the percentage of the increment of failure load, decreases with the number of CFRP wraps. This highlights the fact that the strengthening effect caused by the number of CFRP layers wrapped reaching an optimum limit. So further increment of a number of wraps beyond this optimum limit might not create a greater influence on strength enhancement.

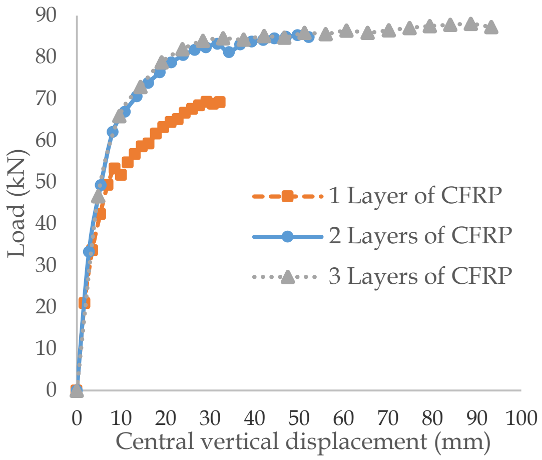

Figure 11 Effects of number of CFRP layers

6. CONCLUSIONS

Wrapping CFRP fabrics closer to the support, enhanced the shear capacity of RC horizontally curved beams until the shear capacity exceeds the flexural capacity. Strength gain in shear due to CFRP wrapping is around 23%. It seems that the CFRP wraps increase the stiffness of the beam since the deflection of the CFRP wrapped 2 m radius curved beam is lower than that of the 2 m radius curved control beam.

Further, the experimental results show that the increase of curvature radius of CFRP wrapped beams enhance the failure load of the beam. This fact can be clearly seen when focusing on the parametric study done on the effects of beam curvature. Moreover, an enhancement in the ductility of the beam was noticed with the increase of curvature of strengthened beams.

Through the parametric analysis, it was concluded that the shear performance of a CFRP wrapped RC curved beam enhances when at least a single support is provided with a pinned restraint. Further, the predicted results depicted that when the number of CFRP wraps increase, strength gain reaches a limit.

7. ACKNOWLEDGMENTS

A special acknowledgment goes to the computer laboratory staff of the Department of Civil Engineering, the University of Moratuwa for their invaluable guidance. The financial support given to the undergraduate project from the University of Moratuwa is greatly appreciated.

8. REFERENCES

Balakrishnan, S., Elwi, A. and Murray, D. (1988). Effect of Modeling on NLFE Analysis of Concrete Structures. *Journal of Structural Engineering*, 114(7), pp.1467-1487.

Rvendran, A., Perera, D. and Gamage, J. (2016). Finite Element Analysis of CFRP Strengthened Concrete Beams. In*: 4th International Symposium on Advances in Civil and Environmental Engineering Practices for Sustainable Development (ACEPS- 2016).*

Ariyachandra, M., Gamage, J., Al-Mahaidi, R. and Kalfat, R. (2017). Effects of surface roughness and bond enhancing techniques on flexural performance of CFRP/concrete composites. *Composite Structures*, 178, pp.476-482.

Premarathne, H. and Gamage, J. (2013). Alternative bonding techniques to delay end debonding of CFRP strengthened reinforced concrete beams. In: *4th International Conference on Structural Engineering and Construction Management*. Kandy, pp.154-160.

Amarasinghe, N. and Gamage, J. (2015). Experimental study on integrated method of NSM and EBR techniques for flexural strengthening of Concrete Beams using CFRP. In: *6 th International Conference on Structural Engineering and Construction Management*. Kandy, pp.170-177.

Chaallal, O., Nollet, M. and Perraton, D. (1998). Shear Strengthening of RC Beams by Externally Bonded Side CFRP Strips. Journal of Composites for Construction, 2(2), pp.111-113.

Tamura, T. and Murata, H. (2010). Experimental study on the ultimate strength of R/C curved beam. In: *Fracture Mechanics of Concrete and Concrete Structures*. Korea Concrete Institute, pp.1783-1788.

Muralidharan, R., Jeyashree, T. and Krishnaveni, C. (2017). Analytical Investigation of RC Curved Beams. *Journal of Industrial Pollution Control.*

Wahalathantri, B.L., Thambiratnam, D.P., Chan, T.H.T. and Fawzia, S., 2011, April. A material model for flexural crack simulation in reinforced concrete elements using ABAQUS. In *Proceedings of the first international conference on engineering, designing and developing the built environment for sustainable wellbeing* (pp. 260-264). Queensland University of Technology.

Sharcnet.ca. n.d., *Abaqus Analysis User's Manual (6.10)*, viewed 10 October 2018, from https://www.sharcnet.ca/Software/Abaqus610/Documentation/docs/v6.10/books/usb/default.htm?startat=pt05ch19s02abm02.html#usb-mat-clinearelastic-orthoterms.

Daud, R., Cunningham, L. and Wang, Y., 2015. Non-linear FE Modelling of CFRP-strengthened RC slabs under cyclic loading. *Athens Journal of Technology and Engineering*, *2*(3), pp.161-180.

X-Calibur Construction Chemistry Inc., n.d. *X-Wrap C300-High strength carbon fiber fabric for structural strengthening*. X-Calibur Construction Chemistry Inc. Available at: https://www.x-calibur.us/files/X-Wrap%20C300.pdf [Accessed 15 Nov. 2018].

British Standards Institution. (2005). *EN 1993-1-1 (2005) (English): Eurocode 3: Design of steel structures - Part 1-1: General rules and rules for buildings*. London, BSi.

British Standards Institution. (2004). *BS EN 10025-3:2004. Hot rolled products of structural steels - Part 3: Technical delivery conditions for normalized/normalized rolled weldable fine grain structural steels*. London, British Standards Institution.

Tejaswini, T. and Raju, M. (2015). Analysis of RCC Beams using ABAQUS. *International Journal of Innovations in Engineering and Technology (IJIET)*, 5(3), pp.248-255

Pereira, J. (2005). *FE Modeling of FRP Strengthening Systems on the White Bayou Bridge.* M.Sc. Chalmers University of Technology.